Central European wildfire regimes under climate change: a sensitivity analysis based on simulations with iLand

A thesis submitted
to the TUM School of Life Sciences
Master's Program Sustainable Resource Management
in partial fulfilment of the requirements for the degree of
Master of Science

by

Franziska Kraft

Supervisor:

Dr. Werner Rammer
Chair of Ecosystem Dynamics and Forest Management in Mountain Landscapes

March 2022

Abstract

Fire disturbance regimes are an important component of the Earth System as they interact with the atmosphere, climate, ecosystems, and human systems. The effects of global change on fire regimes worldwide have already become apparent in recent decades and significant further alterations are expected. An intensification of fire regimes affecting forests is of particular concern due to potential adverse effects on the ecosystem services they provide, such as carbon uptake and storage. In Europe, forest fire disturbances have increased over the last century, affecting a growing number of countries and important ecosystems, including the Alpine region. A further intensification of Central European forest fire regimes due to climate change is widely expected. The main objective of the present thesis was therefore to assess the sensitivity of Central European fire regimes, represented by two exemplary forest landscapes in Germany and Austria, to climatic changes in the RCP4.5 and RCP8.5 scenarios throughout the 21st century based on simulations with the forest ecosystem model iLand. The findings showed that rising temperatures combined with a decline in snow cover will likely have a significant impact on the annual number of fires and the burned area extent in the Central European Alpine region during the 21st century under high emissions scenarios, as well as under moderate scenarios in some areas. Regions experiencing greater changes in temperature and snow cover, while annual precipitation sums remain roughly constant, will most likely also experience greater impacts than others. Fuel availability did not occur to be a limiting factor for fire occurrence, which might promote larger fires, especially as less accessible areas at higher elevations might become increasingly affected. At the same time, the number of high-severity fires in the study areas increased only slightly or not at all. Lastly, the overall impacts on carbon storage in both study landscapes were small, although individual carbon pools were found to be negatively affected during the last 20 years of the century in the most extreme scenario. Even though the results of the present study are only conditionally generalizable to the larger Central European region, a potential doubling or quadrupling of the fire ignition probability in some regions over the course of this century due to climate change would lead to heightened risks for ecosystems and people, and likely also to a significant increase in already substantial firefighting costs and economic losses.

Table of Contents

List of Figures

List of Tables

List of Equations

List of Abbreviations

BGNP	Berchtesgaden National Park
BLE	Bundesanstalt für Landwirtschaft und Ernährung
BOKU	University of Natural Resources and Life Sciences Vienna (Universität für Bodenkultur Wien)
BuWe	Bucklige Welt
CLM	Community Land Model
DEM	Digital Elevation Model
EFFIS	European Forest Fire Information System
EOC	End-of-century
GPP	Gross Primary Production
GTNP	Grand Teton National Park
iLand	individual-based forest landscape and disturbance model
IQR	Interquartile Range
KBDI	Keetch-Byram Drought Index
MK	Mann-Kendall
NEP	Net Ecosystem Productivity

NPP	Net Primary Production
RCP	Representative Concentration Pathway
RU	Resource Unit
StMELF	Bayerisches Staatsministerium für Ernährung, Landwirtschaft und Forsten
TUM	Technical University of Munich

1. Introduction

Burning approximately 450 Mha per year globally (Rego et al., 2021), fire disturbances do not only affect a larger area but also more biomes than any other natural disturbance agent (Lavorel et al., 2006). Fire regimes interact with the atmosphere, climate, ecosystems as well as human systems and are thus an important component of the Earth System. Ongoing global change is therefore also expected to alter current fire regimes worldwide (Bowman et al., 2013; Lavorel et al., 2006). In the following, background information will first be provided on the key factors that influence fire ignition, fire behavior, and fire regimes, followed by a contextualization of fire regimes in the Earth System. In this context, carbon uptake and storage as an ecosystem service of forests and recent changes in global fire regimes as a result of global change will be briefly discussed. Lastly, an overview of the current state of research and the specific research objectives of this thesis follow.

1.1 Factors Influencing Fire Ignition, Fire Behavior, and Fire Regimes

Several factors on various spatial and temporal scales influence fire disturbances (see Figure 1). To ignite a fire, oxygen, heat, and fuel are always required. Wildfire risk, ignition probability, and fire spread are heavily influenced by prevailing weather conditions (e.g. de Rigo et al., 2017; Harris et al.; Lavorel et al., 2006; Migliavacca et al., 2013), especially precipitation, temperature, relative humidity, and wind conditions on a given day, and resulting fuel moisture (Harris et al., 2016; Lavorel et al., 2006). The characteristics of fuels, i.e. biomass affected by fire, significantly determine the behavior of wildfires and their impacts on humans and ecosystems. Wildfires are therefore commonly classified by the predominant fuel type and by the fuel layer that sustains their spread (ground, surface, or crown fires) (Rego et al., 2021). Topography is also a decisive determinant of fire spread, as fires spread faster upslope and at greater slope angles. At the same time, topography also

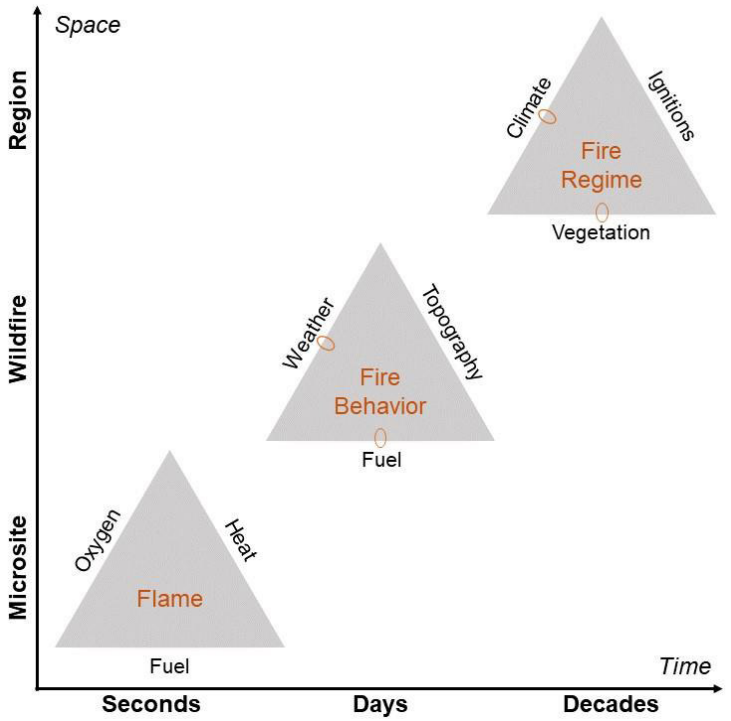

Figure 1: Dominant factors affecting fire at multiple spatial and temporal scales. Loops on the sides of the triangles indicate possible feedbacks (adapted from Parisien and Moritz (2009)).

influences weather and wind conditions as well as fuel availability and characteristics (Rego et al., 2021).

Fire regimes, i.e. the spatio-temporal distribution and characteristics of fires in a region over an extended period of time (Krebs et al., 2010), are largely controlled by climatic conditions (Figure 2, C1), human activities, especially those related to land use (Figure 2, C2) and fire ignitions, as well as land cover (Figure 2, C3). Apart from direct impacts of climatic conditions on fire occurrence, climatic influences also determine the availability, connectivity, and flammability of fuels on longer time scales (Bowman et al., 2013; Harris et al., 2016; Lavorel et al., 2006). While a rise in the atmospheric CO_2 concentration can stimulate biomass production and thus fuel availability in a given ecosystem, changes in climatic conditions, such as more frequent drought occurrence, can also reverse this effect (Bowman et al., 2013; Winkler et al., 2021). Overall, negative effects are expected to predominate in many ecosystems as the CO_2 concentration continues to increase (Winkler et al., 2021). In addition, land use directly impacts land cover, thus fuel loads and fire regimes. Agricultural practices relying on fire for land clearing, for example, or active fire suppression directly control fire occurrence (Lavorel et al., 2006; van Butsic et al., 2015). Lastly, the predominant cause of ignitions, i.e. ignitions caused by humans or in a natural way by volcanic eruptions or lightning strikes, also characterizes the fire regime (Bowman et al., 2013).

1.2 Interactions and Feedbacks Between Fire Regimes and the Earth System

While interactions of different parts of the Earth System control the occurrence of fires (Figure 2, FR), they in turn also affect these and other components of the system. On the one hand, they influence biophysical and biochemical cycles, which in turn causes positive or negative feedbacks on fire occurrence (Figure 2, F1). At the same time, in addition to the direct effects on land cover, there is a more indirect feedback on ecosystem function and services and thereby potential changes in land use (Figure 2, F2) (Lavorel et al., 2006).

Fire disturbances affect land cover composition by promoting vegetation that is resistant or resilient to fire or even depends on fire for its regeneration. This, in turn, can promote fire occurrence, creating a positive feedback loop (Lavorel et al., 2006). While these effects occur on relatively short time scales, fire-induced changes in nutrient availability can also affect land cover over the long term (Figure 2, E1 and C3) (Lavorel et al., 2006). Through these impacts on land cover and potential associated changes in albedo, surface temperature, cloud formation, and hydrologic processes, fire regimes can also indirectly cause climatic changes at regional scales (Figure 2, E5) (Harris et al., 2016; Lavorel et al., 2006). At the same time, fire emissions and released aerosols directly influence the chemical composition of the

atmosphere and promote increased fire occurrence in the long term by affecting the radiative balance and amplifying the greenhouse effect (Bowman et al., 2013; Harris et al., 2016; Lavorel et al., 2006). Aerosols can also have a short-term impact on local weather patterns, for example through a reduction in precipitation (Rosenfeld, 1999; Tosca et al., 2010) or an increase in ignitions from lightning strikes (Altaratz et al., 2010; Lyons et al., 1998). When fire-related carbon emissions exceed the carbon uptake capacity of the vegetation in a region, a carbon sink can ultimately become a carbon source (Figure 2, E2 – 4) (Lavorel et al., 2006). Van der Werf et al. (2017) estimated average global carbon emissions from fires during 1997 – 2016 to be around 2.2 PgC per year, which is roughly equivalent to 19 – 22% of annual average anthropogenic carbon emissions during 2011 – 2020, according to recent estimates (Friedlingstein et al., 2021).

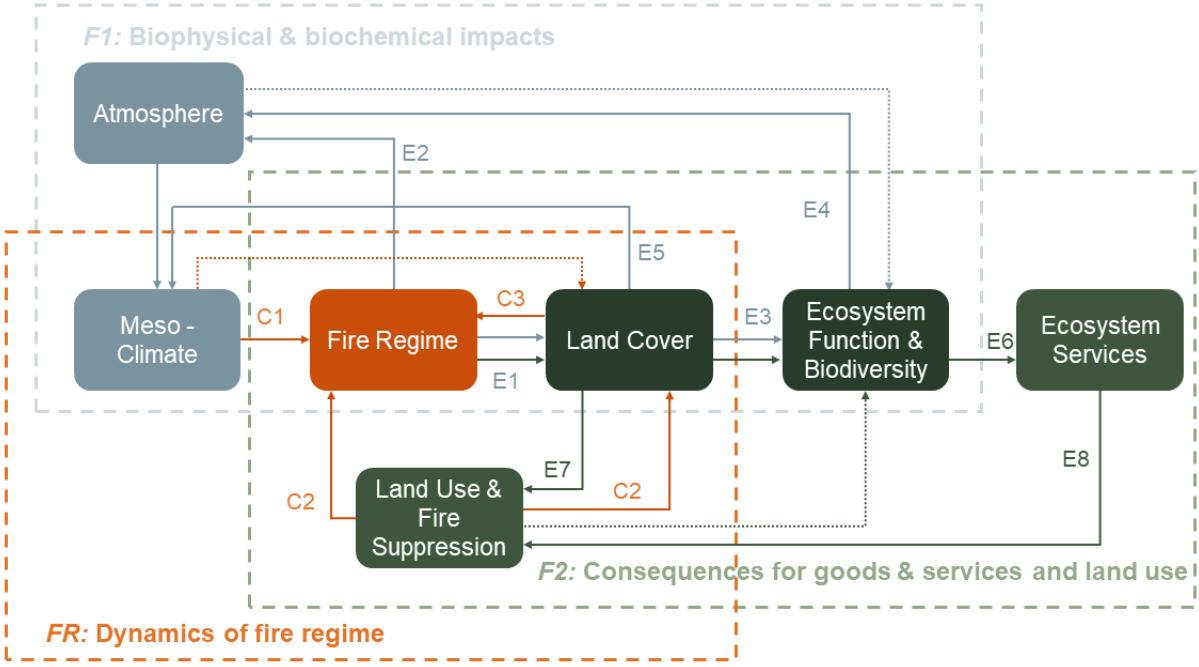

Figure 2: Relationships among different compartments of the human-environment system involved in fire causes (C) and effects (E), which are categorized into one control loop on fire regimes (FR, orange box and arrows) and two feedback loops. The first one drives impacts of fire on biophysical and biochemical processes (F1, blue box and arrows) and the second one (F2, green box and arrows) consequences of fire for ecosystem services and land use. Full arrows indicate topics of direct concern to integrated fire research, while dotted arrows represent other important, often indirect effects (adapted from Lavorel et al. (2006)).

While wildfires are an important natural component of many ecosystems (Bowman et al., 2013; Eastaugh & Hasenauer, 2014), aiding their functioning and regeneration (Rego et al., 2021), they can also have adverse effects on them. With regard to forests specifically, wildfires increase the susceptibility to further disturbances, for example windthrow or bark beetles (M. Müller et al., 2020; Seidl et al., 2017). Both positive and negative effects on forest biodiversity are possible, largely determined by fire regime intensity and tree species, with some species benefitting from open areas after fires and others being negatively affected (M. Müller et al., 2020; Rego et al., 2021). While newly emerging ecological niches could potentially offset a

loss of other species (Moretti et al., 2006), invasive species may also take advantage of them (Lonati et al., 2009; Maringer et al., 2012). Fire suppression activities can also promote the spread of invasive species, which can lead to slope erosion and pollution of waterways and provide new fuel loads, thereby increasing fire frequency and intensity (Bowman et al., 2013). In general, positive impacts are expected to diminish with increasing deviation from the natural regime (M. Müller et al., 2020; Rego et al., 2021). This concerns both a potential intensification of fire regimes due to climatic changes as well as fire suppression measures in naturally flammable ecosystems. The latter leads to an accumulation of fuels and thus to an increased risk of high-severity, stand-killing fires (Bowman et al., 2013).

The impacts of fire disturbances on ecosystem function also affect the provision of many ecosystem services, such as direct forest products or carbon sequestration (Figure 2, E6) (Lavorel et al., 2006). Overall, an intensification of wildfire regimes due to climate change is expected to have negative impacts on ecosystem function (Bonan, 2008) as well as on the provision of essential ecosystem services (Lindner et al., 2010; Turner, 2010), including carbon storage (Seidl, Schelhaas, et al., 2014).

While fire is actively used to alter land cover in view of land use changes, non-intentional fires can also induce these changes (Figure 2, E7) (Lavorel et al., 2006). In addition, fire regimes can induce regulations of, and thus changes in, land use (van Butsic et al., 2015). Lavorel et al. (2006) also argue that a feedback exists between ecosystem function and services and land use (Figure 2, E8), albeit a less obvious and less researched one. Following a decline in or a total loss of ecosystem service provision, reforesting and maintaining the ecosystem in question may no longer be economically viable so that a land use change or land abandonment may occur (Lavorel et al., 2006). These changes will again affect fire occurrence negatively or positively (Figure 2, C2).

1.3 Forests as a Component of the Terrestrial Carbon Sink

Forests account for nearly half of the terrestrial carbon sink, temperate forests alone for about one-tenth (Bonan, 2008). Each year, they absorb a substantial proportion of anthropogenic carbon emissions and thus counteract the ongoing increase in the atmospheric CO_2 concentration (Bonan, 2008). This rise likely caused an increase in the entire terrestrial carbon sink through positive effects on plant growth and biomass as well as soil organic matter towards the end of the last millennium (Walker et al., 2021), an effect that was dominant especially in temperate forests (Winkler et al., 2021). However, the findings of Winkler et al. (2021) also showed that these effects have been declining since and that negative effects of global change are becoming more prevalent in many ecosystems with further increases in the

CO_2 concentration. At the same time, climatic changes induced by a rise in the amount of CO_2 held in the atmosphere have affected the terrestrial carbon sink negatively (Friedlingstein et al., 2021). Friedlingstein et al. (2021) named Central Europe as one of the four most adversely impacted regions worldwide in this context. At the same time, forest cover in Europe has expanded over the last two centuries, resulting in increased carbon uptake while emissions from deforestation continue to rise in many other regions of the world due to ongoing land use changes (Friedlingstein et al., 2021). As mentioned before, wildfires release a substantial amount of carbon each year. Despite a heightened occurrence of extreme fires in many regions in recent years (Friedlingstein et al., 2021), the cumulative global fire area has been steadily decreasing for several decades. However, this trend is driven primarily by a decline in fire occurrence in savannas, not forests (Andela et al., 2017). Nevertheless, wildfire emissions continue to increase on a global scale, reversing the effect of declining global burned area extent (Zheng et al., 2021). Despite these negative impacts of climatic change, the terrestrial carbon sink has remained relatively stable over the past 60 years and continues to absorb about one-third of annual anthropogenic CO_2 emissions (Friedlingstein et al., 2021).

1.4 Changes in Global Fire Regimes Due to Climate Change

Wildfire activity is controlled primarily by prevailing fuel and climatic conditions in a given biome (Krawchuk & Moritz, 2011). In regions with high net primary productivity (NPP) and thus high fuel availability, such as the (sub)tropics, moisture conditions are the most important controlling factor. In areas with high annual precipitation sums, fire occurrence is therefore confined to drought spells. On the other hand, fire occurrence is mainly limited by limited fuel availability in regions characterized by lower biomass productivity as well as hotter and drier conditions (Krawchuk & Moritz, 2011). Overall, regions with medium-high NPP and extended annual dry periods are generally most affected (Bowman et al., 2013). Due to regionally varying impacts of climate change on temperature and precipitation, the response of fire regimes will also not be uniform across the globe. While significant regional alterations are likely to occur in a short period of time, with far-reaching impacts on affected ecosystems, fire occurrence may remain relatively constant on a global scale in the future (Krawchuk et al., 2009; Moritz et al., 2012). Overall, all projections of future fire occurrence are highly uncertain and in many regions, no conclusion can be drawn about the direction of development (Krawchuk et al., 2009; Moritz et al., 2012). However, it is assumed that there could be an increase in fire probability of more than 60% in the mid to high latitudes and a decrease of about 20% in the tropics towards the end of the 21st century (Moritz et al., 2012).

Wildfires have been of particular concern in the western United States since the mid-1980s when a vast increase in fire activity occurred (Westerling, 2016). In recent years, fire regimes

have continued to intensify, with approximately seven additional large fires and 355 km^2 of burned area each year (Dennison et al., 2014). Reasons for this development include the increase in summer and spring temperatures and the resulting earlier onset of snowmelt, which has increased the vulnerability of forest areas at higher elevations in particular (Dennison et al., 2014; Westerling, 2016). Recent simulation studies project a further increase in fire occurrence during the current century. In a study by Hansen et al. (2020), for example, a loss of two-thirds of the original forest area occurred in the Grand Teton National Park in Wyoming (GTNP) due to an increase in the annual burned area of 1,700% by the end of the century in the RCP8.5 scenario[1] compared to the reference period from 1989 to 2017, which was characterized by a return interval of 45 years.

While background information on fire regimes of all land cover types has been introduced previously, the present thesis focuses specifically on fires affecting forest areas in Central Europe. Forest disturbances due to wildfires[2] have increased in Europe during the 20th century (Schelhaas et al., 2003), mainly driven by climatic changes (Seidl et al., 2011). In the past, wildfires in Europe have predominantly been confined to the Mediterranean region, in particular Portugal, Spain, Italy, Greece, and (Southern) France. These five countries generally alone account for an average of 85% of the total annual burned area in Europe. However, other European countries have also become increasingly affected (Costa et al., 2020; de Rigo et al., 2017), especially during the record heat waves and droughts of recent years (San-Miguel-Ayanz et al., 2019). It is estimated that the area impacted by wildfires in Central and Northern Europe in 2018 was nearly 60 times greater than the regional average over the past decade. At the same time, a growing number of important ecosystems, such as the Alpine region, have been affected (San-Miguel-Ayanz et al., 2019). In 2019, for example, almost half of all fires occurred in Natura2000 EU protected regions (San-Miguel-Ayanz et al., 2020). A further intensification of Central European wildfire regimes due to climate change is commonly expected (e.g. Eastaugh & Hasenauer, 2014; Lindner et al., 2010; Wastl et al., 2012).

1.5 State of Knowledge and Research Gap

While Schelhaas et al. (2003) showed that the European fire regime had intensified during the 20th century and Seidl et al. (2011) identified climatic changes as the main reason for the increase in burned forest area between 1958 and 2001, current knowledge about future fire

[1] The Representative Concentration Pathways (RCPs) are trajectories developed by the Intergovernmental Panel on Climate Change to describe potential radiative forcings (in W/m^2, indicated by the number in each scenario's name) caused by different concentrations of CO_2 in the atmosphere by the end of the 21st century (Van Vuuren et al., 2011).

[2] From here on, the terms fire, wildfire, and forest fire are used interchangeably to refer to fires that affect forests.

regimes in Central Europe under climate change is still limited. However, projecting possible responses of wildfire regimes to climate change is critical for developing effective mitigation and adaptation measures to minimize potential adverse impacts on ecosystems and humans. While wildfire risk in Central Europe is generally expected to increase as a result of climate change (Costa et al., 2020; de Rigo et al., 2017), only few simulation studies have been conducted to project potential future patterns of actual fire occurrence. Using the Community Land Model (CLM) and two different climate projections for the SRES A1B scenario for a global-scale study, Kloster et al.'s (2012) simulations showed an increase in fire emissions in Central and Northern Europe due to climatic changes, with population changes having almost no effect. In a similar study on global wildfire emissions under the RCP4.5 and RCP8.5 scenarios using the LPJ-GUESS-SIMFIRE global dynamic vegetation-wildfire model, Knorr et al. (2016) also found a significant increase in burned area and wildfire emissions in Central Europe driven by climatic changes in both scenarios. At the same time, however, this effect was largely offset by the negative impacts of climate on fuel load. The net increase in emissions in the region, therefore, depended largely on the other two drivers considered in their study, namely the CO_2 effect and population changes. In a first simulation effort at the continental scale, also using the CLM model and SRES A1B scenario but a different parameterization than Kloster et al. (2012), Migliavacca et al. (2013) also found a significant increase in fire occurrence and burned area extent in Central and Eastern Europe by the end of the century. In simulations using both the LPJ-GUESS-SIMFIRE and LPJmL-SPITFIRE models with a resolution of 0.5° at continental scale, Wu et al. (2015) observed a significant increase in burned area in Central Europe under the RCP2.6 and RCP8.5 scenarios, despite significant differences between the models. While the increase in all RCP8.5 simulations and in the RCP2.6 simulations using LPJmL-SPITFIRE was mainly due to climatic changes, the effect of human population density dominated in the RCP2.6 scenario using LPJ-GUESS-SIMFIRE. While none of these studies considered the effect of wildfires on carbon storage, Seidl, Schelhaas, et al. (2014) observed a further intensification of European forest disturbance regimes by 2030 under a range of different climate scenarios (compared to the second half of the last century) in simulations using the EFISCEN and REGIME models, which could lead to a reduction in the carbon storage potential of forests of approximately 500 TgC across Europe. However, wildfires had a negligible effect on carbon storage in Central Europe in the study. Overall, simulation studies with higher spatial resolution focusing on individual areas in Central Europe specifically are still lacking and could contribute to a better understanding of potential small-scale changes of the regions' fire regimes under climate change. Given that the aforementioned studies mainly showed an increase in wildfire activity in Central Europe toward the end of the century, a longer-term study on the region's carbon storage potential is also needed.

1.6 Research Objectives and Questions

The main goal of the present master thesis is to use the wildfire module of the high-resolution forest landscape model iLand (short for the **i**ndividual-based forest **lan**dscape and **d**isturbance model) in a European context for the first time and to thereby gain insights into potential responses of Central European fire regimes to climatic changes throughout the 21st century. Two of the European study areas of the Chair of Ecosystem Dynamics and Forest Management at the Technical University of Munich (TUM), the Berchtesgaden National Park (BGNP) in Germany and the "Bucklige Welt" (BuWe) in Austria, were used for the simulations. As a basis for the simulations, the first part of this thesis characterizes the current and historic fire regimes of these regions. As present fire regimes are dominated by human activity and the resulting fire return intervals are too long to return meaningful results in simulations, estimates of historic return intervals for the Holocene were used for the parametrization of the model. Thus, this study represents a sensitivity analysis of the potential influence of climate change on fire regimes in Central Europe rather than an attempt to accurately project future fire occurrence.

More precisely, this thesis will be guided by four research questions:

(1) What characterizes current and historic wildfire regimes in Central Europe, in particular in Germany and Austria?

(2) How can these findings be leveraged to parameterize iLand's fire module for two exemplary forest landscapes in Germany and Austria?

(3) How sensitively do the fire regimes of these two landscapes respond to climatic changes in the RCP4.5 and RCP8.5 scenarios by the end of the 21st century in simulations with the iLand model?

(4) What are the effects of potential changes in the fire regimes on carbon storage in the two study landscapes?

2. Methods

To answer the research questions, a literature review and simulations using the iLand model were conducted, followed by an analysis of the model outputs in R (see Figure 3).

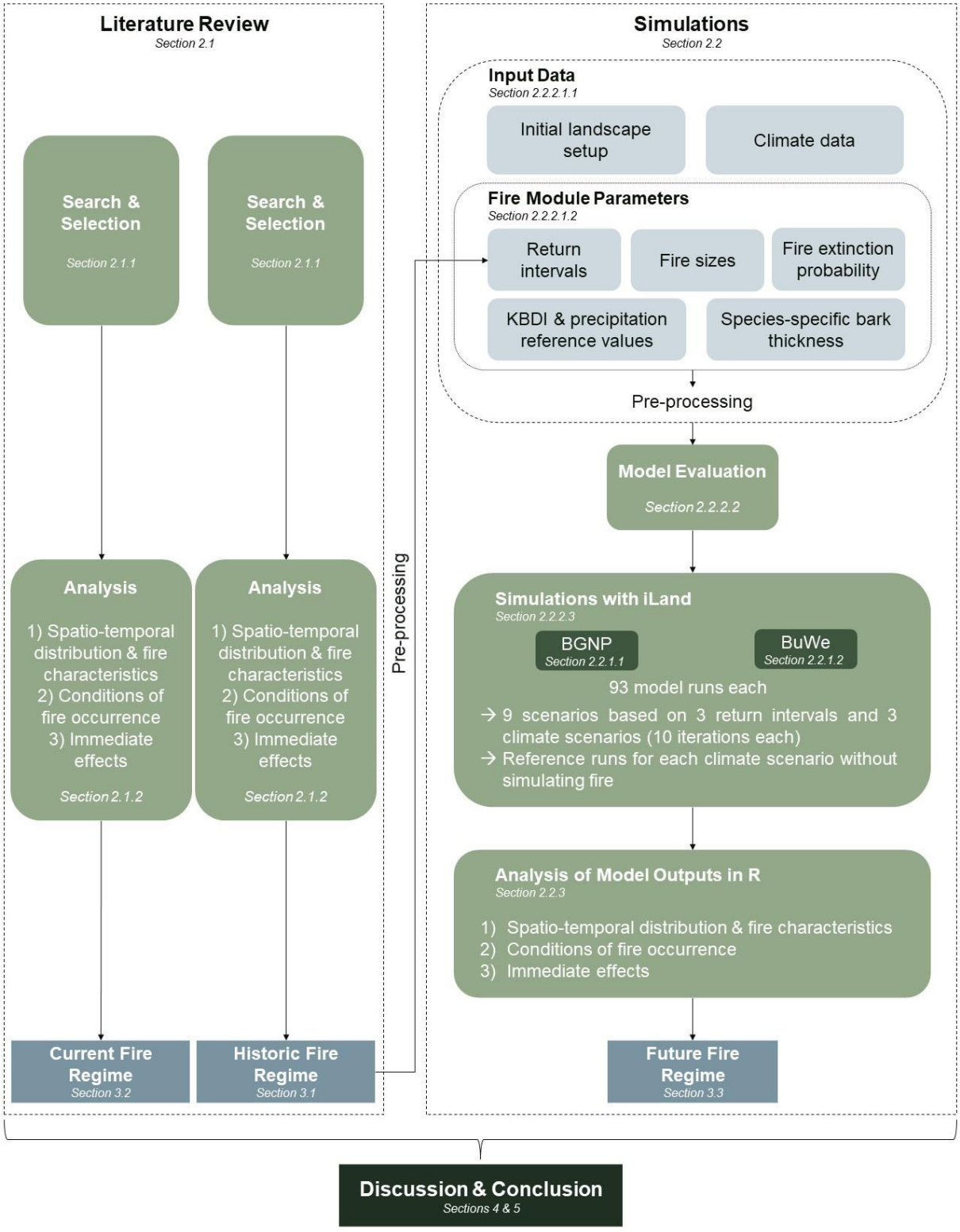

Figure 3: Flowchart illustrating the workflow of the present thesis.

2.1 Literature Review of the Historic and Current Fire Regimes

The literature review aimed at providing background information on current and historic fire regimes in Central Europe, with a focus on Germany and Austria, as well as relevant data for the parameterization of the fire module of iLand.

2.1.1 Literature Search and Selection

For the characterization of the current fire regimes, the databases Web of Science and Scopus as well as Google Scholar were used to find academic literature. Keywords for the search included “wildfires”, “fire regime”, “forest fires”, “fire frequency”, “fire intervals”, and “return intervals”, which were used in combination with terms like “Central Europe” or “European Alps” to limit the geographical focus of studies. Due to the small number of relevant results, databases and reports released by governmental institutions on the current forest fire occurrence at the European level, in Germany, and in Austria were consulted in addition to academic literature. However, data availability regarding the spatial and temporal distribution of wildfires was still quite limited and most data sources only provided aggregated data for a short timeframe and were often incomplete. One of the most comprehensive sources, which formed the basis of the assessment, was the WebGIS-based database operated by the University of Natural Resources and Life Sciences Vienna (Universität für Bodenkultur Wien (BOKU)), which provides information on around 5,000 forest fires in Austria since 1993 (including the type of fire, date, state and municipality, total burned area in m², cause of fire, and the number of fire departments and emergency personnel involved) (Institut für Waldbau, 2021). In addition, the German Federal Agency for Agriculture and Food (Bundesanstalt für Landwirtschaft und Ernährung, BLE) has published an annual report summarizing the number of fires and areas burned at the federal and state levels in Germany since 1991.

The previously mentioned scientific databases were also used to find academic literature for the characterization of the historic fire regimes. Additional keywords for the search included “fire history”, “charcoal”, and “paleoecology”. Only literature focusing on the Holocene, which stated specific fire return intervals for a location in the European Alps, was selected. Nine relevant studies with 42 return intervals for different time periods and regions were found in this search, an overview of which can be found in Table 1. All of these studies inferred fire frequency and return intervals from sedimentary charcoal remains (Blarquez et al., 2010; Blarquez & Carcaillet, 2010; Carcaillet, 1998; Carcaillet et al., 2009; Colombaroli et al., 2010; Genries et al., 2009; Kaltenrieder et al., 2010; Leys et al., 2014; Stähli et al., 2006).

Table 1: Overview of studies used to determine historic fire return intervals.

Study	Geographical Focus	Time Period	Number of Return Intervals
Blarquez and Carcaillet (2010)	Western Italian Alps (Lago Perso) and Northern French Alps (Lac du Loup)	8,000 - 0 BP	2
Blarquez et al. (2010)	Western Italian Alps (Lago Perso)	8,000 - 0 BP	3
Carcaillet (1998)	Northern French Alps (Aussois and Saint Michel)	6,750 - 210 BP	12
Carcaillet et al. (2009)	Northern French Alps (Lac du Loup, Lac du Thyl, & Lac du Lait)	9,000 - 0 BP	11
Colombaroli et al. (2010)	Central Swiss Alps (Gouille Rion)	10,000 - 0 BP	2
Genries et al. (2009)	Northern French Alps (Lac du Thyl)	9,000 - 5,500 BP	2
Kaltenrieder et al. (2010)	Southern Italian Alps (Euganean Hills)	16,500 – 0 BP	1
Leys et al. (2014)	Dolomites (Lago di Colbricon Inferiore)	12,000 – 0 BP	6
Stähli et al. (2006)	Switzerland (Swiss National Park)	6,000 BC - 1,000 AD	3

2.1.2 Theoretical Framework

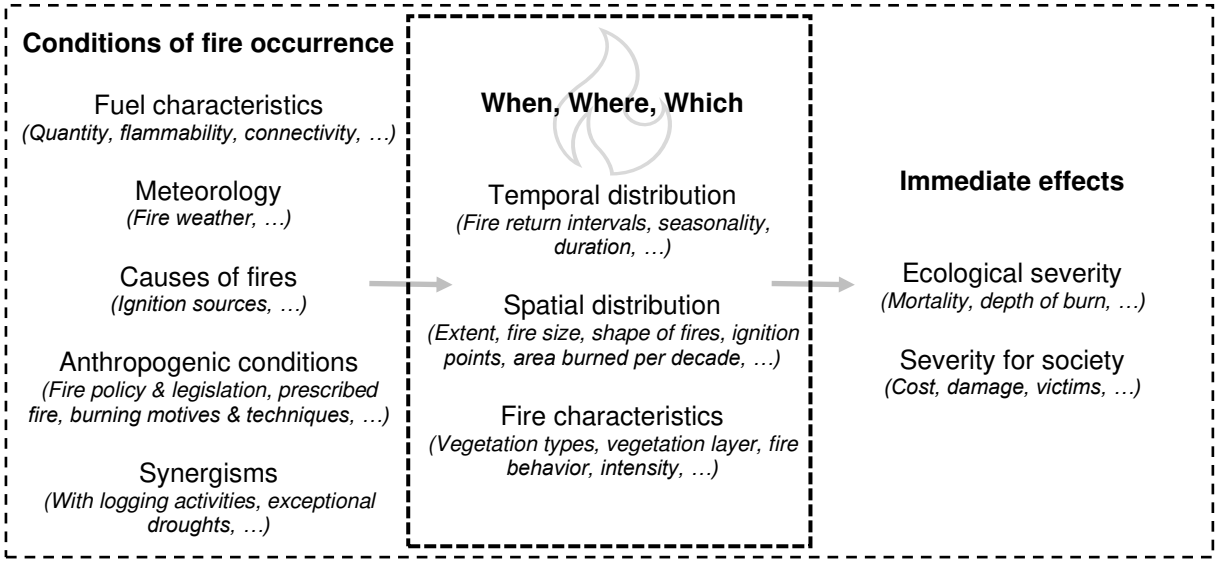

Figure 4: Theoretical framework to characterize fire regimes (Adapted from Krebs et al. (2010)).

There is currently no established definition for the term fire regime, which is why it often serves as an umbrella term for a set of differing parameters. This thesis followed the concept proposed by Krebs et al. (2010), according to which a fire regime, in the narrowest sense, is

characterized by the temporal and spatial distribution of fires as well as by fire characteristics. In addition, in a broader sense, the conditions of fire occurrence and immediate social and ecological effects can also be used to define the fire regime (see Figure 4) (Krebs et al., 2010). Due to the limited data availability, not all aspects could be covered extensively in the analysis.

2.2 Simulations with iLand

2.2.1 Study Areas

Among the Central European study areas of the Chair of Ecosystem Dynamics, the BGNP and BuWe (see Figure 5 below) were chosen for this master thesis because they represent different climatic conditions in Central Europe, whose fire regimes are expected to be affected differently by climate change. This ensured that the results of this master thesis are transferable to larger parts of Central Europe.

Figure 5: Approximate location of the two study landscapes BGNP and BuWe in Central Europe (shown as red dots) (Basemap: Esri).

2.2.1.1 Berchtesgaden National Park

The BGNP in southeastern Bavaria was established in 1978 and covers an area of 20,808 ha. It is situated in a transitional zone between oceanic and continental climatic influences. The terrain and the considerable difference in altitude of about 2,000 m between the lowest and the highest point have significant effects on air masses, temperature, humidity but also on the radiation balance. Therefore, a typical mountain climate with a high spatial and temporal variability prevails. The altitude-dependent annual mean temperatures range from +7 °C to -2 °C and the average annual precipitation from 1,500 to 2,600 mm (Nationalparkverwaltung Berchtesgarden, 2001). This climatic variation also results in natural altitude-dependent vegetation stages (Nationalparkverwaltung Berchtesgarden, 2001). The timberline is located

above 2,000 m above sea level and approximately 8,645 ha are covered by forests (Thom et al., 2022). Originally, the lower altitude areas were dominated by submontane mixed beech forests while spruce-fir-beech forests were found in montane areas. However, due to past use, the composition became more coniferous in many areas (Nationalparkverwaltung Berchtesgarden, 2001). Today, the most common tree species at mid-high elevations (as well as across the entire landscape) is Norway spruce (*Picea abies*) while silver fir (*Abies alba*) and European beech (*Fagus sylvatica*) are predominant at lower elevations. The higher altitudes are dominated by Dwarf mountain pine (*Pinus mugo*), European Larch (*Larix decidua*), or Swiss stone pines (*Pinus cembra*). Today, the core zone of the BGNP comprises more than 60% of the total area and is completely excluded from any human interventions. In the remaining management zone, only restoration and preventive measures are carried out (Thom et al., 2022). Figure 6 below shows the current composition of the landscape as configured in iLand.

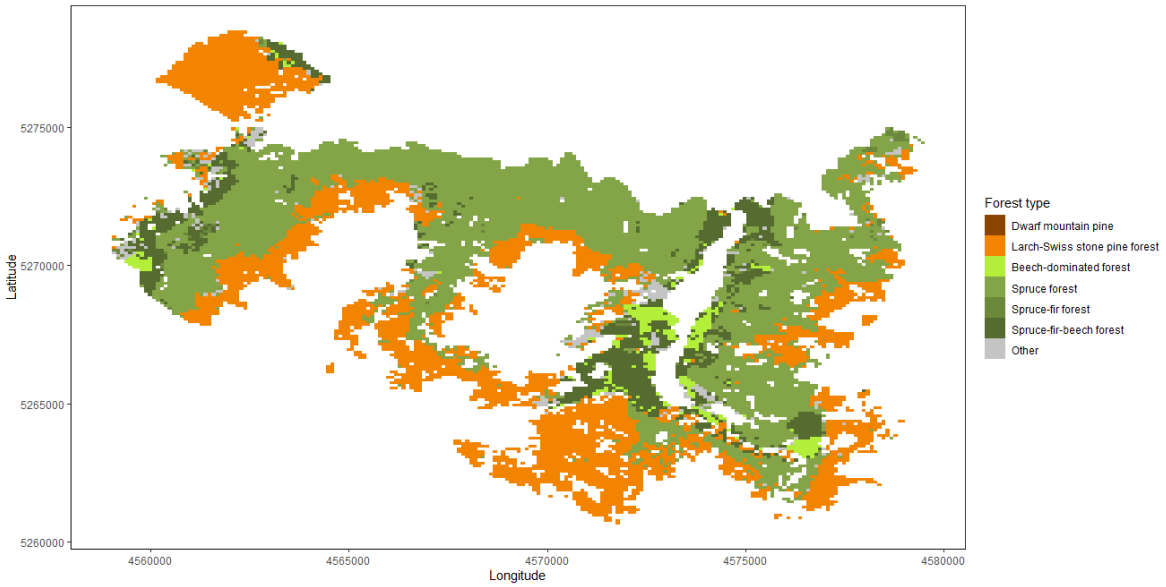

Figure 6: Initial vegetation composition of the BGNP (Forest type classification based on Thom et al. (2022)'s approach).

2.2.1.2 Bucklige Welt

The BuWe is located in the eastern Austrian lowlands and covers a total area of about 9,180 ha at altitudes ranging from 270 to 735 m above sea level, of which about 6,700 ha are forested areas. The climate of the study area is warm, subcontinental-Pannonian. In the reference period of 1981 – 2010, the annual average temperatures ranged from 7.9 to 9.6 °C and the annual precipitation from 640 to 940 mm, with lower temperatures and more precipitation at higher altitudes. The forests of the landscape are dominated by Norway spruce (*Picea abies*), which was commonly planted in pure stands in the past, so that its share in the total stand is about 45% today (Honkaniemi et al., 2020). Figure 7 below shows the current vegetation composition of the BuWe as configured in iLand.

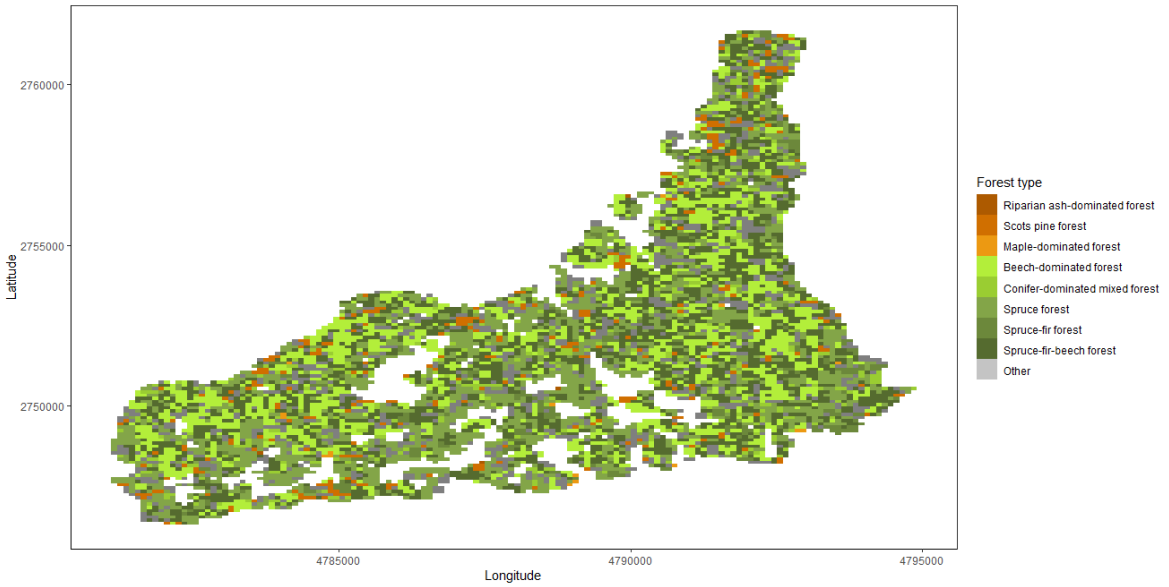

Figure 7: Initial vegetation composition of the BuWe (Forest type classification based on Thom et al. (2022)'s approach).

2.2.2 iLand Fire Module

iLand is a process-based model that simulates forest ecosystem dynamics at the landscape level, which was developed by members of the Chair of Ecosystem Dynamics and Forest Management at TUM. It simulates competition, growth, mortality, and regeneration of individual trees and takes climatic conditions, disturbances, and forest management into account (Seidl et al., 2012). In this context, the availability of resources such as light, water, and nutrients is determined at the level of so-called resource units (RU) with a default size of 100 m x 100 m (Seidl et al., 2012). For an extensive description of the model see Seidl et al. (2012) or Seidl and Rammer (2021) for the technical documentation.

iLand also includes a spatially explicit forest fire module, which was initially developed for simulations of wildfire regimes in the United States (Seidl, Rammer, & Spies, 2014) and has not yet been applied to European landscapes. Wildfires are dynamically simulated at 20 m x 20 m resolution by the module based on historical fire occurrence and burned area, available fuel load (namely surface litter and fallen coarse wood, but not including live fuels and dead canopy fuels), and fire weather based on the prevailing drought conditions determined via the Keetch-Byram Drought Index (KBDI) (Seidl, Rammer, & Spies, 2014). The key processes involved in determining fire ignition, spread, extent, and effects as well as relevant impacts on carbon pools and flows are briefly described below. For an extensive description, see Seidl, Rammer, and Spies (2014).

Fire ignition. Since fire ignition largely depends on the availability of sufficient fuel, more than 0.05 kg of fuel biomass per square meter are required to ignite a given cell. The base

probability of fire ignition ($P_{base\ ignition}$, Eq. 1) is determined as the inverse of the historic fire return interval ($MFRI_i$) and adjusted by the proportion of the area of the cell ($area_j$) relative to the site-specific average fire size ($size_i$) (Seidl, Rammer, & Spies, 2014).

$$P_{base\ ignition} = \frac{1}{MFRI_i} \times \frac{area_j}{size_i} \quad \text{(Eq. 1)}$$

The odds of ignition ($odds_{ignition}$, Eq. 2) are then further modified to account for fire weather (the KBDI) and fire suppression (r_{mgmt})[3]. The KBDI reflects the fuel layer moisture deficit with respect to an assumed maximum storage capacity of 203 mm (in 1/100 inch), where a value of zero represents no drought and the maximum value of 800 represents severe drought (Keetch & Byram, 1968; Seidl, Rammer, & Spies, 2014). This value is adjusted daily at RU level for any precipitation that has occurred and reached the fuel layer (i.e. excluding interception losses; *dP*, Eq. 2) as well as for a drought factor (*dQ*, Eq. 2; Keetch & Byram, 1968; Seidl, Rammer, & Spies, 2014). The latter is determined based on the daily maximum temperature (T_{max}, Eq. 3) and the mean annual precipitation (*MAP*, Eq. 3) of the landscape, but is set to zero in case of snow cover or a daily maximum temperature of less than 10 °C (Keetch & Byram, 1968; Seidl, Rammer, & Spies, 2014).

$$KBDI_t = KBDI_{t-1} + dQ - \frac{dP}{25.4} \times 100 \quad \text{(Eq. 2)}$$

with the daily drought factor *dQ* computed as (Eq. 3)

$$\mathrm{dQ} = 10^{-3} \times \left(800 - \left(\mathrm{KBDI}_{t-1} - \frac{dP}{25.4} \times 100\right)\right) \times \frac{0.9676 \times e^{0.0486 \times \left(T_{max} \times \frac{9}{5} + 32\right) - 8.299}}{1 + 10.88 \times e^{-0.0441 \times \frac{MAP}{25.4}}}$$

In iLand, a relative annual fire weather index of each RU (*rcKBDI*, Eq. 4) is calculated as the ratio of the cumulative annual sum over the daily KBDI values to its maximum value (i.e., 365 days with a KBDI of 800), thereby also capturing changes in the length of the fire season, which would not be the case when determining an average value over a given fire period. The ratio of this annual indicator to a previously determined historic reference value ($rcKBDI_{ref}$, Eq. 4), which reflects the fuel moisture conditions of the historic fire regime, is then used to adjust the odds of ignition (Seidl, Rammer, & Spies, 2014).

$$odds_{ignition} = odds_{base\ ignition} \times \frac{rcKBDI}{rcKBDI_{ref}} \times \frac{1}{r_{mgmt}} \quad \text{(Eq. 4)}$$

[3] Fire suppression was not considered in the present study and therefore not further elaborated here; for a description of the approach, see Seidl, Rammer, and Spies (2014).

with

$$odds_{base\ ignition} = \frac{P_{base\ ignition}}{1 - P_{base\ ignition}}$$

Ultimately, a uniform random number between 0 and 1 is drawn, whereupon a fire ignites in a given cell if the drawn number is less than or equal to the probability of ignition (Seidl, Rammer, & Spies, 2014).

Fire size and spread. Using a cellular automaton approach, fire spreads dynamically across the simulation landscape after ignition. The probability of fire spreading to any of the eight adjacent cells is again dependent on sufficient fuel load but also wind and slope (Seidl, Rammer, & Spies, 2014). Wind is modeled independently for each fire, with a varying direction of ±45° for every fire and speed randomly selected from a previously defined range. Slopes are determined based on a digital elevation model (DEM) of the simulation landscape (Seidl, Rammer, & Spies, 2014). Transition probabilities can also be further modified to reflect lower spread rates of a land type if necessary (see Seidl, Rammer, and Spies (2014)). Actual fire spread from a cell is again ultimately decided by a uniform random number. In addition, a fire also goes out with a predefined extinguishing probability before spreading further (Seidl, Rammer, & Spies, 2014). Fire spread stops either when no further spread is possible (e.g., due to fuel limitation) or when the predefined minimum fire size is reached (see below).

To determine the extent of individual fires, a maximum potential fire size is drawn from a negative exponential distribution matched to the historical fire regime and individual fire sizes (*fsize*, Eq. 5) between the minimum and maximum size are stochastically established based on the previously specified mean fire size ($fsize_{mean}$, Eq. 5) and a uniform random number (*rnd*, Eq. 5) (Seidl, Rammer, & Spies, 2014).

$$fsize = -\ln(rnd) \times fsize_{mean} \quad \text{(Eq. 5)}$$

Fire severity. In simulating fire severity, the iLand fire module considers the effects of fuel availability and moisture (again based on the KBDI) as well as tree size- and species-specific resilience (Seidl, Rammer, & Spies, 2014). The availability and structure of fuels are approximated by the detritus pools simulated by the model. The pools are differentiated according to their drying rates, with fast-drying fuels such as dead leaves and twigs in the litter pool and slower-drying fuels such as larger branches and logs in the downed woody debris pool. The fuel available in each pool is determined by its respective moisture conditions (Seidl, Rammer, & Spies, 2014).

The proportion of crown kill (i.e., tree mortality) during a fire is related to the size of the affected trees, their crown shape, and the scorch height, which is estimated using available fuel as a proxy for fire intensity (Seidl, Rammer, & Spies, 2014). Equation 6 is used to determine individual tree mortality probability (P_{mort}) from a wildfire event, where *bt* is the tree's bark thickness (cm) and *ck* is the proportion of crown kill. The absolute bark thickness is calculated from the species-specific parameter *barkThickness*, which corresponds to the relative proportion of bark in the tree diameter at breast height (Seidl, Rammer, & Spies, 2014).

$$P_{mort} = \frac{1}{1 + e^{-1.466 + 1.91 \times bt - 0.1775 \times bt \times bt - 5.41 \times ck \times ck}} \quad \text{(Eq. 6)}$$

On the other hand, all saplings affected by fire die. When a tree is killed during a fire, the foliage, branch, and stem pools are adjusted based on respective consumption rates, and any remaining carbon is absorbed into the standing and dead detritus pools. However, for sapling layer trees, it is added to the litter pool. Within the fire perimeter, it is also assumed that a small amount of soil organic matter will be lost because of erosion and that seeds will not be able to establish in the same year of a fire (Seidl, Rammer, & Spies, 2014).

Carbon flows. Gross primary production (*GPP*) in iLand is derived monthly at RU-level based on a radiation use efficiency approach as the product of utilizable photosynthetic active radiation and effective radiation use efficiency (Seidl et al., 2012). The approach accounts for radiation interception by individual trees based on their leaf area, position in the canopy, and radiation use strategy, and thus for competition between trees, as well as different environmental influences on individual species. The decreasing productivity potential of individual trees with increasing age is also considered by including the current age and height relative to the respective maxima of each species (see Seidl et al. (2012) for more details).

Net primary production (*NPP*, Eq. 7) is derived from the GPP in a simplified manner, assuming a constant proportion of autotrophic respiration (*Ra*, Eq. 7) (Seidl et al., 2012).

$$NPP = GPP \times Ra \quad \text{(Eq. 7)}$$

Net ecosystem productivity (*NEP*, Eq. 8) is finally calculated from NPP by subtracting the absolute amounts of heterotrophic respiration (*Rh*, Eq. 8), disturbance losses, and, if relevant, management losses (Seidl et al., 2012).

$$NEP = NPP - Rh - disturbance\ losses - management\ losses \quad \text{(Eq. 8)}$$

2.2.2.1 Parameterization

2.2.2.1.1 Initial Landscape Setup and Climate Data

The initial state of the vegetation of both landscapes had already been configured for earlier studies and was kept unchanged for the present thesis. Similarly, this study also used the same climate data for the climate change scenarios under RCP4.5 and RCP8.5 forcing (see Table 2 for details). All details on the parametrization of these sections of the model can be found in Thom et al. (2022) for the BGNP and Honkaniemi et al. (2020) for the BuWe. Only the changes in temperatures and precipitation under the climate change scenarios as well as the parameters for the additional parametrization of the fire module will be described in the following.

Table 2: Overview of the GCM-RCM combinations from which the climate model data were obtained (Honkaniemi et al., 2020; Thom et al., 2022).

Study Area	Climate Scenario	Climate Model Data (GCM-RCM Combinations)
BGNP	RCP4.5	ICHEC-EC-EARTH_r12i1p1 and CLMcom-CCLM4-8-17 ICHEC-EC-EARTH_r12i1p1 and KNMI-RACMO22E ICHEC-EC-EARTH_r12i1p1 and SMHI-RCA4 ICHEC-EC-EARTH_r12i1p1 and KNMI-RACMO22E MPI-M-MPI-ESM-LR_r1i1p1 and CLMcom-CCLM4-8-17 MPI-M-MPI-ESM-LR_r1i1p1 and SMHI-RCA4
	RCP8.5	ICHEC-EC-EARTH_r12i1p1 and CLMcom-CCLM4-8-17 ICHEC-EC-EARTH_r12i1p1 and KNMI-RAQMO22E ICHEC-EC-EARTH_r12i1p1 and SMHI-RCA4 ICHEC-EC-EARTH_r12i1p1 and KNMI-RACMO22E MIROC-MIROC5_r1i1p1 and CLMcom-CCLM4-8-17 MOHC-HadGEM2-ES_r1i1p1 and UHOH-WRF361H MPI-M-MPI-ESM-LR_r1i1p1 and CLMcom-CCLM4-8-17 MPI-M-MPI-ESM-LR_r1i1p1 and SMHI-RCA4 MPI-M-MPI-ESM-LR_r1i1p1 and UHOH-WRF361H
BuWe	RCP4.5	EC-EARTH and KNMI-RACMO22E
	RCP8.5	EC-EARTH and KNMI-RACMO22E IPSL-CM5A-MR and IPSL-INERISWRF331F HadGEM2-ES and CLMcom-CCLM4-8-17

As shown in Figure 8 below, both annual precipitation sums (solid lines) and summer precipitation in the months of June, July, and August (dashed lines) remain relatively constant in both landscapes and all climate scenarios until the end of the century. In contrast, there is an increase in minimum and maximum temperatures in both landscapes, especially in the second half of the century, which is stronger in the RCP8.5 than in the RCP4.5 scenario (see Figure 9). With regard to summer temperatures, this trend is even more pronounced in the BGNP, but less so in the BuWe. Despite the stronger increase in temperatures in the BGNP,

the maximum temperatures in the BuWe remain significantly higher than those in the BGNP in all scenarios until the end of the century.

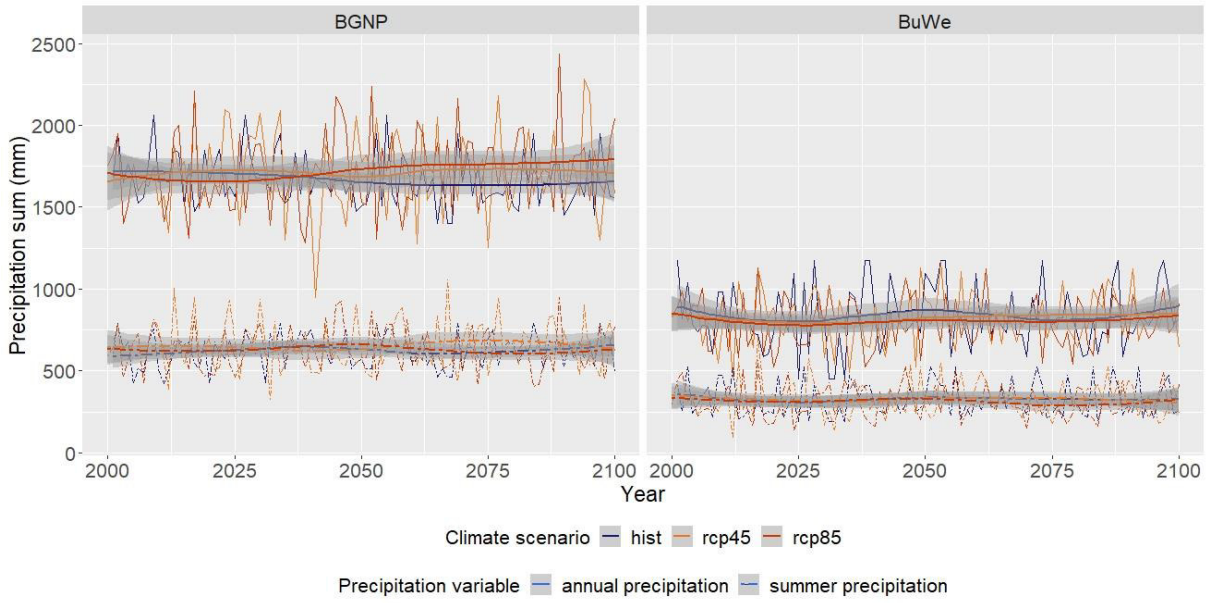

Figure 8: Development of average annual and summer precipitation sums across the BGNP (first column) and BuWe (second column) landscapes under the different climate scenarios. Solid lines show annual precipitation sums while dash-dotted lines represent summer precipitation sums in the months June, July, and August.

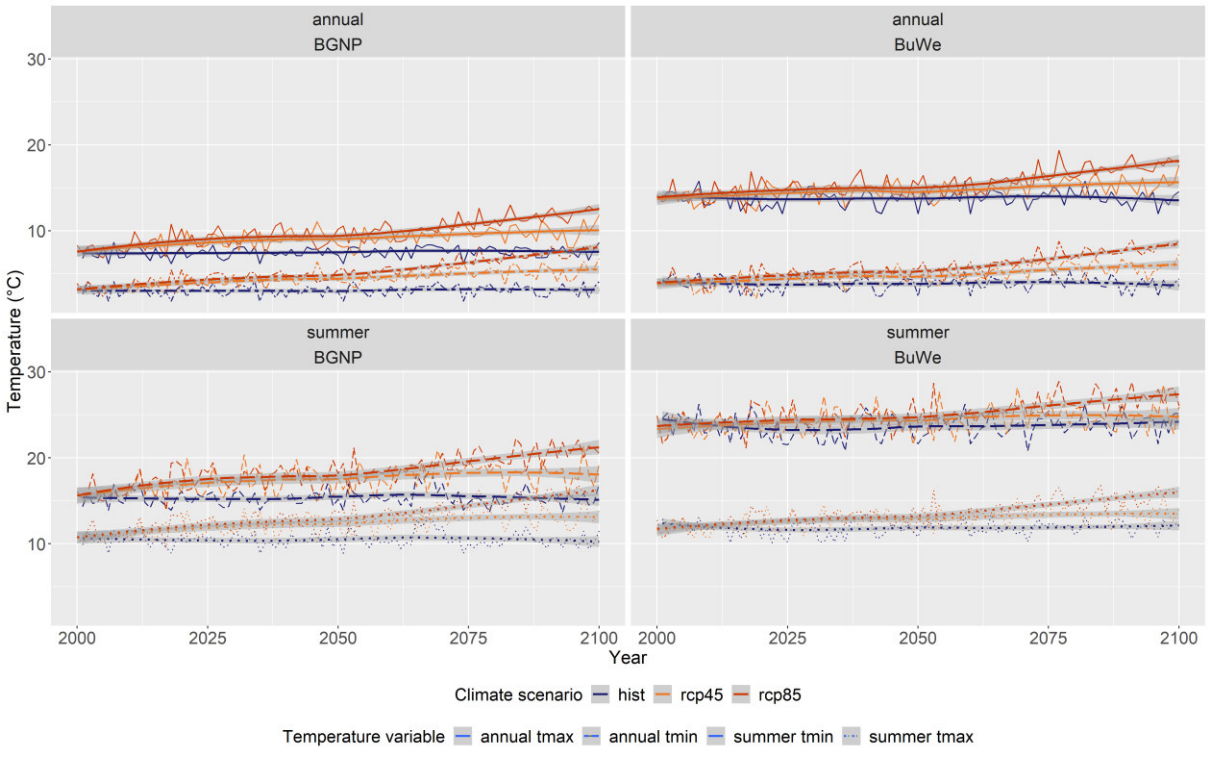

Figure 9: Development of average annual (first line) and summer (second line) minimum and maximum temperatures across the BGNP (first column) and BuWe (second column) landscapes under the different climate scenarios. Annual minimum (dash-dotted lines) and maximum (solid lines) temperatures are shown in the first line, while the second line displays the minimum (dotted lines) and maximum (dashed lines) summer temperatures in the months of June, July, and August.

2.2.2.1.1 Fire Module Parameters

The parameters of the iLand fire module and the selected values for the present thesis are summarized in Table 3 below. The most essential parameters used to characterize the initial fire regime of the study areas are the fire return intervals as well as the minimum, mean, and maximum fire sizes. The fire return intervals were determined from the nine studies previously summarized in Table 1. The assumption was made that the mean return interval across all locations is transferable to the two study areas. However, to better cover the wide range of intervals and to appropriately address the associated large uncertainty, simulations were also run with the lowest and highest of the 42 values.

Table 3: Overview of the fire module parameters.

	Parameter Key	Description	Unit	Value(s)	Source
Fire ignition	*fireReturnInterval*	Average number of years between two fires affecting a single pixel.	years	min 124 mean 534 max 1,520	Blarquez et al. (2010), Blarquez and Carcaillet (2010), Carcaillet (1998), Carcaillet et al. (2009), Colombaroli et al. (2010), Genries et al. (2009), Kaltenrieder et al. (2010), Leys et al. (2014), Stähli et al. (2006)
	rFireSuppression	Scalar for fire suppression.		1	Default value
Fire spread	*averageFireSize*	Average fire size.	m^2	235,009	Senf and Seidl (2021)
	minFireSize	Minimum fire size.	m^2	11,700	Senf and Seidl (2021)
	maxFireSize	Maximum fire size.	m^2	2,773,800	Senf and Seidl (2021)
	rLand	Multiplier for the fire spread probability. If below 1 (or 100%), fire spreads with a reduced probability.	%	100	Default value
	FireExtinctionProbability	Probability that a fire on a burning pixel will go out without spreading further.	%	34	Hansen et al. (2020), validated through testing
Fuel	*fuelKFC1*	Parameter kfC1 for calculation of fuel amount using compartment specific moisture relations.		0.75	Default value (outdated)[4]
	fuelKFC2	Parameter kfC2 for calculation of fuel amount using compartment specific moisture relations.		0.75	Default value (outdated)[4]

[4] In the provided templates of the project files, wrong values were given for the three fuel parameters.

	fuelKFC3	Parameter kfC3 for calculation of fuel amount using compartment specific moisture relations.		0.75	Default value (outdated)[4]
Wind	*speedMin*	Minimum wind speed.	m/s	10	This study
	speedMax	Maximum wind speed. The wind speed is randomly selected between the minimum and maximum for each fire event.	m/s	20	This study
	direction	Main wind direction (in degrees). North=0, East=90, South=180, West=270. For each fire event the wind direction is calculated as direction +- 45°.	m/s	270	This study
Mortality	*crownKill1*	Parameter kCK1 to calculate fraction of crown kill.	%	0.21111	Default value
	crownKill2	Parameter kCK2 to calculate fraction of crown kill.	%	-0.00445	Default value
	crownKillDbh	Dbh-threshold (dbh_thres) used in crown kill calculations.	cm	40	Default value
	burnSOMFraction	Fraction of SOM biomass that is assumed to be lost by a fire.	%	2	Hansen et al. (2020)
	burnStemFraction	Fraction of stem biomass of died trees that is combusted.	%	11	Hansen et al. (2020)
	burnBranchFraction	Fraction of branch biomass of died trees that is combusted.	%	51	Hansen et al. (2020)
	burnFoliageFraction	Fraction of foliage biomass of died trees that is combusted.	%	90	Hansen et al. (2020)

The minimum, mean, and maximum fire sizes were calculated from Senf and Seidl (2021)'s dataset covering forest disturbance events in Europe. With regard to the fire extinction probability, values from previous studies focusing on different study areas in the United States were obtained and tested for the best reproduction of the historical return interval and realistic fire shapes, whereupon the value of 0.34 based on a study by Hansen et al. (2020) was chosen. For all other parameters, either the default value or a predetermined value was used.

Additional parameters relevant for the simulation of wildfires in iLand are site and RU-specific reference values for the KBDI index and the mean annual precipitation. Annual values for both parameters were first simulated in iLand based on historical climate data from 1981 - 2010 for each RU in each landscape and then averaged to determine one historic reference value for each parameter and RU. In addition, bark thickness parameters had not been determined for the European tree species configured in iLand. They were calculated based on the Schönbrunn bark removal table (Schönbrunner Rindenabzugstabelle (WaldSchweiz, 2021)) as averages across all diameters to represent the entire life cycle and can be found in Table 4.

Table 4: Mean bark thickness as the proportion of the diameter at breast height of all European tree species configured in iLand (based on WaldSchweiz (2021)).

Short name	Name	Bark thickness
piab	Picea abies	0.102
abal	Abies alba	0.125
lade	Larix decidua	0.216
pisy	Pinus sylvestris	0.107
fasy	Fagus sylvatica	0.072
quro	Quercus robur	0.167
acps	Acer pseudoplatanus	0.094
frex	Fraxinus excelsior	0.128
cabe	Carpinus betulus	0.072
bepe	Betula pendula	0.128
alin	Alnus incana	0.094
qupe	Quercus petraea	0.167
psme	Pseudotsuga menzisii	0.129
algl	Alnus glutinosa	0.094
casa	Castanea sativa	0.094
pini	Pinus nigra	0.107
acca	Acer campestre	0.094
acpl	Acer platanoides	0.094
qupu	Quercus pubescence	0.167
pice	Pinus cembra	0.107
soau	Sorbus aucuparia	0.072
soar	Sorbus aria	0.072
coav	Corylus avellana	0.128
alvi	Alnus viridis	0.094
potr	Populus tremula	0.167
poni	Populus nigra	0.167
tico	Tilia cordata	0.128
tipl	Tilia platyphyllos	0.128
ulgl	Ulmus glabra	0.128
saca	Salix caprea	0.094
rops	Robinia pseudoacacia	0.167
pimu	Pinus mugo	0.107

2.2.2.2 Model Validation

Before starting the simulations, the model's ability to reproduce the return intervals was evaluated based on 300-year simulations in iLand with the historic climate data of both landscapes. For this purpose, the simulated return intervals were calculated based on the burned area modeled by iLand, with the interval corresponding to the number of years that passed until the cumulative annual burned area equaled the total forested area of the respective study area. During the evaluation, it became clear that the fire module overestimated the forest area in the BGNP by about 1,000 ha. The reason for this mismatch is that in recent European iLand studies, not all RUs are considered to be fully stockable. Consequently, the iLand fire module was updated to incorporate also only partially stockable cells. However, an adjusted value of 9,500 ha instead of 8,645 ha was still used in calculations for BGNP where the total forest area played a role. Taking these corrections into account, the model's reproduction of the given return intervals was satisfactory. In addition, the severity of the simulated fires was analyzed, showing sufficient agreement with the results of Dupire et al. (2019) on the mortality of forests with different compositions and in biogeographic zones.

2.2.2.3 Simulation Design

All simulated scenarios, which are summarized in Table 5 below, were based on the current landscape composition of the two study areas and simulated for the entire 21st century.

Table 5: Overview of all simulated scenarios.

Study Area	Fire Return Interval	Climate Scenario	Scenario
BGNP	124	Historical	*BGNP-124-HIST*
		RCP4.5	*BGNP-124-RCP45*
		RCP8.5	*BGNP-124-RCP85*
	534	Historical	*BGNP-534-HIST*
		RCP4.5	*BGNP-534-RCP45*
		RCP8.5	*BGNP-534-RCP85*
	1,520	Historical	*BGNP-1520-HIST*
		RCP4.5	*BGNP-1520-RCP45*
		RCP8.5	*BGNP-1520-RCP85*
BuWe	124	Historical	*BuWe-124-HIST*
		RCP4.5	*BuWe-124-RCP45*
		RCP8.5	*BuWe-124-RCP85*
	534	Historical	*BuWe-534-HIST*
		RCP4.5	*BuWe-534-RCP45*
		RCP8.5	*BuWe-534-RCP85*
	1,520	Historical	*BuWe-1520-HIST*
		RCP4.5	*BuWe-1520-RCP45*
		RCP8.5	*BuWe-1520-RCP85*

Management activities in the BuWe were not included in the simulations so that the fire intervals could be simulated without potential interference from human activities and to ensure better comparability of the two study areas. Thus, the simulated scenarios differed only in terms of the fire return intervals and climatic conditions. For both study areas, a baseline scenario with historical climate conditions (corresponding to the years 1981 – 2010) and two climate scenarios, the intermediate RCP4.5 and the high emissions RCP8.5 scenario, were simulated for the three different fire return intervals listed before in Table 4. Each of the nine scenarios for each landscape was simulated 10 times to account for the stochasticity of the processes. In addition, a reference simulation without any fire occurrence was run for both landscapes and all three climate scenarios. Thus, 186 model runs were performed in total.

2.2.3 Analysis of Model Outputs

In general, the analysis of all model outputs followed a similar process: outputs were first read into the R environment (R Core Team, 2020) using either the package *RSQLite* (K. Müller et al., 2021) or *raster* (Hijmans, 2022) depending on the file format, where they were then filtered for relevant variables, organized and aggregated by scenario, and analyzed with the R package *tidyverse* (Wickham, 2021). The packages *ggplot2* (Wickham et al., 2021), *gghighlight* (Yutani, 2021), *ggpubr* (Kassambara, 2020), and *RColorBrewer* (Neuwirth, 2014) were utilized to visualize results.

To answer the third research question, variables were analyzed in the three areas "spatio-temporal distribution and fire characteristics", "conditions of fire occurrence" as well as "immediate effects" (see section 2.1.2), mainly focusing on the averages over the ten iterations per scenario to achieve more robust results. The period to which the analyses refer is always indicated, but in most cases, it corresponded to either to the simulation years 20 – 100 (also referred to as future period) or the years 80 – 100 (referred to as EOC period). To ensure comparability between landscapes, values relative to each site's baseline scenario with historic climate conditions but also relative to other site-specific characteristics, such as the total forested area, were determined where necessary.

The first section focused mainly on analyzing the "fire" output of iLand, more precisely the annual number of fires and annual burned area extent (mostly relative to the total landscape area). To determine whether differences in the annual number of fires and the annual burned area extent between the climate change scenarios and the baseline scenario were statistically significant, the two-sided, paired Wilcoxon test (Wilcoxon, 1945) was employed using the base R function *wilcox.test().* It is a non-parametric test, i.e., not requiring a normal distribution of the data, and was chosen after not-normal distributions of the data were confirmed using a

Shapiro-Wilk normality test (Royston, 1982). To then assess if the annual number of fires and burned area followed a certain trend over the simulation period, Mann-Kendall (MK) (Kendall, 1975; Mann, 1945) and Sen's Slope tests (Sen, 1968) were employed using the *Kendall* (McLeod, 2011) and *trend* (Pohlert, 2020) R packages, respectively. The statistical MK test is commonly used to detect trends in climatic or hydrologic time series (Hamed & Ramachandra Rao, 1998) but has also been used to analyze fire regimes (e.g. Jiménez-Ruano et al., 2017; Salguero et al., 2020). It is also a non-parametric test and operates based on the null hypothesis that no trend exists in a given time series. The standard MK test requires the input data not to be serially autocorrelated (Hamed & Ramachandra Rao, 1998), which was confirmed also using the *Kendall* package. The significance level was defined at $\alpha = 0.05$. The MK tau values ranging from -1 to +1 indicate if the trend is negative or positive, with larger values reflecting more consistent trends (Kendall, 1975; Mann, 1945). The Sen's Slope test, on the other hand, indicates the magnitude of a trend (Sen, 1968). It was used to further define the previously identified significant trends at a 95% confidence interval.

Future return intervals were calculated based on the mean annual burned area extent, the same way as during the model evaluation. They were then put in relation to the simulated historical interval in each scenario to account for the deviations between the simulated intervals and the input intervals. Lastly, the annual number of fires per RU in each study landscape and iteration were extracted from iLand in raster files but spatial patterns were analyzed only for the minimum return intervals since clusters were more obvious due to the greater number of fires compared to the longer intervals.

The second part of the analysis focused on anomalies in fuel moisture conditions under the climate change scenarios, as represented by the KBDI as well as causes of these anomalies. First, the average annual KBDI of each RU in the simulation years 80 – 100 was determined and then put in relation to the RU's historical reference KBDI. In addition, the deviation of the number of snow cover days during the same period from historical conditions was determined, since these have a significant influence on the fuel moisture conditions. The annual number of snow cover days is given in the iLand "water" output. Lastly, the relationship between the annual average KBDI at the landscape level and the number of fires in the same year was analyzed based on a scatterplot.

The third part of the analysis addressed post-fire tree mortality, resulting fire severity, and influences on carbon fluxes and storage. Mortality rates for each fire were calculated based on the number of trees that died during the fire relative to the total number of trees affected. Fire severity was classified as low if the mortality rate was below 30%, medium if it was between

30% and 80%, and high if it was above 80%. After the annual number of fires in each class and iteration was determined, an annual average was computed over the ten iterations.

Ultimately, the “carbon” and “carbonflow” outputs were analyzed with a focus on disturbance losses, NEP, and carbon pools to answer the third research question. Here, the focus was on quantifying the relationship between carbon losses caused by fire disturbances and NEP. Since a non-normal distribution of the data was determined with the Shapiro-Wilk normality test, the non-parametric Kendall's tau test was employed for the analysis, using the R basis function *cor.test()*.

3. Results

3.1 Historic Fire Regime

To date, knowledge of historic fire regimes in the study areas is very limited. However, historic forest fire occurrence in other parts of the Central European Alpine region has been researched more extensively, in some cases as far back as 16,500 years ago (see Table 1). A summary of these research findings will be presented below, assuming that these regime characteristics are also broadly transferable to the study areas.

3.1.1 Spatio-Temporal Distribution and Fire Characteristics

The historic temporal distribution of wildfires and resulting return intervals have been reconstructed from sedimentary charcoal remains for locations in the Northern French Alps, the Western, Southern, and Northern Italian Alps as well as the Swiss Alps (see Table 1 for more details). The range of these return intervals from 124 to 1,520 years is very wide (see Table 3) as they represent a variety of fire regimes due to the large reference time span and different study areas, and thus different climatic conditions, prevailing vegetation compositions, and varying influence of human activities. These conditions will be discussed in more detail in the following subsection. In addition to the temporal aspects, there were also small-scale spatial differences in the fire regimes of individual regions, with lower fire occurrence at higher elevations and on northern slopes (Carcaillet et al., 2009; Colombaroli et al., 2010). Stähli et al. (2006) also analyzed the fire regimes of different forest types, namely mountain pine forests, mixed forests, and Norway spruce forests. The frequency of fires in mountain pine forests was about 2.5 times higher than in Norway spruce and mixed forests. However, while they characterized fire intensity in their mountain pine-dominated study area as moderate, reflecting a mix of surface and crown fires, they assumed that individual fires were more severe in the Norway spruce forests (Stähli et al., 2006). The other studies did not provide information on the intensity of the fire regimes or specific return intervals for certain vegetation types.

3.1.2 Conditions of Fire Occurrence

There is agreement among the analyzed studies that natural fire regimes prevailed in the Alps during the early Holocene, driven mainly by climatic, vegetation and thus fuel conditions (Carcaillet, 1998; Carcaillet et al., 2009; Colombaroli et al., 2010; Kaltenrieder et al., 2010; Stähli et al., 2006). Typically, the first fires in the Alps occurred naturally a few decades or centuries after the original forestation, because woody vegetation was always necessary as fuel, regardless of climatic conditions (Leys et al., 2014). In general, however, the occurrence of forest fires was driven to a significant degree by the moisture content of the fuel, as this affected its flammability, but also its general availability, leading to an increased occurrence of fires under warm and dry conditions (Carcaillet, 1998; Colombaroli et al., 2010; Stähli et al.,

2006). In turn, Blarquez et al. (2010) found that the presence of these conditions over an extended period of time - nearly 3,000 years in the study – actually lead to a low incidence of fire because it inhibited the accumulation of fuel, while periods characterized by more precipitation resulted in a higher number of fires.

In addition, species richness (Blarquez et al., 2010) as well as the presence of certain key species (Blarquez & Carcaillet, 2010; Carcaillet, 1998; Carcaillet et al., 2009; Genries et al., 2009; Leys et al., 2014) promoted more intense fire regimes. Several of the studies identified *Pinus cembra* as a key species providing flammable biomass as fuel for wildfires so that forests dominated by this species were more likely to experience fires than those with a different vegetation composition (Blarquez & Carcaillet, 2010; Carcaillet et al., 2009; Genries et al., 2009). Similarly, *Pinus mugo* promoted wildfire spread through its high flammability and dense canopy, which may have also increased fuel connectivity across landscapes (Leys et al., 2014). Leys et al. (2014) estimated the influence of this tree species to be substantial enough to offset the fire-limiting effects of the wet climate in the Dolomites.

Locally, differences between fire regimes were also driven by topography, slope, and elevation (Carcaillet et al., 2009; Colombaroli et al., 2010). Independent of the presented drivers, the ignition of natural forest fires occurred mainly through lightning strikes (Carcaillet, 1998).

Several of the studies detected changes in the fire regimes that were most likely due to human activity starting in the Neolithic period around 8,000 years ago, which influenced not only vegetation composition due to the cultivation of certain plants but also local fire regimes directly (Carcaillet, 1998; Carcaillet et al., 2009; Colombaroli et al., 2010; Kaltenrieder et al., 2010; Leys et al., 2014; Stähli et al., 2006). While the human impact on fire regimes was negligible before (Stähli et al., 2006), fires were actively utilized as a means in agriculture to clear forested areas for the first time in this period (Carcaillet, 1998; Carcaillet et al., 2009; Kaltenrieder et al., 2010). Even though attributing changes in fire regimes to a specific cause, natural or human, is difficult when relying only on sedimentary reconstructions (Colombaroli et al., 2010), human activity was most likely the dominating factor influencing fire regimes in the European Alps throughout the late Holocene (Carcaillet et al., 2009; Leys et al., 2014). While several studies saw an intensification of the fire regime in response to land use on a temporary or longer-term basis (Colombaroli et al., 2010; Leys et al., 2014; Stähli et al., 2006), Stähli et al. (2006) recorded an overall decline in fire activity in the late compared to the early Holocene. Thus, the precise effect of human activity on the fire regime, i.e., whether an amplification or suppression occurred, differed between study sites.

3.1.3 Immediate Effects

While some of the studies considered wildfires an important factor influencing deforestation (Carcaillet, 1998) as well as vegetation dynamics in general (Colombaroli et al., 2010; Kaltenrieder et al., 2010) during the Holocene, Stähli et al. (2006) stated that the impact in the Alpine region is usually masked by other disturbance factors. Furthermore, the authors could not detect any change in tree composition, at least in the short term (Stähli et al., 2006), which is also in agreement with the findings of Leys et al. (2014) according to which subalpine mixed forests appeared to be tolerant in their composition to return intervals between 30 and 735 years. Likewise, Genries et al. (2009) concluded that fires favored the diversity and preserved the open structure of the dense subalpine forests of the Holocene. With respect to the impact of wildfires on individual species, there were substantial differences between the studies as well as between the study sites in individual studies, so that no general conclusions could be drawn. Only *Betula* appeared to benefit consistently from fires (Blarquez & Carcaillet, 2010; Genries et al., 2009).

3.2 Current Fire Regime

3.2.1 Spatio-Temporal Distribution and Fire Characteristics

On average, 144 fires occurred annually in Austria and 1,035 fires in Germany between 1993 and 2019. These fires resulted in a cumulative average annual burned area of 52 ha in Austria (Institut für Waldbau, 2022) and 656 ha in Germany (BLE 1995 – 2021; BMEL, 1994; Michael Lachmann, 2006 – 2010; Michaela Lachmann, 2011 – 2015). However, interannual variability can be large in both countries, as visible in Figure 10.

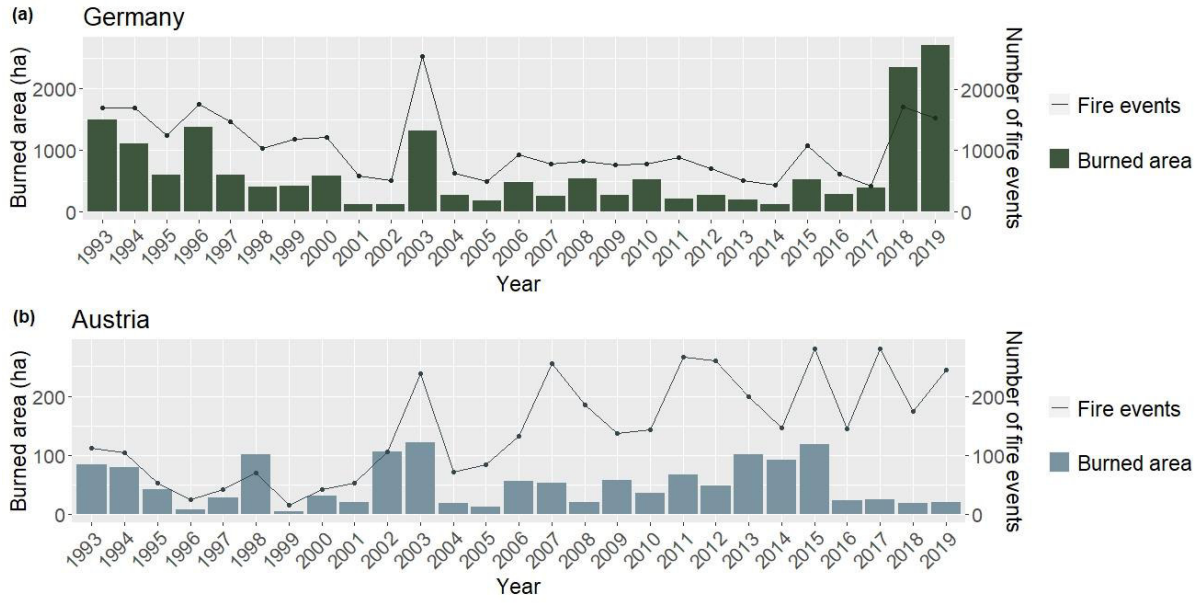

Figure 10: Annual number of fire events and cumulative burned area in ha from 1993 until 2019 in (a) Germany (BLE 1995 – 2021; BMEL, 1994; Michael Lachmann, 2006 – 2010; Michaela Lachmann, 2011 – 2015) and (b) Austria (Institut für Waldbau, 2022).

While an increasing trend in the number of fires in Austria can be observed since 1999, the cumulative annual burned area does not follow the same trend. The fire regime in Germany, on the other hand, is rather characterized by extreme years with otherwise relatively constant values. Not only interannual but also intra-annual variability of fire occurrence tends to be high in both countries. In the Central European Alps, two fire seasons can usually be observed throughout the year: the first in spring and the second in summer. The cause in both cases is drought; in spring due to frost and stable weather conditions, in summer due to high temperatures and low precipitation (M. Müller et al., 2020). Fire occurrence in Germany and Austria usually follows this trend, while peak values are normally reached in summer in Germany (BLE, 2021) and in April in Austria (San-Miguel-Ayanz et al., 2019). While the fire regimes of the entire countries reflect the fire regimes of the study landscapes only to a very limited extent, those of the states Bavaria and Burgenland should provide a better approximation.

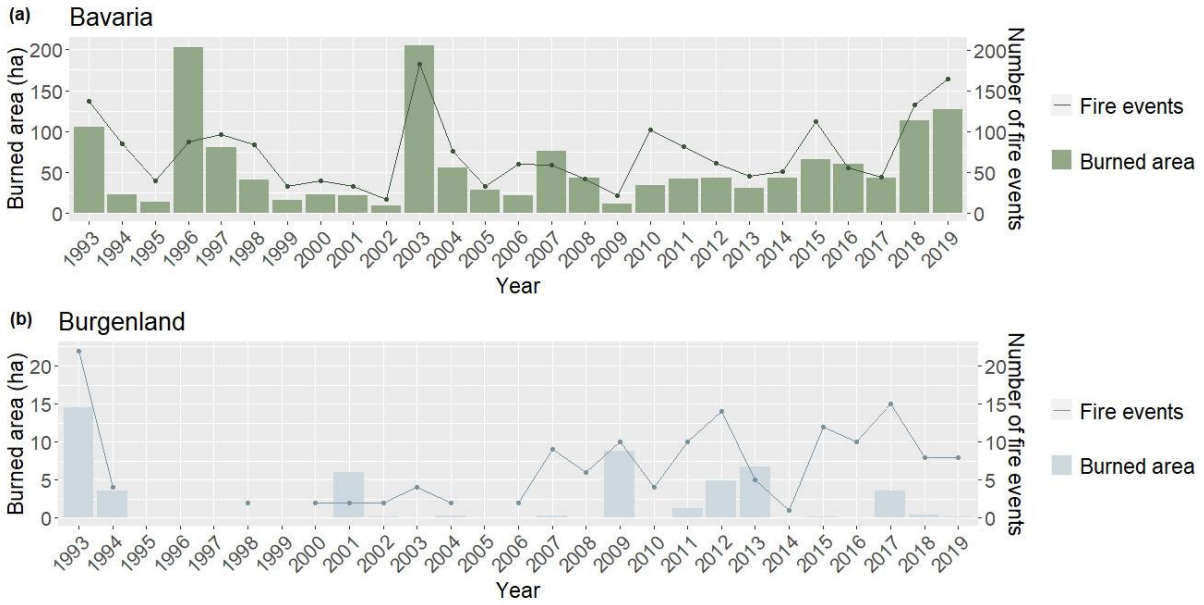

Figure 11: Annual number of fire events and cumulative burned area in ha from 1993 until 2019 in (a) Bavaria (BLE 1995 – 2021; BMEL, 1994; Michael Lachmann, 2006 – 2010; Michaela Lachmann, 2011 – 2015) and (b) Burgenland (Institut für Waldbau, 2021).

Bavaria's share of the annual number of forest fires in Germany ranged from 2 to 13% between 1993 and 2019, and its share of the total burned area per year from 2 to 36%. The average number of fires per year during the same period was 74 and the average burned area was 58 ha (BLE 1995 – 2021; BMEL, 1994; Michael Lachmann, 2006 – 2010; Michaela Lachmann, 2011 – 2015). The number of annual forest fires in Burgenland represented between just under one and almost 20% of the total in Austria during the same time period. The proportion of burned areas varied between slightly above zero and 30%. On average, there were eight fires per year burning a mean area of just below three hectares (Institut für Waldbau, 2021). However, these values are rather approximate, as records are missing entirely for the years

1995, 1996, 1997, 1999, and 2005 and for the sizes of several fires in other years. While the development of fire numbers and areas in Bavaria follows approximately the same pattern as in Germany as a whole, the fire regime of Burgenland seems to differ more from the rest of Austria (see Figures 10 and 11). However, Burgenland is also significantly smaller than Bavaria, which is why greater fluctuations in the annual volume of fires are to be expected.

Based on the annual average burned areas, current return intervals can be determined based on the total forest areas of the countries or states, analogous to the approach used for the model evaluation described in chapter 2.2.2.1. As shown in Table 6 below, there is a vast discrepancy of tens of thousands of years between the average return interval of the historic regime and the current regimes.

Table 6: Overview of current return intervals at the national and state level.

	Germany	**Bavaria**	**Austria**	**Burgenland**
Mean Return Interval	17,434	44,931	77,265	46,091

The deviation is mainly due to the fact that current regimes are dominated by human activities to a much greater extent. Among other factors, such as forest management, this is mainly due to active fire prevention as well as effective firefighting, which also limits fire sizes and duration. Individual forest fires in Germany and Austria are therefore usually very small, mostly below 0.1 ha (M. Müller et al., 2020), and of short duration. Most fires in Austria, for example, are extinguished within the first hour, while first firefighting attempts usually occur within 20 minutes of ignition (San-Miguel-Ayanz et al., 2019).

Available information on fire characteristics is rather limited. The vast majority of wildfires in Austria in 2018 were low-intensity surface fires (San-Miguel-Ayanz et al., 2019). None of the analyzed reports contained information on the intensity of wildfires in Germany. With respect to affected vegetation, forest fires usually affect conifers to a greater extent than deciduous species (BLE, 2021; M. Müller et al., 2020). In addition, coniferous forests on southern slopes and on limestone in the northern Alps are at higher risk of fire (M. Müller et al., 2020).

3.2.2 Conditions of Fire Occurrence

On average, human actions, directly or indirectly, cause over 95% of all forest fires in Europe and over 90% of fires in the Alpine region, however in many cases, the exact reason is unknown (M. Müller et al., 2020; San-Miguel-Ayanz et al., 2019; San-Miguel-Ayanz et al., 2020). Consequently, fire occurrence is higher in densely populated areas and recreational areas, as well as along roads and railways, than in remote regions. Wildfires are often caused by negligence or accident, e.g. by cigarettes, out-of-control fires, flying sparks, and power lines

(M. Müller et al., 2020). However, arson also plays a role; in Germany, about 15% of all forest fires are started intentionally each year, while the share in Austria is less than 10% (BLE, 2021; M. Müller et al., 2020). Clear-cutting increases the susceptibility of forests to both fire ignition and spread in both countries due to lower fuel moisture coupled with dry, grass-dominated fine fuel (M. Müller et al., 2020). Natural causes of fire ignition are limited to lightning strikes, which play a larger role in the southern and eastern central Alps and in the summer months. In Austria, an average of 15% of all forest fires are caused by lightning strikes, but in the summer months this value can reach up to 50% (M. Müller et al., 2020). In recent years, the share has been much greater, while in Germany only a good five percent of fires were due to natural causes (BLE, 2021; San-Miguel-Ayanz et al., 2019; San-Miguel-Ayanz et al., 2020).

As previously mentioned, weather conditions play a major role in wildfire regimes in Central Europe, and fires often occur in association with heatwaves, drought, and dry foehn winds (de Rigo et al., 2017; Migliavacca et al., 2013; M. Müller et al., 2020). While Zumbrunnen et al. (2009) identified summer temperature as an important determinant of fire occurrence in subalpine areas, foehn winds and non-climatic variables had a larger impact in colline-montane regions. However, they also found that precipitation three years prior to a given year correlated positively with fire frequency as these conditions allow for a buildup of fuel (Zumbrunnen et al., 2009). Overall however, the importance of precipitation and temperature became increasingly overshadowed by the effects of human activity and fuel availability in the second half of the 20th century, also in subalpine areas (Zumbrunnen et al., 2009). A study by Wastl et al. (2013) analyzing the correlation between eleven different weather patterns, fire risk, and actual fire occurrence in the Alpine region showed that anticyclonic weather conditions were generally associated with higher fire risk than cyclonic conditions. They also led to higher, more seasonally uniform fire danger in the southern Alps than in northern parts, where fire risk is substantially elevated in summer (Wastl et al., 2013). While the correlation between weather patterns and actual fire occurrence is usually weaker where fire regimes are heavily influenced by human activity (Wastl et al., 2013; Weibel et al., 2010), Wastl et al. (2013) found that it followed a similar pattern as fire risk and was highest during anticyclonic weather conditions, such as high-pressure systems, which causes fuels to dry out.

Enhanced forest connectivity and fuel buildup in the European Alpine region are expected as a result of increasing land abandonment (Blarquez et al., 2010; Carcaillet et al., 2009; Leys et al., 2014) and active fire suppression (Colombaroli et al., 2010; M. Müller et al., 2020). Since fuel availability is a major determinant of fire occurrence, these factors might promote more intense fire regimes with larger and more severe fires (Blarquez et al., 2010; Carcaillet et al., 2009; Colombaroli et al., 2010; Leys et al., 2014; M. Müller et al., 2020).

The legal regulations for forest fire suppression, firefighting, and post-fire restoration are enacted at the state level in Germany and Austria (M. Müller et al., 2020). The legislation of both countries includes restrictions on prescribed fires, which are generally not permitted. An exception is Lower Austria, where prescribed burning of railroad embankments is allowed to prevent fires caused by flying sparks on railroad embankments (M. Müller et al., 2020). In addition, bans on controlled fires and smoking in forests and surrounding areas can be imposed in both regions. Originally intended for periods of high fire risk, these restrictions are often in effect continuously from March through October in many areas (M. Müller et al., 2020). According to Article 17 of the Bavarian Forest Act (Bayerisches Waldgesetz, BayWaldG), private individuals in Bavaria always need a permit for fires at a distance of fewer than 100 m from forest areas (BayWaldG, 2005).

3.2.3 Immediate Effects

In addition to the environmental impacts of forest fires already discussed in Chapter 1, socio-economic impacts are also of central importance in regions with high population density such as Germany and Austria. Wildfires pose a direct risk to people and infrastructure, especially when urban structures are adjacent to forests. Adverse health impacts can stem, for example, from smoke inhalation (M. Müller et al., 2020) or burns, although the number of fire-related injuries in the study regions is generally very low (San-Miguel-Ayanz et al., 2019). In addition, fires can decrease the protective function of forests (Eastaugh & Hasenauer, 2014), resulting in other natural hazards and therefore further risks for society. In the Alpine region, these include in particular greater avalanche risk, increased water runoff, landslides, rockfall, or soil erosion (M. Müller et al., 2020) caused by a decrease in the stability of the roots after fires (Gehring et al., 2019; Vergani et al., 2017).

At the same time, wildfires are associated with high costs for firefighting operations, especially in inaccessible areas (Eastaugh & Hasenauer, 2014; M. Müller et al., 2020), and for post-fire management measures. These amount to around 650,000 euros per year in Austria (M. Müller et al., 2020). In Germany, this sum has been exceeded by a factor of five to eight in recent years (San-Miguel-Ayanz et al., 2019; San-Miguel-Ayanz et al., 2020). In total, around 45 million euros are currently invested annually in direct fire suppression measures throughout the Alpine region (M. Müller et al., 2020). The annual economic damage caused by wildfires amounted to approximately 1.8 million euros in Germany in the period from 1991 to 2019 (BLE, 2021; San-Miguel-Ayanz et al., 2020), which corresponds to approximately 2,500 € per hectare of burned area (BLE, 2021). Economic damages in Austria are less well documented and were not indicated in the analyzed literature and data sets.

3.3 Future Fire Regime

3.3.1 Spatio-Temporal Distribution and Fire Characteristics

Figures 12 through 15 show the annual number of fires and annual share of the total area burned in each study landscape under the two climate change scenarios compared to the respective baseline value over the future period as well as the annual means averaged over the ten simulations in bold. In many instances, there were only minor absolute differences in the annual number of fires and burned area extent between scenarios with and without climate change, especially under the RCP4.5 scenario and in simulations with longer return intervals (see Table A, Appendix A). To confirm that deviations were not just due to the inherent stochasticity of fire occurrence but indeed caused by climatic changes, the Wilcoxon test was used to determine statistical significance. The test was carried out for both the future and EOC periods since the future return intervals were also calculated for the same periods.

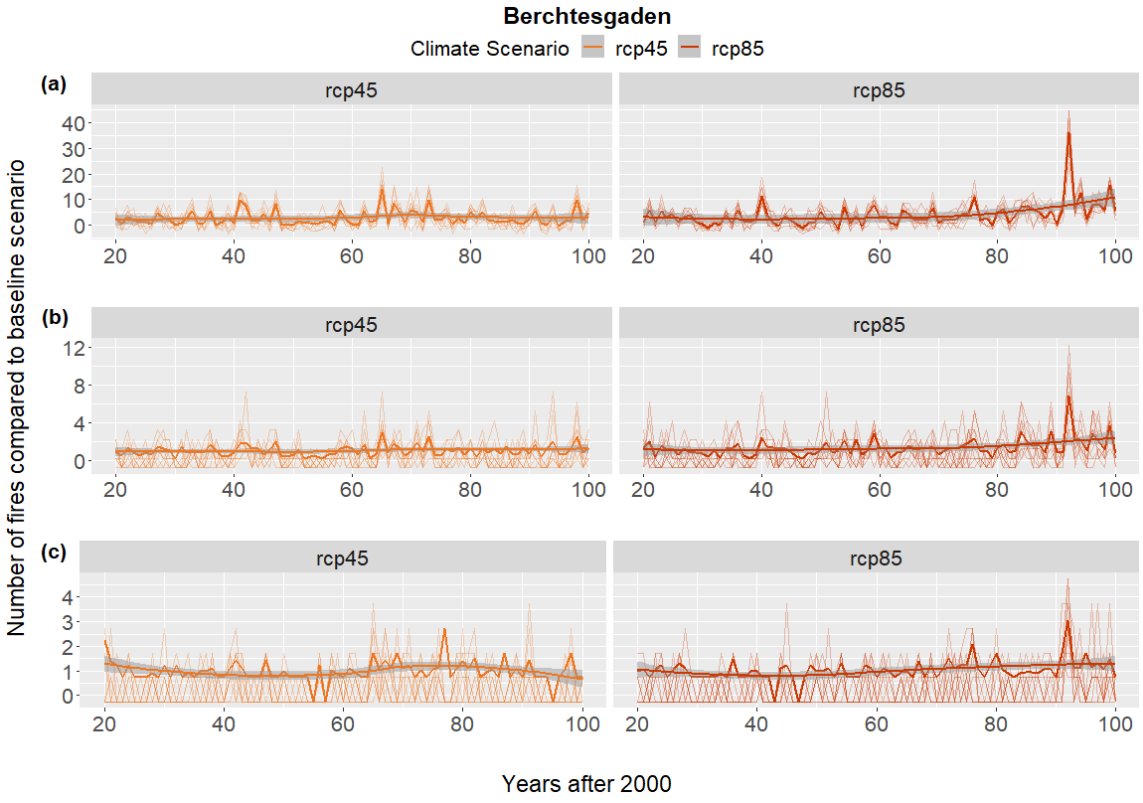

Figure 12: Deviation of the annual number of fires in the BGNP from the mean of the baseline simulation in the two climate change scenarios in the simulation years 20 – 100 for simulations with (a) the minimum, (b) the mean, and (c) the maximum return interval. Thin lines show the ten individual iterations while the bold lines represent annual means as well as the overall mean, smoothed using the loess method.

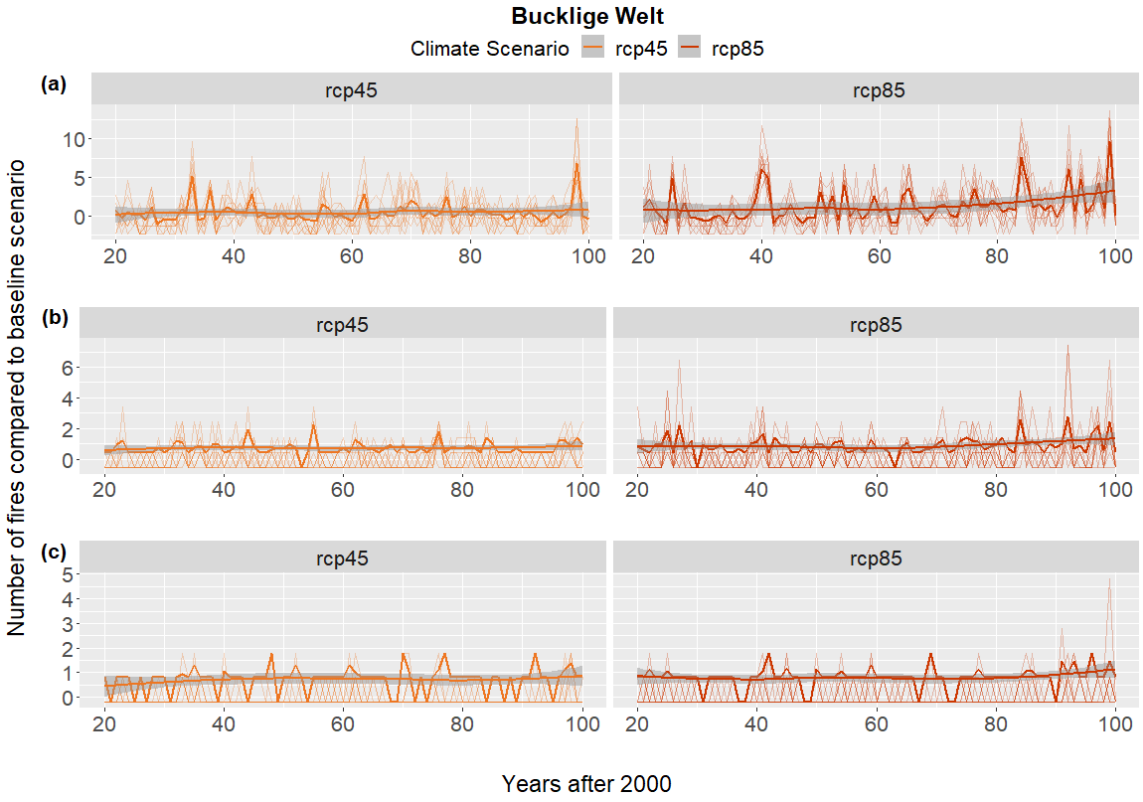

Figure 13: Deviation of the annual number of fires in the BuWe from the mean of the baseline simulation in the two climate change scenarios in the simulation years 20 – 100 for simulations with (a) the minimum, (b) the mean, and (c) the maximum return interval. Thin lines show the ten individual iterations while the bold lines represent annual means as well as the overall mean, smoothed using the loess method.

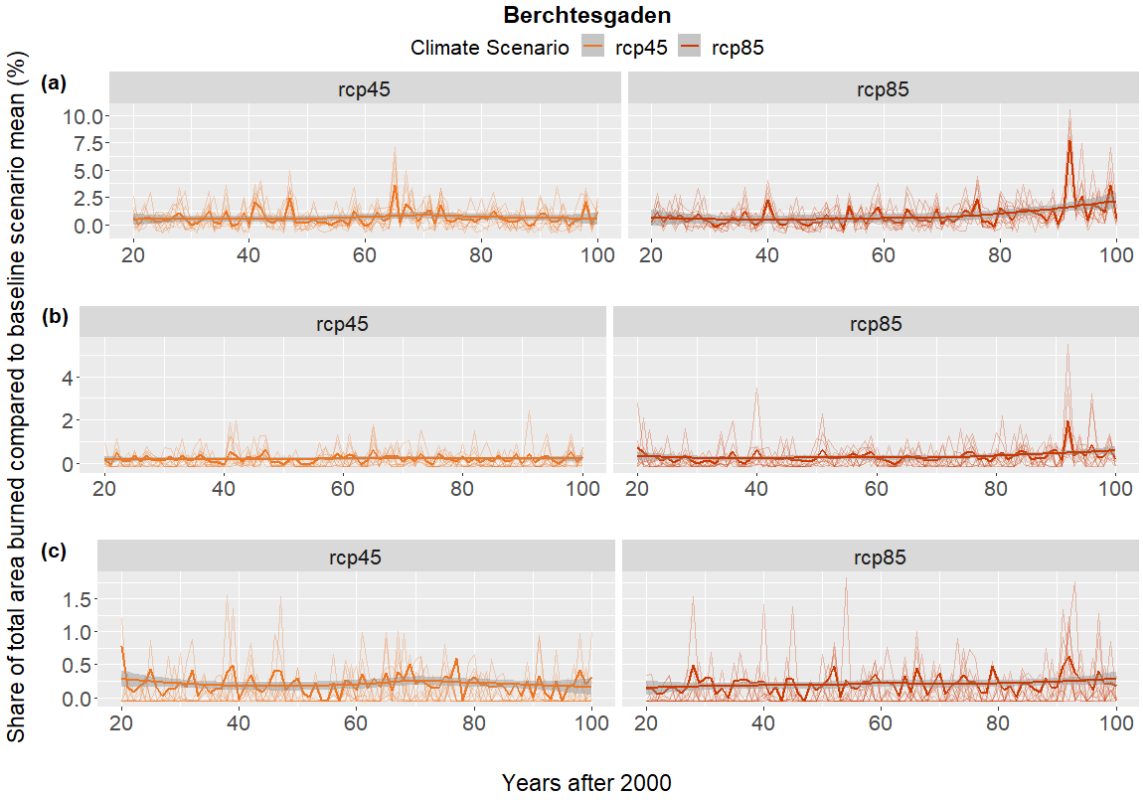

Figure 14: Deviation of the annual share of the total area burned in the BGNP from the mean of the baseline simulation in the two climate change scenarios in the simulation years 20 – 100 for simulations with (a) the minimum, (b) the mean, and (c) the maximum return interval. Thin lines show the ten individual iterations while the bold lines represent annual means as well as the overall mean, smoothed using the loess method.

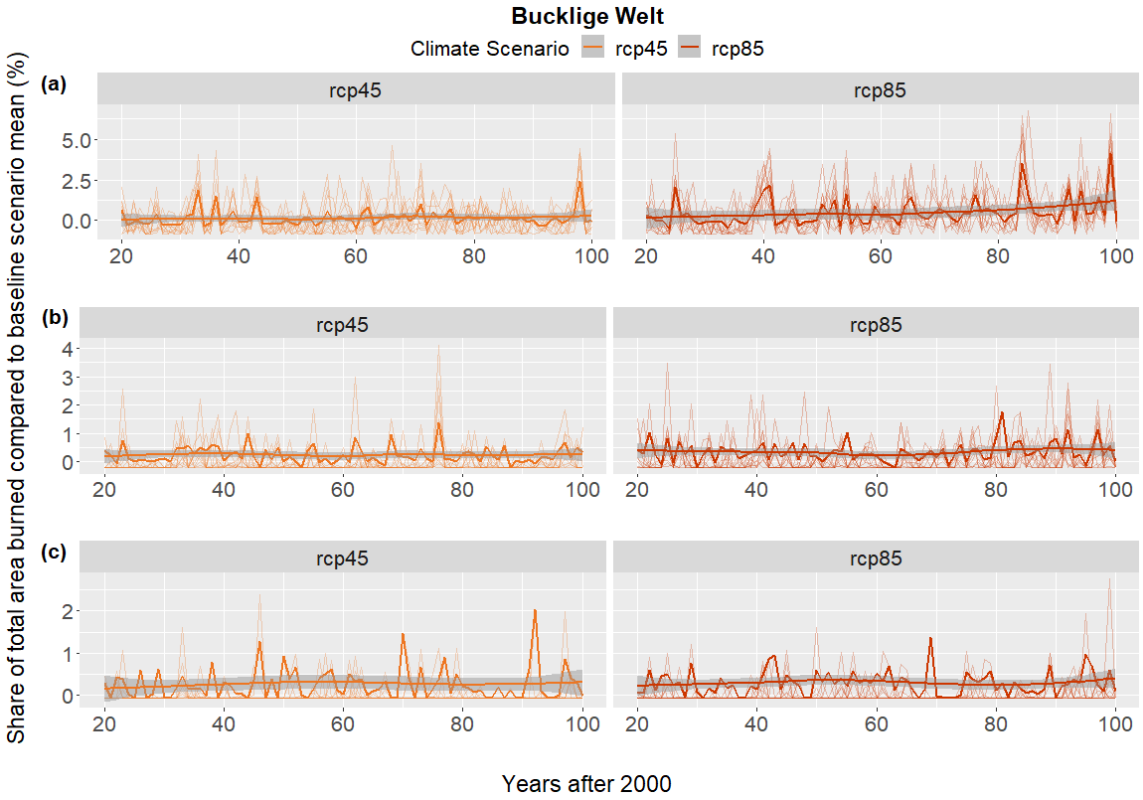

Figure 15: Deviation of the annual share of the total area burned in the BuWe from the mean of the baseline simulation in the two climate change scenarios in the simulation years 20 – 100 for simulations with (a) the minimum, (b) the mean, and (c) the maximum return interval. Thin lines show the ten individual iterations while the bold lines represent annual means as well as the overall mean, smoothed using the loess method.

The results of the test show that there was a significant difference between the annual number of fires and burned area extent in all scenarios in the years 2020 – 2100 in the BGNP compared to the baseline scenario (see Table 7). During this period, the number of fires increased by 62% – 86% in the RCP4.5 scenarios and by 108% – 119% in the RCP8.5 scenarios. In the BuWe, changes in the number of fires and burned area were significant only in the BuWe-124-RCP8.5 and BuWe-534-RCP8.5 scenarios, with an increase in fire frequency of about 45% in both cases, but not in any of the RCP4.5 simulations. A more pronounced difference in simulations with a significantly shorter return interval is to be expected since fire occurrence and thus the base ignition probability are significantly higher than with longer intervals. In the EOC period, in contrast, significant differences did not occur in the BGNP in all cases, and the changes in the RCP4.5 scenarios were also less pronounced than during the entire future period. It is clear from the figures that there were pronounced increases in the annual number of fires approximately between the years 2065 and 2075 in these scenarios, after which the curve flattened out again, while fire occurrence continuously increased from the year 2080 onwards in the RCP8.5 scenarios. In the BuWe, on the other hand, the pattern in the EOC period was the same as in the entire future period, although the last 20 years of the century saw a greater increase in fires and burned area.

Table 7: Change in the overall annual mean number of fires and relative burned area in the two climate change scenarios compared to the baseline scenario in the future and EOC period. Statistically significant differences between the annual means of the different scenarios determined using the Wilcoxon test are shown in bold.

Study Area	Climate Scenario	Return Interval	Variable	Future		EOC	
				Change	p-value	Change	p-value
BGNP	RCP4.5	124	Number of fires	+80.4%	**4.5e-12***	+58.2%	**0.0027***
			Burned area share	+83.2%	**5.1e-11***	+60.4%	**0.0029***
		534	Number of fires	+61.7%	**5.4e-06***	+26.3%	**0.0123***
			Burned area share	+49.0%	**0.0415***	+18.2%	0.3926
		1520	Number of fires	+85.5%	**0.0009***	+47.1%	0.2563
			Burned area share	+91.0%	**0.0289***	+17.2%	0.4524
	RCP8.5	124	Number of fires	+119.0%	**1.3e-12***	+192.0%	**9.9e-05***
			Burned area share	+113.0%	**5.7e-12***	+190.0%	**4.8e-06***
		534	Number of fires	+108.0%	**4.9e-10***	+151.0%	**0.0004***
			Burned area share	+109.0%	**1.9e-07***	+172.0%	**0.0001***
		1520	Number of fires	+113.0%	**5.2e-05***	+140.0%	**0.0074***
			Burned area share	+113.0%	**0.0090***	+103.0%	0.7854
BuWe	RCP4.5	124	Number of fires	+3.1%	0.3493	-4.8%	0.9256
			Burned area share	+2.0%	0.7740	-5.9%	0.5168
		534	Number of fires	-4.0%	0.4678	-9.5%	0.8128
			Burned area share	-7.3%	0.9437	-14.7%	0.9729
		1520	Number of fires	-9.9%	0.6435	-34.0%	0.8334
			Burned area share	-9.9%	0.3738	-35.0%	0.3803
	RCP8.5	124	Number of fires	+44.4%	**0.0010***	+76.1%	**0.0158***
			Burned area share	+49.5%	**0.0027***	+81.5%	**0.0384***
		534	Number of fires	+45.4%	**0.0009***	+75.6%	**0.0156***
			Burned area share	+43.5%	**0.0156***	+82.7%	**0.0325***
		1520	Number of fires	+25.3%	0.2829	+46.0%	0.1304
			Burned area share	+22.2%	0.8728	+37.0%	0.4120

* indicates statistical significance ($p<0.05$)

Based on Figures 12 – 15 alone, no clear trend can be identified in most cases. Therefore, the time series were examined for the presence of a statistically significant trend using the MK test and, if relevant, the magnitude of the trend was determined using the Sen's Slope test (see Table 8). The results show that no significant trend existed in either landscape under the RCP4.5 scenario. In the RCP8.5 scenario, on the other hand, the MK test indicated a significant positive trend in the annual number of fires under climate change in all simulated scenario combinations in the BGNP as well as in simulations with the minimum return interval of 124 years in the BuWe. In a direct comparison, the positive trend in the BGNP was stronger than in the BuWe in this scenario. Overall, stronger trends under the assumption of shorter return intervals are again expected.

Table 8: Results of MK and Sen's Slope tests for trends in the annual number of fires and share of the total area burned in the simulation years 20 – 100 of each simulated scenario compared to the respective reference time series without climate change. Statistically significant trends are shown in bold.

Study Area	Climate Scenario	Return Interval	Time Series	Mann-Kendall tau value	Mann-Kendall p-value	Sen's Slope
BGNP	RCP4.5	124	Number of fires	0.0606	0.4286	-
			Burned area share	0.0420	0.5819	-
		534	Number of fires	0.0965	0.2123	-
			Burned area share	0.0330	0.6655	-
		1520	Number of fires	0.0069	0.9354	-
			Burned area share	0.0071	0.9285	-
	RCP8.5	124	Number of fires	**0.2860**	**0.0002***	**0.0581**
			Burned area share	**0.2720**	**0.0003***	**0.0101**
		534	Number of fires	**0.2240**	**0.0034***	**0.0093**
			Burned area share	**0.2290**	**0.0025***	**0.0026**
		1520	Number of fires	**0.2270**	**0.0046***	**0.0031**
			Burned area share	0.1190	0.1183	-
BuWe	RCP4.5	124	Number of fires	0.0468	0.5430	-
			Burned area share	0.1110	0.1420	-
		534	Number of fires	0.0484	0.5558	-
			Burned area share	-0.0216	0.7784	-
		1520	Number of fires	0.0771	0.3751	-
			Burned area share	0.0016	0.9869	-
	RCP8.5	124	Number of fires	**0.2450**	**0.0013***	**0.0217**
			Burned area share	**0.2250**	**0.0030***	**0.0076**
		534	Number of fires	0.1130	0.1478	-
			Burned area share	0.0179	0.8162	-
		1520	Number of fires	0.1100	0.2045	-
			Burned area share	0.0149	0.8479	-

* indicates statistical significance ($p<0.05$)

Future return intervals for each landscape were calculated based on the mean annual burned area in each simulated scenario (see Figure 16 and Table B, Appendix A). However, since the differences between the mean annual burned area in the climate change scenarios and the baseline scenario were not always statistically significant, these should be evaluated cautiously. In the BGNP, simulated return intervals of the climate change scenarios were consistently well below those under historical conditions, with this effect being more pronounced in the RCP8.5 scenario. Moreover, previously detected positive trends in the development of relative fire areas in the scenarios BGNP-124-RCP8.5 and BGNP-534-RCP8.5 were also reflected in shorter EOC intervals. In the two scenarios with significant differences in the relative burned area in the BuWe (BuWe-124-RCP8.5 and BuWe-534-RCP8.5), substantially shorter return intervals of more than 25% in the future period and almost 50% in the EOC period were observed. In these scenarios, which are the only two that allowed for a reliable comparison between the landscapes, the return interval deviations under climate change were larger in the BGNP, which is consistent with the previous findings. In the RCP4.5 scenario, longer return intervals were consistently found for the BuWe in all scenarios, but the

underlying deviations of the mean annual burned areas were not actually significantly different from the baseline scenario.

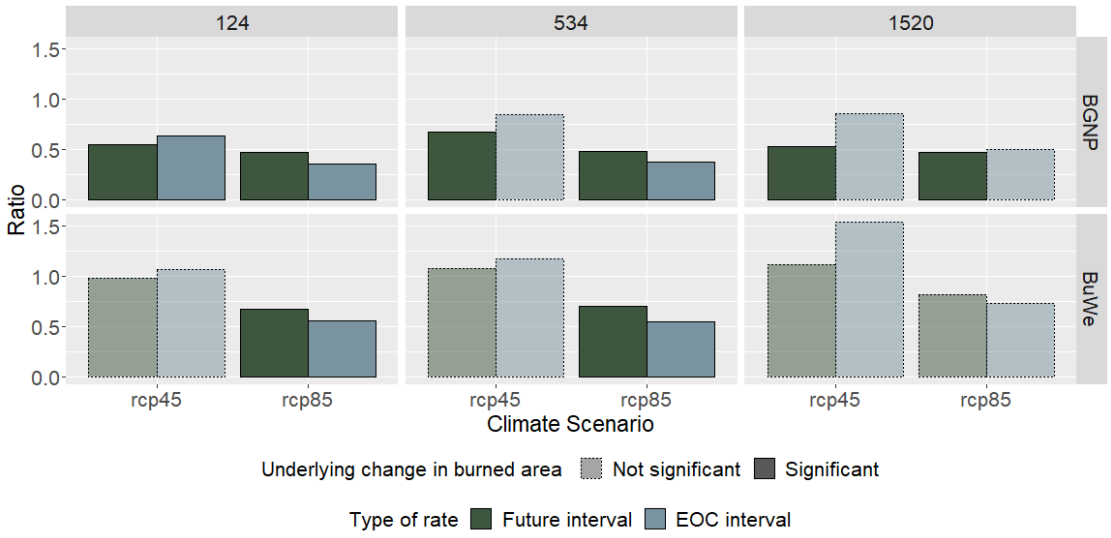

Figure 16: Ratio of the simulated return intervals under historic conditions to those under climate change for the simulation years 20 – 100 and 80 – 100 for each combination of climate scenario and historic return interval in the BGNP (first row) and the BuWe (second row). Solid outlines indicate statistically significant changes in the underlying differences in the burned area between the respective climate change scenario and the historic baseline scenario, while transparent bars with dotted outlines stand for non-significant differences.

Overall, fire occurrence in the BGNP was far more spatially differentiated than in the BuWe (see Figure 17). While clear clusters of high fire occurrence emerged in the BGNP in both climate change scenarios, the distribution of fires was more uniform across the BuWe landscape, except for a slight concentration in the east in the RCP8.5 scenario. In comparison to historic conditions, higher altitudes in the BGNP were increasingly affected by wildfires under climate change, especially in the RCP8.5 scenario.

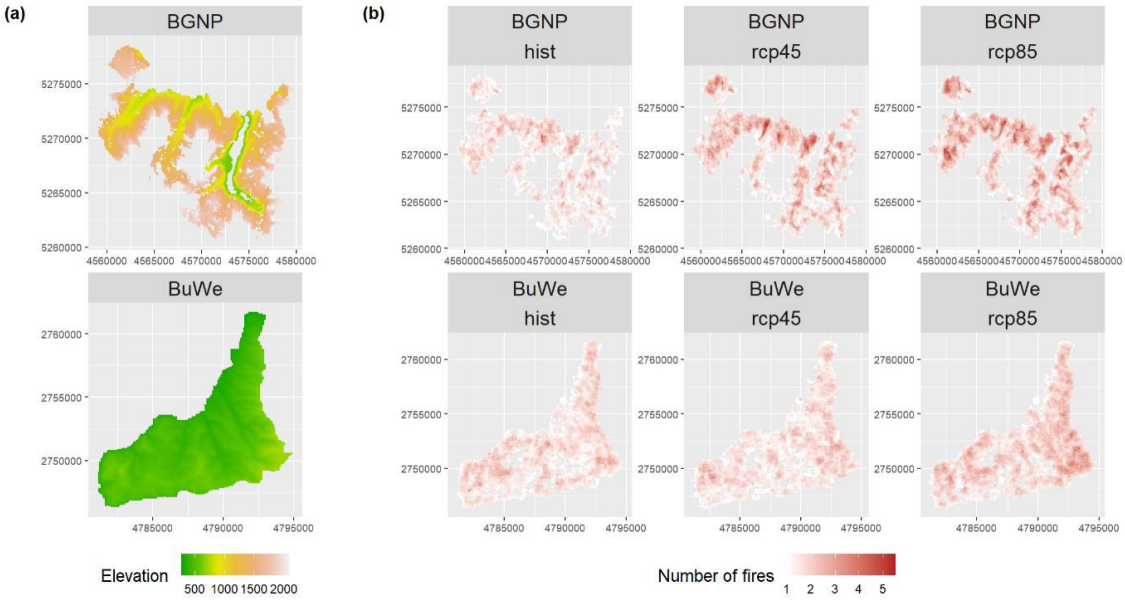

Figure 17: Plots of the BGNP (first line) and the BuWe (second line) showing (a) the elevation of each pixel and (b) the number of fires in each pixel throughout the entire simulation period, averaged over all ten iterations with the minimum fire interval of 124 years.

3.3.2 Conditions of Fire Occurrence

Fire occurrence in a particular RU of a landscape in iLand is heavily influenced by the prevailing fuel moisture conditions, as represented by the KBDI. Figure 18 below shows the ratio of the mean EOC KBDI (averaged over the simulation years 80 – 100) to the reference KBDI of the historic fire regime (see Figure F, Appendix B) for each RU in both landscapes.

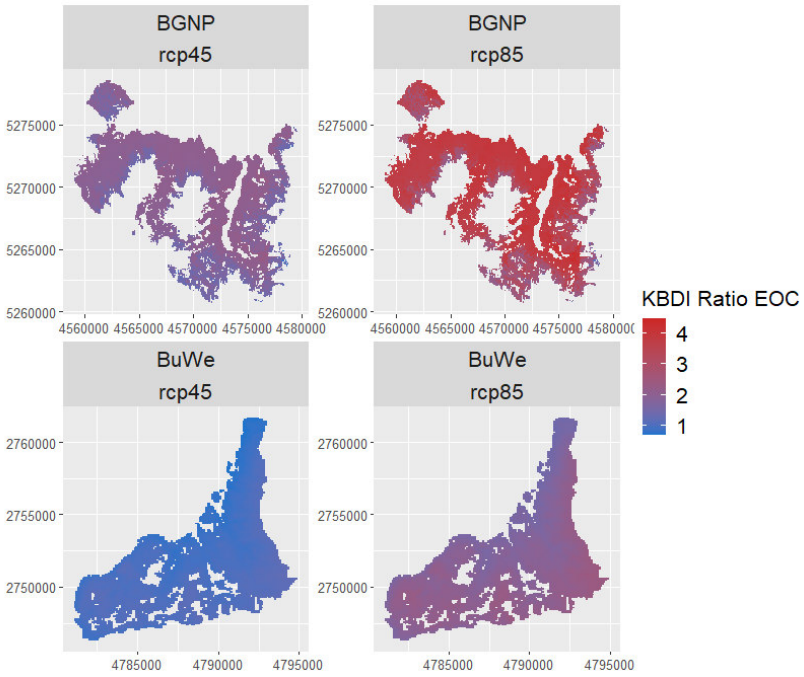

Figure 18: Maps showing the ratio of the mean end-of-century KBDI (simulation years 80 – 100) to the historic reference value for each RU in the BGNP (first row) and the BuWe (second row).

In the BGNP, a substantial increase in the KBDI values, and thus drying of fuels and elevated fire risk, by a factor of about two in the RCP4.5 scenario and about four in the RCP8.5 scenario was observed in the majority of the RUs. The BuWe landscape responded much less sensitively with KBDI values remaining constant over large areas in the RCP4.5 scenario and an increase of roughly a factor of two in the RCP8.5 scenario. While precipitation remained relatively stable throughout the simulation period in both landscapes, maximum temperatures, which also affect the KBDI, increased in both landscapes. In BGNP, however, the increase was stronger, especially during summer, which can explain part of the more pronounced change. Another important factor influencing the KBDI is snow cover since fuels can only dry out in its absence. Under historical conditions, at least 30 days of annual snow cover occurred in the BGNP in each RU with significantly higher values up to year-round snow cover at higher elevations. In the BuWe, on the other hand, the number of snow days ranged from five to 135 days (see Figure G and H, Appendix B). In comparison, there was a pronounced decrease in the number of days with snow cover in the vast majority of RUs in both landscapes in the simulations with climate change towards the end of the century. While both climate change scenarios had similar impacts in the BuWe, with the number of snow cover days roughly halved

over a large part of the landscape, the BNGP saw more dramatic declines overall as well as greater differences between scenarios. In the RCP4.5 scenario, there was a decrease of about 75% in many RUs at lower elevations. In the RCP8.5 scenario, a larger area and higher elevations were affected, and the decrease was even more severe at the same time (see Figure 19).

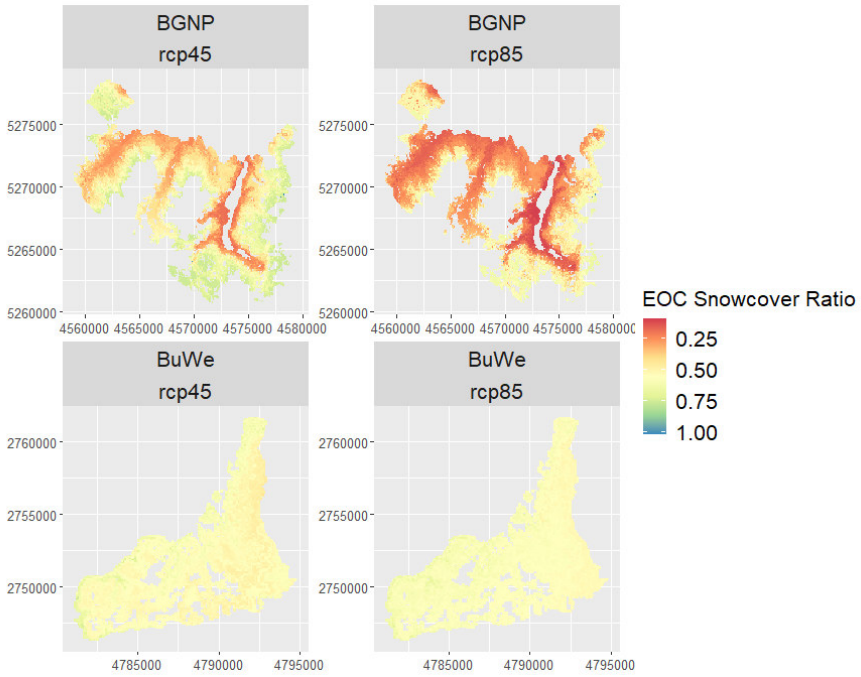

Figure 19: Ratio of the annual number of days with snow cover above 0 mm in the years 20 – 100 in the simulations with historic climate compared to the RCP4.5 (first column) and RCP8.5 (second column) scenarios in each RU of the BNGP (first row) and the BuWe (second row) landscapes.

Since the ratio of the current KBDI to the reference KBDI of a RU directly affects the risk of ignition, and since this ratio is generally higher in the BGNP than in the BuWe for the same KBDI due to lower historic reference values, more fires ignite in the BGNP than the BuWe for the same future KBDI in the climate change scenarios (see Figure 20).

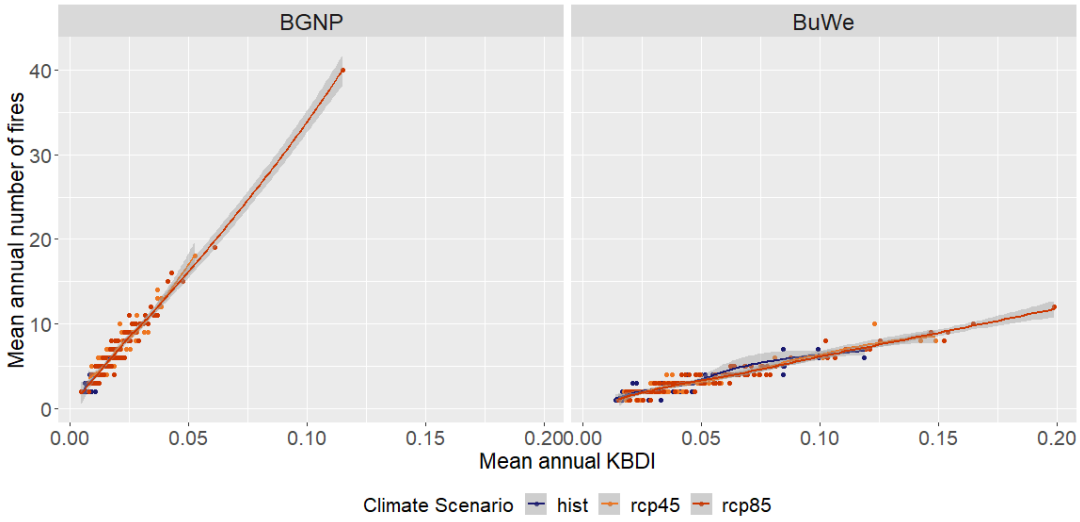

Figure 20: Mean annual number of fires plotted against mean annual KBDI in both landscapes under the different climate scenarios in simulations with the minimum return interval of 124 years.

Ultimately, the increase in burned area, and thus the shortening of return intervals, was due to an increase in the number of fires, rather than increasing fire sizes due to climatic conditions; these remain roughly constant in the comparison between scenarios (see Figure E, Appendix A). This effect is to be expected because KBDI anomalies affect ignition probabilities in iLand but generally not fire spread.

3.3.3 Immediate Effects

The annual number of fires assigned to a specific severity class based on the mortality rate of the affected trees is shown in Figure 21. In the RCP4.5 scenario, the relative distribution of fires among the three severity classes was quite stable over the simulation period and overall similar to the baseline scenario, except for more moderate severity fires in the BGNP. Due to the higher number of fires overall in the RCP8.5 scenario towards the end of the century, there was also an increase in the number of trees per severity class. However, this effect was more pronounced in the low and moderate severity class while there was a weaker increase in high severity fires in the BGNP and no increase in the BuWe. The mortality rate ultimately determines the amount of carbon released during a wildfire. The annual amount of carbon lost due to fire disturbances in the study landscapes under the different climate scenarios is shown in Figure 22. Relatively frequently, a higher loss of carbon occurred despite a lower number of fires in a given year in the BuWe. This is due to the higher overall tree volume in the BuWe, which increased continuously throughout the century despite a strong decrease in the number of trees per hectare (see Figures I and J, Appendix C).

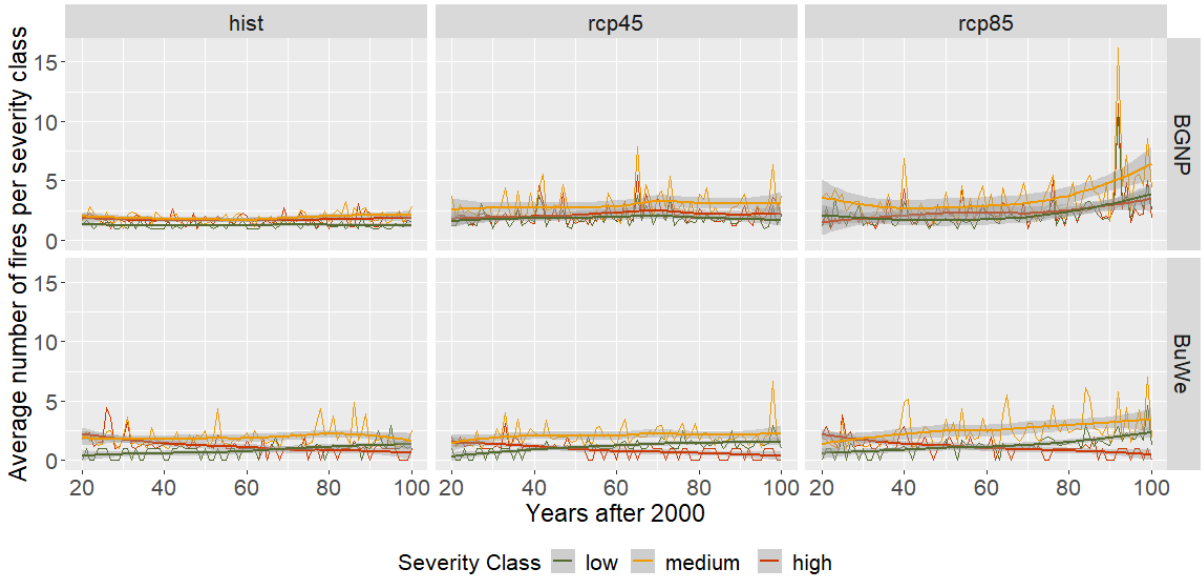

Figure 21: Number of fires per severity class in each climate scenario averaged over the ten iterations with the minimum return interval in the BGNP (first row) and the BuWe (second row).

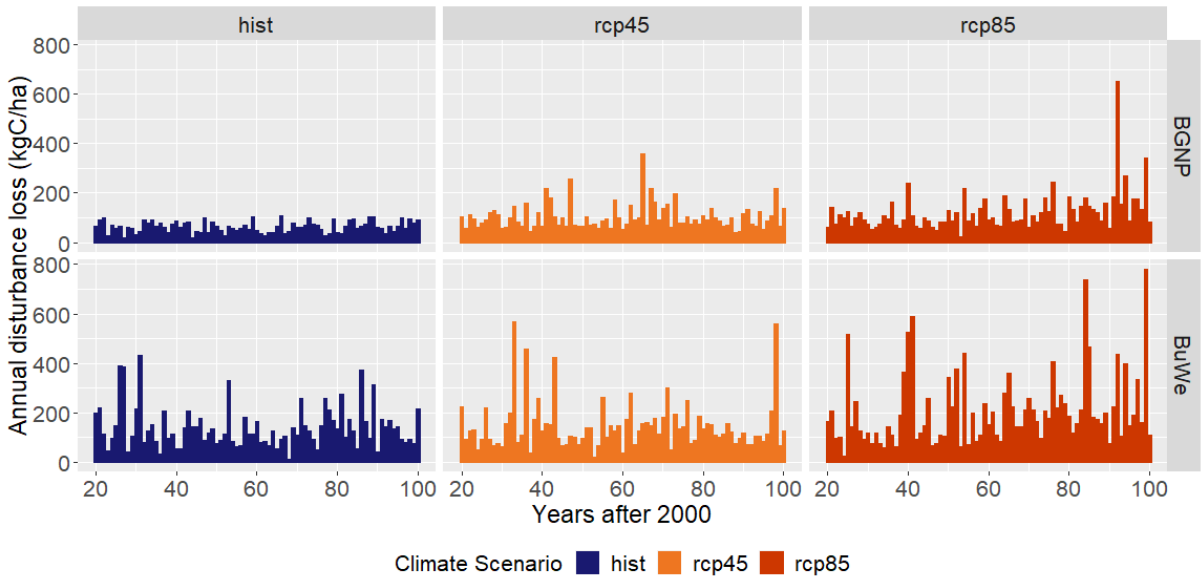

Figure 22: Annual carbon losses due to fire disturbances in kg per hectare in each climate scenario in the BGNP (first row) and the BuWe (second row), averaged over the ten iterations using the minimum historic return interval.

Annual NEP, which equals the net changes over all ecosystem carbon pools and is directly affected by disturbance losses, is shown in Figure 23 below. Since NEP is primarily dependent on the net NPP of the same year, very high fire-related carbon losses in a given year do not necessarily also translate into a net loss of carbon in the landscape.

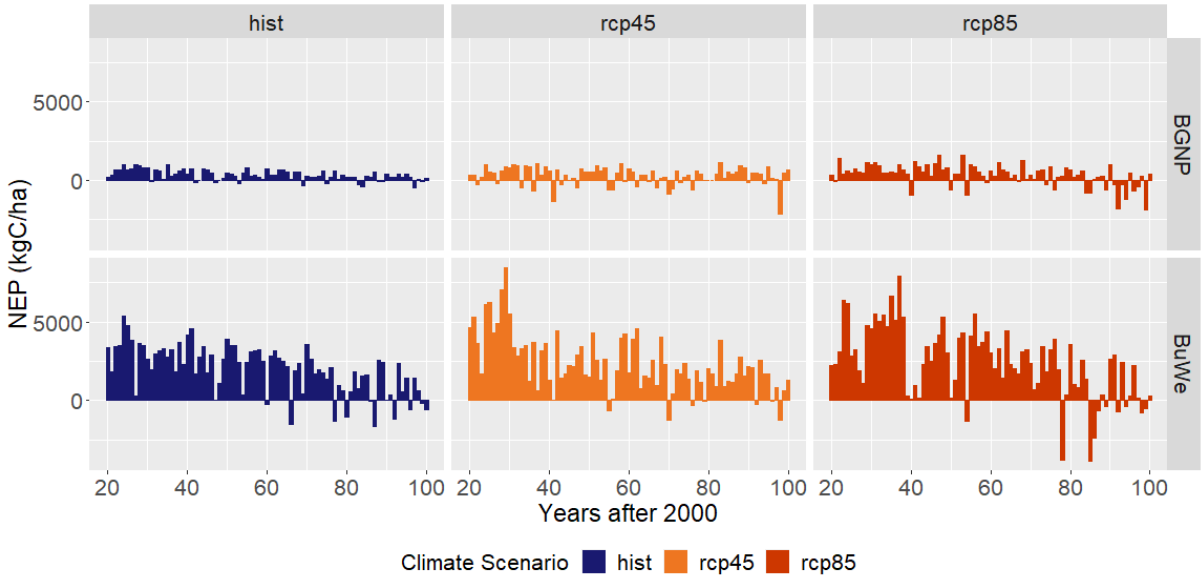

Figure 23: Annual NEP, or total net changes over all ecosystem carbon pools, in kg carbon per hectare in each climate scenario in the BGNP (first row) and the BuWe (second row), averaged over the ten iterations using the minimum historic return interval.

A Kendall's tau test was therefore used to determine the exact effect of disturbance loss on NEP in the different climate scenarios (see Table 9). It revealed significant negative correlations between disturbance losses and NEP in all climate scenarios in both landscapes,

which were stronger in the climate change scenarios than the baseline scenario and stronger in the RCP8.5 than the RCP4.5 scenario.

Table 9: Correlations between disturbance carbon losses and NEP in simulations with the minimum return interval as determined by Kendall's tau.

Study Area	Baseline Scenario	RCP4.5	RCP8.5
BGNP	-0.2865 *	-0.4036 *	-0.4590 *
BuWe	-0.1499 *	-0.2141 *	-0.4061 *

* indicates statistical significance ($p<0.05$)

Nevertheless, NEP was only rarely negative, meaning that a net decline of the total carbon stored occurred, even in years with high carbon losses due to fire disturbances so that the overall impact of the fire regime on carbon storage was small (see also Figure K, Appendix C). In the RCP8.5 scenario, however, NEP started to be negative regularly during the EOC period in both landscapes. A comparison of the amount of carbon stored in the different pools in RCP8.5 simulations with the minimum return interval and the RCP8.5 reference simulation without fire during this period showed that most carbon pools of both study areas were reduced by between 5 and 15% by the fire disturbances (see Figure 24). The pools "Snags" and "Snags Other", i.e., standing dead wood and the branches and coarse roots of standing dead trees (Seidl & Rammer, 2021), increased by around 9 and 10%, respectively, in both landscapes. An exception is the pool "Regeneration" in BuWe, which increased by about 260% in the scenario with fire. It is possible that fire disturbance may promote regeneration locally in the landscape, where regeneration might be limited in the absence of disturbances.

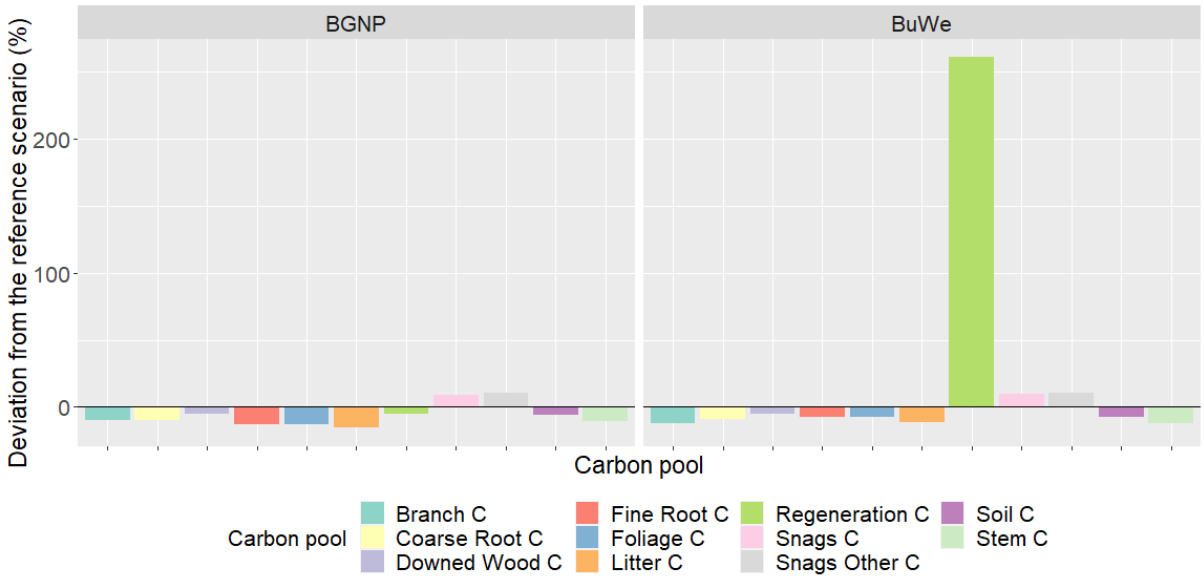

Figure 24: Deviation of the amount of carbon stored in each carbon pool in RCP8.5 scenarios with the minimum return interval (averaged over the ten iterations) in relation to the RCP8.5 reference scenario without fire during the EOC period (±%).

4. Discussion

4.1 Evolution of Central European Fire Regimes up to the Present

Even though historic fire regimes in the Central European Alpine region, and the two study landscapes in particular, have not yet been studied extensively, the few existing studies have already shown an enormous variability in fire occurrence between regions, but also over time. While fire regimes after the original afforestation were initially driven solely by natural factors, i.e., climatic and weather conditions, ignitions by lightning strikes, and the presence of certain key tree species, the influence of human activities has become evident since the early Neolithic. Today, fire regimes are almost entirely governed by humans, who have almost completely altered them as the main source of ignitions in much of the region, but also overall, primarily through active fire suppression and management. As a result, contemporary fire regimes in the extended study areas are characterized by much longer return intervals and the virtual absence of large fires. However, there has been little research on the precise fire characteristics of past and present regimes, such as particularly affected tree species or fire intensity, and on the specific impacts on biodiversity and ecosystem service provision. Currently, the main focus in managing fire regimes is on preventing or mitigating economic losses and, especially in the Alps, maintaining the protective functions of forests.

An intensification of current Central European fire regimes due to climate change is commonly expected, potentially exacerbated by land abandonment and thus enhanced forest connectivity and fuel buildup in the Alpine region, which would lead to an increased risk of damage to humans and ecosystems even with similarly effective fire management measures. However, the simulation results of the present thesis only partially confirmed this expectation since climatic changes did not always result in statistically significant deviations from the historic regimes in the Central European study landscapes.

4.2 Projected Sensitivity of the Fire Regimes to Climatic Changes Throughout the 21st Century

Overall, a stronger response of the BGNP fire regime to climatic changes was observed in both climate change scenarios. In the RCP4.5 scenario, the fire regime of the BGNP was already significantly different from the baseline scenario, while this was not the case in the BuWe. While there was a significant increase in fire occurrence in both landscapes in the RCP8.5 scenarios, apart from the BuWe-1520-RCP8.5 scenario, this effect was more pronounced in the BGNP, as reflected in the shorter return intervals. This development seems counterintuitive at first since the BuWe experienced more favorable conditions for fire occurrence under both historic climate and the climate change scenarios, i.e., higher absolute (summer) temperatures and less precipitation. However, there was a stronger shift in fire-

promoting weather conditions in the BGNP compared to those that characterized the historic fire regime, such as a greater increase in (summer) temperatures and a substantial decrease in snow cover days, both of which directly affect the base ignition probability in iLand (see Equation 2). Thus, the decrease in return intervals in the climate change scenarios compared to the baseline scenario (see Figure 17) was also roughly of the same magnitude as the overall KBDI increase in BGNP (see Figure 19). Since there was no substantial change in the KBDI at the landscape level in the RCP4.5 scenario in the BuWe, the future fire regime was also not significantly different from the historic fire regime. In the RCP8.5 scenario, on the other hand, the landscape-level KBDI roughly doubled. The resulting changes were only significant in scenarios with the minimum and mean return interval while no significant difference from the historical regime could be detected using the longer, maximum interval due to the already very low fire occurrence. No significant trend in the annual number of fires and burned area extent was found in either landscape in the RCP4.5 scenario and the only instance, in which trends were found in both study areas, was in the simulations with the minimum return interval and the RCP8.5 scenario. In comparison, a stronger positive trend was again found in the BGNP in this scenario.

More frequent fire occurrence was also the cause of the increase in total burned area extent, while the size of individual fires remained relatively constant due to the way the model was parametrized. However, anthropogenic climate change has been shown to promote the occurrence of large fires in many areas worldwide (e.g. Abram et al., 2021; Dennison et al., 2014), which was not considered in the present study. In future studies, the impact of climate and weather conditions on fire sizes could be incorporated by defining certain thresholds, above which a larger minimum fire size is set, similar to the approach by Hansen et al. (2020).

The analysis also showed that in the BGNP, forested areas at higher elevations will likely be increasingly affected by wildfires. In addition to potential adverse impacts on ecosystems, this would most likely also be associated with an increase in the difficulty and cost of firefighting efforts due to the more restricted accessibility and ultimately likely also result in an increasingly greater risk for larger fires.

While a significant negative correlation between carbon losses due to fire disturbances and NEP was detected, which was stronger in scenarios assuming a higher atmospheric CO_2 concentration, the overall impact of the fire regimes on carbon storage pools in the landscapes throughout the entire simulation period were minor. Only in occasional years did the disturbance losses result in a negative NEP and thus a net loss of carbon. Nevertheless, an accumulation of years characterized by net carbon losses was observable towards the end of

the 21st century in the RCP8.5 scenario in both landscapes. While other factors besides fire disturbance may also play a role in this context, such as a decline in productivity due to tree aging, the analysis showed that the amount of carbon stored in the individual pools declined due to fires in both study areas during the EOC period. However, while this trend is an important indicator for potential future developments, its magnitude was likely grossly overestimated due to the choice of the most severe climate change scenario combined with an extremely short return interval considering the current intervals of the study areas. As mentioned in section 2.2.2.1.1, an error occurred in the parameterization of the fuel parameters, although it likely had very little effect on the amount of fuel consumed.

4.3 Contextualization of the Results within the Current State of Research

While Knorr et al. (2016) noted that the increase in burned area in Europe due to climatic changes under the RCP4.5 and RCP8.5 scenarios was largely offset by a negative effect of climatic changes on fuel loads, fuel availability did not become a limiting factor of fire occurrence in either study landscape under the same climate change scenarios in this study. Wu et al. (2015) even found a positive effect of the increasing atmospheric CO_2 concentration on fuel loads and burned area extents across Europe in the RCP 8.5 scenario. In simulations using LPJ-GUESS-SIMFIRE, the authors found no significant difference between the projected mean annual burned fractions in the last 20 years of the 21st century compared to those at the end of the 20th century in the RCP8.5 scenario in the approximate location of the study areas of this thesis (considering a much coarser spatial resolution of about 55 km). The LPJmL-SPITFIRE model, on the other hand, simulated a climate-driven increase in mean annual burn fractions between 3.25 and 4.75 in the RCP8.5 scenario in both regions (Wu et al., 2015). These results are consistent with the projected increase in fire occurrence in the BGNP in this study but not with that in the BuWe.

A direct comparison of the results with the other two simulation studies presented in the introduction is only possible to a limited extent, among other factors because these are based on a different climate change scenario, which can be classified roughly between the RCP4.5 and RCP8.5 scenarios. Nonetheless, Migliavacca et al.'s (2013) study also provided supportive evidence for the finding that fuel availability in Central Europe will remain sufficient during the 21st century so that changes in temperature and precipitation have the greatest impact on fire occurrence. In addition, a significant increase in burned areas was found in the wider Central and Eastern European region, although this did not apply to the two study regions. No significant difference from the baseline scenario was found there. However, fire suppression was also considered in the study (Migliavacca et al., 2013), which should explain much of this discrepancy with the present thesis. In the global study by Kloster et al. (2012), there was a

significant increase in annual fire emissions compared to the baseline scenario in Europe over the last 25 years of the 21st century, which also affected the regions where the two study regions of the present thesis are located. While there was an increase in fire probability in both regions during this period due to changes in moisture conditions and an elongation of the fire season, eastern Austria also experienced a simultaneous decrease in fire probability due to negative changes in fuel availability (Kloster et al., 2012). However, an estimation of the exact magnitude of these effects in individual small-scale regions and thus a direct comparison to the present work is not possible due to the low spatial resolution. In addition, iLand does not specify the month in which a fire occurred, so no conclusions about seasonality can be drawn.

Lastly, the findings regarding the impact of changes in the fire regimes on carbon sequestration and storage in the study landscapes are consistent with those of Seidl, Schelhaas, et al. (2014), who also showed a negligible effect of forest fires on carbon storage by 2030 under a range of different climate scenarios.

This comparison of the results with the current state of research shows the considerable influence of the choice of model and its parameterization on the results. While the studies predominantly predicted an increase in fire occurrence in Central Europe and the study areas due to climatic changes during the 21st century, there were considerable differences between the studies, especially concerning the magnitude of this increase and the impact of climate change on fuel availability. All studies reflected the enormous local differences in fire activity in the different regions of Central Europe, reconfirming the need for small-scale studies with high spatial resolution such as the present work. These types of studies can contribute to a clearer understanding of local impacts of climate change on fire regimes and thus provide a more solid basis for regional adaptation and mitigation measures.

Lastly, a comparison with the similarly designed study by Hansen et al. (2020), who used iLand to examine the effects of climatic changes in the RCP4.5 and RCP8.5 scenarios on the fire regime of the GTNP in the United States during the 21st century, provides an opportunity to place the results in an international context. The study area encompassed 40,000 ha of forested area at elevations between 1,600 m and 3,400 m, receiving 540 mm of precipitation annually (Hansen et al., 2020). The study showed an increase in the mean annual number of fires by almost 70% in the RCP8.5 scenario, from 3.3 fires per year on average from 1989 – 2017 to 5.6 fires per year from 2018 – 2098 (Hansen et al., 2020). To compare these results with those of the present study, the simulations with the minimum interval are best suited because the fire occurrence is most similar. While the rise in fire occurrence in the BuWe was lower than in the GTNP at 44%, the BGNP reacted much more sensitively with an increase of

almost 120%. While there was a substantial increase in fire occurrence in the GTNP by the middle of the century in the RCP8.5 scenario, which was less pronounced in the present thesis, there was also a further intensification toward the end of the century (Hansen et al., 2020), similar to this study. However, due to the different approach in simulating fire sizes under climate change (see section 4.2), the mean fire sizes increased along with the other indicators in the Wyoming study, leading to a significantly stronger increase in the annual burned area extent than the number of fires. While fire sizes only exceeded 200 ha once in each landscape in all RCP8.5 simulations in the present study, fires larger than 225 ha became very common in GTNP in the second half of the 21st century, so that more than 37% of the total area was affected by fires in many years (Hansen et al., 2020). In contrast to the trends observed in the two study landscapes in the European Alps, high-severity fires also occurred more frequently, causing a large decrease in the total forested area of the GTNP after the middle of the century (Hansen et al., 2020). Thus, while the relative increase in the number of annual fires could potentially be within a similar range in the two regions, or even greater in the European Alps, the intensification of fire regimes in Central Europe and the associated severity of negative impacts will not be comparable to current and potential future developments in the western United States.

4.4 Discussion of iLand's Fire Modeling Approach Based on the KBDI Index

The simulation results show that, as expected due to iLand's fire modeling approach, the future occurrence of fires is primarily controlled by the change in future fuel moisture conditions compared to those of the historical regime. The soundness of this probability-based modeling approach has been validated with observational data in several studies focusing on forest landscapes in the United States (e.g. Braziunas et al., 2018; Hansen et al., 2020; Seidl, Rammer, & Spies, 2014). The change in fuel moisture conditions is calculated and reflected in iLand via the KBDI index. It is one of the most widely used indices to assess fire danger, especially in the United States but also in many other regions worldwide, in part because it is easy to calculate and requires comparatively few inputs (Liu et al., 2010; Taufik et al., 2015). Originally, the index was created for use in the United States, primarily Florida (Keetch & Byram, 1968), which is reflected directly in its computational approach: the drying rate included in the index and the method of computing potential evapotranspiration as part of the drought factor were both tailored to Florida's climatic conditions (Keetch & Byram, 1968; Liu et al., 2010; Taufik et al., 2015). As a result, various studies have shown that using the KBDI in other regions is not always suitable (e.g. Liu et al., 2010). More specifically, the index appears to underestimate fire risk (Petros et al., 2011; Spano et al., 2005) and not to detect the end of the summer drought season (Pellizzaro et al., 2007) in regions with less precipitation than Florida, such as the Mediterranean, and overestimate fire danger in regions with more precipitation,

such as tropical wetlands in Indonesia (Taufik et al., 2015). The prevalence of soil types other than those found in Florida has also been found to reduce the predictive power of the KBDI (Reardon et al., 2009; Sparks et al., 2002).

Studies have also shown that the KBDI is not a suitable indicator for assessing fire danger in winter in Austria but can capture it well in summer, especially at extreme values (Arpaci et al., 2013; Eastaugh & Hasenauer, 2014). At the same time, Arpaci et al. (2013) found that simply using the daily mean temperature to assess fire danger provided a better estimate at more sites in Austria than the best performing of the 22 indices included, which the authors also attributed to the lack of adaptation of the indices to local conditions. They recommended the use of a combination of different indices during the summer and winter seasons and generally in areas with large differences in topography and prevailing climatic conditions like Austria (Arpaci et al., 2013). Similarly, the use of relative humidity alone for projections of fire occurrence in Germany, and also in Bavaria, outperformed a number of fire indices in a study by Holsten et al. (2013). Among commonly used indices, the M-68, which has been developed for use in Germany, seems to provide the best results (Holsten et al., 2013; Schunk et al., 2017). Nevertheless, the KBDI and litter moisture conditions are still significantly correlated in Bavaria (Schunk et al., 2017). At the same time, an increase in fire-promoting conditions in the region over the last six decades has coincided with a decrease in actual fire occurrence, most likely due to changes in human activities (Wastl et al., 2012). Because weather conditions play a subordinate role for ignitions caused by humans, as discussed earlier, fire indices cannot always adequately predict fire occurrence in areas where the vast majority of ignitions are human-caused. For example, in a Swiss study by Reineking et al. (2010), the KBDI performed well in a comparison of 14 fire indices for natural ignitions but was not among the best indices for human ignitions. In this context, the Angstroem index performed best. The authors therefore also recommended employing different indices for the two causes of ignition and, if the use of only one index is feasible, to base the choice on the main cause in the area (Reineking et al., 2010).

While the relative impacts of changes in temperature and precipitation on fire regimes outside the southeastern United States can still be reasonably estimated using the KBDI in any case (Liu et al., 2010), several efforts of varying complexity have been made to adapt the index to different local conditions. The simplest way to modify the KBDI is to adjust the parameters used to determine the drought factor to the local annual mean precipitation. Petros et al. (2011), for example, have reported a better performance of the KBDI for fire regimes in the Mediterranean region after modifying it in this way. Snyder et al. (2006) also obtained better KBDI results for California by adjusting the drying rate using the Hargreaves-Samani method

to estimate reference evapotranspiration instead of the originally utilized potential evapotranspiration estimation method. Taufik et al. (2015) calculated a modified KBDI, incorporating local annual precipitation and a revised calculation of potential evapotranspiration, but were only able to achieve a comparatively small improvement in predictive power using this approach. Therefore, and in agreement with the recommendations of Reardon et al. (2009) and Pellizzaro et al. (2007), further improvements were made by the authors to also include soil hydrologic characteristics in a modified version of the index. The addition of a water table factor to account for the typically low water tables in wetland ecosystems that affect soil moisture content led to a significant improvement of the KBDI's performance compared to its original form as well as the version adapted to the local climate (Taufik et al., 2015). However, these are all individual efforts to adapt the KBDI to a specific area, and to date, there are no guidelines or a framework to facilitate the adaptation of the index to new study areas.

Despite the aforementioned drawbacks of using the KBDI outside the southeastern United States, the results of the present thesis were probably not significantly affected by not adjusting the KBDI to local conditions, as the analysis was based entirely on relative changes due to climatic changes. However, an adjustment of the KBDI or the addition of supplementary indices should be considered in future studies using iLand to obtain reliable results.

4.5 Study Limitations

Among the main limitations of the present work is the limited data availability and research on historical and current fire regimes in Central Europe, and the study regions in particular, which hampered the parameterization of the model. Even official records by governmental entities are often unreliable as they tend to be incomplete and alternative data sources, such as satellite data, are of little help as fires in the study regions are usually too small to detect. Although the sensitivity of the study areas' fire regimes to climatic changes could still be estimated, the results can therefore not offer a realistic picture of future fire occurrence. At the same time, the modeling approach itself was highly simplified and additional factors such as fire suppression, forest management, a potential increase of fire sizes due to climate change, or interactions with other natural disturbance agents were not considered due to the limited scope of the study. Furthermore, simulations were performed under only two of the currently available RCP scenarios, but these likely underestimate or overestimate real developments. While it is still helpful to get a better understanding of the range of potential impacts, a study considering the most likely business-as-usual scenario at present, the RCP6.0 scenario, could provide more accurate results. Since future fire regimes were simulated and studied for only two exemplary landscapes, the transferability of the results to other regions in the Alps and

wider Central Europe is limited and further studies are needed to enhance spatial coverage. Ultimately, the present thesis is based on one model only and its specific fire modeling approach built around deviations of fuel moisture conditions as measured by the KBDI from those that characterized the historic fire regime, as discussed in the previous subsection, and the results should be compared and verified with those of other models.

5. Conclusion

The present study has shown that an increase in (summer) temperatures as well as a decrease in snow cover will likely have a significant impact on fire occurrence in Central Europe during the 21st century under moderate and high emissions scenarios, similar to other regions such as the western United States. Counterintuitively, areas such as the BGNP, where annual precipitation sums are likely to remain at a constantly high level, might experience more pronounced impacts than warmer and drier regions if these two influencing factors change more strongly. Fuel availability did not occur to be a limiting factor for fire activity in Central Europe under climate change, which could promote the occurrence of larger fires, especially if less accessible areas at higher elevations will be increasingly affected. While the results of the present study at landscape level are evidently only conditionally transferable to larger parts of Central Europe, a potential climate-induced increase in the fire ignition probability by a factor of two to four in some regions over the next 80 years would be associated with high risks for ecosystems, people, and infrastructure, and likely also a significant increase in firefighting costs and economic losses. A comparison of the findings with previously conducted simulation studies indicated that continental-scale studies are often insufficient to predict the magnitude of changes at smaller scales despite an overall agreement regarding the direction of the change, which is important, for example, to develop specific local policies.

Several areas for improvement and topics for further research have emerged from the findings of this study. For one, the month in which each fire occurred could be added to the fire-specific outputs in iLand to analyze potential changes in the seasonality of fire regimes based on this information. Furthermore, an approach should be developed to adapt the KBDI to local conditions of new study areas to ensure that results are reliable when it is applied outside of the United States. Alternatively, a different or additional drought index could be introduced, considering that certain indices perform better in modeling human-induced ignitions. With respect to the present study and its study regions, the parameterization should be improved as much as possible and important influencing factors, such as management and fire suppression as well as interactions with other disturbance agents, should be considered in potential future attempts to improve the projections. In addition, the possibility of larger fires developing under extreme conditions should be considered in future studies, for example by

using certain thresholds of the KBDI, which has been shown to provide solid results in another iLand study. While impacts on carbon storage were mostly minor in the present study, carbon pools were noticeably reduced during the EOC period in the most extreme scenario. A longer-term study beyond the 21st century might therefore be needed to gain a better understanding of potential long-term trends. In addition, impacts on other ecosystem services may be more relevant and should also be the focus of future studies. The findings of the present thesis should also be compared to those of other models that are based, for example, on a different drought index for modeling fire danger, as different modeling approaches have significant impacts on the magnitude of the simulated results. To gain a better understanding of potential changes in Central European fire regimes, additional landscapes with different climatic characteristics as well as a greater variety of climate change scenarios should be investigated. Overall, the study showed that further research of the effects of global change on Central European fire regimes will initially also require further improvement of existing models that have not been developed or adapted for this purpose.

References

Abram, N. J., Henley, B. J., Sen Gupta, A., Lippmann, T. J. R., Clarke, H., Dowdy, A. J., Sharples, J. J., Nolan, R. H., Zhang, T., Wooster, M. J., Wurtzel, J. B., Meissner, K. J., Pitman, A. J., Ukkola, A. M., Murphy, B. P., Tapper, N. J., & Boer, M. M. (2021). Connections of climate change and variability to large and extreme forest fires in southeast Australia. *Communications Earth & Environment*, *2*(1). https://doi.org/10.1038/s43247-020-00065-8

Altaratz, O., Koren, I., Yair, Y., & Price, C. (2010). Lightning response to smoke from Amazonian fires. *Geophysical Research Letters*, *37*(7), n/a-n/a. https://doi.org/10.1029/2010GL042679

Andela, N., Morton, D. C., Giglio, L., Chen, Y., van der Werf, G. R., Kasibhatla, P. S., DeFries, R. S., Collatz, G. J., Hantson, S., Kloster, S., Bachelet, D., Forrest, M., Lasslop, G., Li, F., Mangeon, S., Melton, J. R., Yue, C., & Randerson, J. T. (2017). A human-driven decline in global burned area. *Science (New York, N.Y.)*, *356*(6345), 1356–1362. https://doi.org/10.1126/science.aal4108

Arpaci, A., Eastaugh, C. S., & Vacik, H. (2013). Selecting the best performing fire weather indices for Austrian ecoregions. *Theoretical and Applied Climatology*, *114*(3-4), 393–406. https://doi.org/10.1007/s00704-013-0839-7

Bayerisches Waldgesetz, (GVBl. S. 313, BayRS 7902-1-L) (2005).

Blarquez, O., Bremond, L., & Carcaillet, C. (2010). Holocene fires and a herb-dominated understorey track wetter climates in subalpine forests. *Journal of Ecology*, *98*(6), 1358–1368. https://doi.org/10.1111/j.1365-2745.2010.01721.x

Blarquez, O., & Carcaillet, C. (2010). Fire, Fuel Composition and Resilience Threshold in Subalpine Ecosystem. *PLoS ONE*, *5*(8), e12480. https://doi.org/10.1371/journal.pone.0012480

Bonan, G. B. (2008). Forests and climate change: Forcings, feedbacks, and the climate benefits of forests. *Science (New York, N.Y.)*, *320*(5882), 1444–1449. https://doi.org/10.1126/science.1155121

Bowman, D. M., O'Brien, J. A., & Goldammer, J. G. (2013). Pyrogeography and the Global Quest for Sustainable Fire Management. *Annual Review of Environment and Resources*, *38*(1), 57–80. https://doi.org/10.1146/annurev-environ-082212-134049

Braziunas, K. H., Hansen, W. D., Seidl, R., Rammer, W., & Turner, M. G. (2018). Looking beyond the mean: Drivers of variability in postfire stand development of conifers in Greater Yellowstone. *Forest Ecology and Management*, *430*, 460–471. https://doi.org/10.1016/j.foreco.2018.08.034

Bundesanstalt für Landwirtschaft und Ernährung [BLE] (1995). *Waldbrandstatistik der Bundesrepublik Deutschland für das Jahr 1994*. Frankfurt am Main. Bundesanstalt für Landwirtschaft und Ernährung. https://www.bmel-statistik.de/fileadmin/daten/FHB-0302250-1994.pdf

Bundesanstalt für Landwirtschaft und Ernährung [BLE] (1996). *Waldbrandstatistik der Bundesrepublik Deutschland für das Jahr 1995*. Frankfurt am Main. Bundesanstalt für Landwirtschaft und Ernährung. https://www.bmel-statistik.de/fileadmin/daten/FHB-0302250-1995.pdf

Bundesanstalt für Landwirtschaft und Ernährung [BLE] (1997). *Waldbrandstatistik der Bundesrepublik Deutschland für das Jahr 1996*. Frankfurt am Main. Bundesanstalt für Landwirtschaft und Ernährung. https://www.bmel-statistik.de/fileadmin/daten/FHB-0302250-1996.pdf

Bundesanstalt für Landwirtschaft und Ernährung [BLE] (1998). *Waldbrandstatistik der Bundesrepublik Deutschland für das Jahr 1997*. Frankfurt am Main. Bundesanstalt für Landwirtschaft und Ernährung. https://www.bmel-statistik.de/fileadmin/daten/FHB-0302250-1997.pdf

Bundesanstalt für Landwirtschaft und Ernährung [BLE] (1999). *Waldbrandstatistik der Bundesrepublik Deutschland für das Jahr 1998*. Frankfurt am Main. Bundesanstalt für Landwirtschaft und Ernährung. https://www.bmel-statistik.de/fileadmin/daten/FHB-0302250-1998.pdf

Bundesanstalt für Landwirtschaft und Ernährung [BLE] (2000). *Waldbrandstatistik der Bundesrepublik Deutschland für das Jahr 1999*. Frankfurt am Main. Bundesanstalt für Landwirtschaft und Ernährung. https://www.bmel-statistik.de/fileadmin/daten/FHB-0302250-1999.pdf

Bundesanstalt für Landwirtschaft und Ernährung [BLE] (2001). *Waldbrandstatistik der Bundesrepublik Deutschland für das Jahr 2000*. Frankfurt am Main. Bundesanstalt für Landwirtschaft und Ernährung. https://www.bmel-statistik.de/fileadmin/daten/FHB-0302250-2000.pdf

Bundesanstalt für Landwirtschaft und Ernährung [BLE] (2002). *Waldbrandstatistik der Bundesrepublik Deutschland für das Jahr 2001*. Frankfurt am Main. Bundesanstalt für Landwirtschaft und Ernährung. https://www.bmel-statistik.de/fileadmin/daten/FHB-0302250-2001.pdf

Bundesanstalt für Landwirtschaft und Ernährung [BLE] (2003). *Waldbrandstatistik der Bundesrepublik Deutschland für das Jahr 2002*. Frankfurt am Main. Bundesanstalt für Landwirtschaft und Ernährung. https://www.bmel-statistik.de/fileadmin/daten/FHB-0302250-2002.pdf

Bundesanstalt für Landwirtschaft und Ernährung [BLE] (2004). *Waldbrandstatistik der Bundesrepublik Deutschland für das Jahr 2003*. Frankfurt am Main. Bundesanstalt für Landwirtschaft und Ernährung. https://www.bmel-statistik.de/fileadmin/daten/FHB-0302250-2003.pdf

Bundesanstalt für Landwirtschaft und Ernährung [BLE] (2005). *Waldbrandstatistik der Bundesrepublik Deutschland für das Jahr 2004*. Bonn. Bundesanstalt für Landwirtschaft und Ernährung. https://www.bmel-statistik.de/fileadmin/daten/FHB-0302250-2004.pdf

Bundesanstalt für Landwirtschaft und Ernährung [BLE] (2021). *Waldbrandstatistik der Bundesrepublik Deutschland 2020*. Bonn. Bundesanstalt für Landwirtschaft und Ernährung. https://www.bmel-statistik.de/fileadmin/daten/FHB-0302250-2020.pdf

Bundesministerium für Ernährung, Landwirtschaft und Forsten [BMEL] (1994). *Waldbrandstatistik der Bundesrepublik Deutschland für das Jahr 1993*. Bonn. Bundesministerium für Ernährung, Landwirtschaft und Forsten. https://www.bmel-statistik.de/fileadmin/daten/FHB-0302250-1993.pdf

Carcaillet, C. (1998). A spatially precise study of Holocene fire history, climate and human impact within the Maurienne valley, North French Alps. *Journal of Ecology*, *86*(3), 384–396. https://doi.org/10.1046/j.1365-2745.1998.00267.x

Carcaillet, C., Ali, A. A., Blarquez, O., Genries, A., Mourier, B., & Bremond, L. (2009). Spatial variability of fire history in subalpine forests: From natural to cultural regimes. *Écoscience*, *16*(1), 1–12. https://doi.org/10.2980/16-1-3189

Colombaroli, D., Henne, P. D., Kaltenrieder, P., Gobet, E., & Tinner, W. (2010). Species responses to fire, climate and human impact at tree line in the Alps as evidenced by palaeo-environmental records and a dynamic simulation model. *Journal of Ecology*, *98*(6), 1346–1357. https://doi.org/10.1111/j.1365-2745.2010.01723.x

Costa, H., de Rigo, D., Libertà, G., Houston Durrant, T., & San-Miguel-Ayanz, J. (2020). *European wildfire danger and vulnerability in a changing climate: towards integrating risk dimensions*. Luxembourg. Publications Office of the European Union. https://doi.org/10.2760/46951

De Rigo, D., Libertà, G., Houston Durrant, T., Artés Vivancos, T., & San-Miguel-Ayanz, J. (2017). *Forest fire danger extremes in Europe under climate change: variability and uncertainty*. https://doi.org/10.2760/13180

Dennison, P. E., Brewer, S. C., Arnold, J. D., & Moritz, M. A. (2014). Large wildfire trends in the western United States, 1984-2011. *Geophysical Research Letters*, *41*(8), 2928–2933. https://doi.org/10.1002/2014GL059576

Dupire, S., Curt, T., Bigot, S., & Fréjaville, T. (2019). Vulnerability of forest ecosystems to fire in the French Alps. *European Journal of Forest Research*, *138*(5), 813–830. https://doi.org/10.1007/s10342-019-01206-1

Eastaugh, C. S., & Hasenauer, H. (2014). Deriving forest fire ignition risk with biogeochemical process modelling. *Environmental Modelling & Software: With Environment Data News*, *55*, 132–142. https://doi.org/10.1016/j.envsoft.2014.01.018

Friedlingstein, P., Jones, M. W., O'Sullivan, M., Andrew, R. M., Bakker, D. C. E., Hauck, J., Le Quéré, C., Peters, G. P., Peters, W., Pongratz, J., Sitch, S., Canadell, J. G., Ciais, P., Jackson, R. B., Alin, S. R., Anthoni, P., Bates, N. R., Becker, M., Bellouin, N., Bopp, L., Chau, T. T. T., Chevallier, F., Chini, L. P., Cronin, M., Currie, K. I., Decharme, B., Djeutchouang, L., Dou, X., Evans, W., Feely, R. A., Feng, L., Gasser, T., Gilfillan, D., Gkritzalis, T., Grassi, G., Gregor, L., Gruber, N., Gürses, Ö., Harris, I., Houghton, R. A., Hurtt, G. C., Iida, Y., Ilyina, T., Luijkx, I. T., Jain, A. K., Jones, S. D., Kato, E., Kennedy, D., Klein Goldewijk, K., Knauer, J., Korsbakken, J. I., Körtzinger, A.,

Landschützer, P., Lauvset, S. K., Lefèvre, N., Lienert, S., Liu, J., Marland, G., McGuire, P. C., Melton, J. R., Munro, D. R., Nabel, J. E. M. S.; Nakaoka, S.-I., Niwa, Y., Ono, T., Pierrot, D., Poulter, B., Rehder, G., Resplandy, L., Robertson, E., Rödenbeck, C., Rosan, T. M., Schwinger, J., Schwingshackl, C., Séférian, R., Sutton, A. J., Sweeney, C., Tanhua, T., Tans, P. P., Tian, H., Tilbrook, B., Tubiello, F., van der Werf, G., Vuichard, N., Wada, C., Wanninkhof, R., Watson, A., Willis, D., Wiltshire, A. J., Yuan, W., Yue, C., Yue, X., Zaehle, S., & Zeng, J. (2021). *Global Carbon Budget 2021.* https://doi.org/10.5194/essd-2021-386

Gehring, E., Conedera, M., Maringer, J., Giadrossich, F., Guastini, E., & Schwarz, M. (2019). Shallow landslide disposition in burnt European beech (Fagus sylvatica L.) forests. *Scientific Reports*, *9*(1), 8638. https://doi.org/10.1038/s41598-019-45073-7

Genries, A., Mercier, L., Lavoie, M., Muller, S. D., Radakovitch, O., & Carcaillet, C. (2009). The effect of fire frequency on local cembra pine populations. *Ecology*, *90*(2), 476–486. https://doi.org/10.1890/07-1740.1

Hamed, K. H., & Ramachandra Rao, A. (1998). A modified Mann-Kendall trend test for autocorrelated data. *Journal of Hydrology*, *204*(1-4), 182–196. https://doi.org/10.1016/S0022-1694(97)00125-X

Hansen, W. D., Abendroth, D., Rammer, W., Seidl, R., & Turner, M. G. (2020). Can wildland fire management alter 21st-century subalpine fire and forests in Grand Teton National Park, Wyoming, USA? *Ecological Applications*, *30*(2), e02030. https://doi.org/10.1002/eap.2030

Harris, R. M. B., Remenyi, T. A., Williamson, G. J., Bindoff, N. L., & Bowman, D. M. J. S. (2016). Climate–vegetation–fire interactions and feedbacks: trivial detail or major barrier to projecting the future of the Earth system? *WIREs Climate Change*, *7*(6), 910–931. https://doi.org/10.1002/wcc.428

Hijmans, R. J. (2022). *Geographic Data Analysis and Modeling [R package raster version 3.5-15]*. Comprehensive R Archive Network (CRAN). https://cran.r-project.org/package=raster

Holsten, A., Dominic, A. R., Costa, L., & Kropp, J. P. (2013). Evaluation of the performance of meteorological forest fire indices for German federal states. *Forest Ecology and Management*, *287*, 123–131. https://doi.org/10.1016/j.foreco.2012.08.035

Honkaniemi, J., Rammer, W., & Seidl, R. (2020). Norway spruce at the trailing edge: The effect of landscape configuration and composition on climate resilience. *Landscape Ecology*, *35*(3), 591–606. https://doi.org/10.1007/s10980-019-00964-y

Institut für Waldbau (2021). *Waldbranddaten von 1993 – 2021 für die Bundesländer Salzburg und Burgenland (inkl. Datum, Brandart, Brandfläche und Brandursache)* [Data File]. Universität für Bodenkultur Wien.

Institut für Waldbau (2022). *Waldbrand-Datenbank Österreich.* Universität für Bodenkultur Wien. https://fire.boku.ac.at/firedb/de/#

Jiménez-Ruano, A., Rodrigues Mimbrero, M., & De La Riva Fernández, J. (2017). Exploring spatial–temporal dynamics of fire regime features in mainland Spain. *Natural Hazards and Earth System Sciences*, *17*(10), 1697–1711. https://doi.org/10.5194/nhess-17-1697-2017

Kaltenrieder, P., Procacci, G., Vannière, B., & Tinner, W. (2010). Vegetation and fire history of the Euganean Hills (Colli Euganei) as recorded by Lateglacial and Holocene sedimentary series from Lago della Costa (northeastern Italy). *The Holocene*, *20*(5), 679–695. https://doi.org/10.1177/0959683609358911

Kassambara, A. (2020). *'ggplot2' Based Publication Ready Plots [R package ggpubr version 0.4.0]*. Comprehensive R Archive Network (CRAN). https://cran.r-project.org/package=ggpubr

Keetch, J. J., & Byram, G. M. (1968). A Drought Index for Forest Fire Control. *U.S.D.A. Forest Service Research Paper SE-38*. https://www.srs.fs.usda.gov/pubs/rp/rp_se038.pdf

Kendall, M. G. (1975). *Rank correlation measures*. Charles Griffin.

Kloster, S., Mahowald, N. M., Randerson, J. T., & Lawrence, P. J. (2012). The impacts of climate, land use, and demography on fires during the 21st century simulated by CLM-CN. *Biogeosciences*, *9*(1), 509–525. https://doi.org/10.5194/bg-9-509-2012

Knorr, W., Jiang, L., & Arneth, A. (2016). Climate, CO_2 and human population impacts on global wildfire emissions, 267–282. https://doi.org/10.5194/bg-13-267-2016

Krawchuk, M. A., & Moritz, M. A. (2011). Constraints on global fire activity vary across a resource gradient. *Ecology*, *92*(1), 121–132. https://doi.org/10.1890/09-1843.1

Krawchuk, M. A., Moritz, M. A., Parisien, M.-A., van Dorn, J., & Hayhoe, K. (2009). Global pyrogeography: The current and future distribution of wildfire. *PLoS ONE*, *4*(4), e5102. https://doi.org/10.1371/journal.pone.0005102

Krebs, P., Pezzatti, G. B., Mazzoleni, S., Talbot, L. M., & Conedera, M. (2010). Fire regime: History and definition of a key concept in disturbance ecology. *Theory in Biosciences*, *129*(1), 53–69. https://doi.org/10.1007/s12064-010-0082-z

Lachmann, M. [Michael] (2006). *Waldbrandstatistik der Bundesrepublik Deutschland für das Jahr 2005*. Bonn. Bundesanstalt für Landwirtschaft und Ernährung. https://www.bmel-statistik.de/fileadmin/daten/FHB-0302250-2005.pdf

Lachmann, M. [Michael] (2007). *Waldbrandstatistik der Bundesrepublik Deutschland für das Jahr 2006*. Bonn. Bundesanstalt für Landwirtschaft und Ernährung. https://www.bmel-statistik.de/fileadmin/daten/FHB-0302250-2006.pdf

Lachmann, M. [Michael] (2008). *Waldbrandstatistik der Bundesrepublik Deutschland für das Jahr 2007*. Bonn. Bundesanstalt für Landwirtschaft und Ernährung. https://www.bmel-statistik.de/fileadmin/daten/FHB-0302250-2007.pdf

Lachmann, M. [Michael] (2009). *Waldbrandstatistik der Bundesrepublik Deutschland für das Jahr 2008*. Bonn. Bundesanstalt für Landwirtschaft und Ernährung. https://www.bmel-statistik.de/fileadmin/daten/FHB-0302250-2008.pdf

Lachmann, M. [Michael] (2010). *Waldbrandstatistik der Bundesrepublik Deutschland für das Jahr 2009*. Bonn. Bundesanstalt für Landwirtschaft und Ernährung. https://www.bmel-statistik.de/fileadmin/daten/FHB-0302250-2009.pdf

Lachmann, M. [Michaela] (2011). *Waldbrandstatistik der Bundesrepublik Deutschland für das Jahr 2010*. Bonn. Bundesanstalt für Landwirtschaft und Ernährung. https://www.bmel-statistik.de/fileadmin/daten/FHB-0302250-2010.pdf

Lachmann, M. [Michaela] (2012). *Waldbrandstatistik der Bundesrepublik Deutschland für das Jahr 2011*. Bonn. Bundesanstalt für Landwirtschaft und Ernährung. https://www.bmel-statistik.de/fileadmin/daten/FHB-0302250-2011.pdf

Lachmann, M. [Michaela] (2013). *Waldbrandstatistik der Bundesrepublik Deutschland für das Jahr 2012*. Bonn. Bundesanstalt für Landwirtschaft und Ernährung. https://www.bmel-statistik.de/fileadmin/daten/FHB-0302250-2012.pdf

Lachmann, M. [Michaela] (2014). *Waldbrandstatistik der Bundesrepublik Deutschland für das Jahr 2013*. Bonn. Bundesanstalt für Landwirtschaft und Ernährung. https://www.bmel-statistik.de/fileadmin/daten/FHB-0302250-2013.pdf

Lachmann, M. [Michaela] (2015). *Waldbrandstatistik der Bundesrepublik Deutschland für das Jahr 2014*. Bonn. Bundesanstalt für Landwirtschaft und Ernährung. https://www.bmel-statistik.de/fileadmin/daten/FHB-0302250-2014.pdf

Lavorel, S., Flannigan, M. D., Lambin, E. F., & Scholes, M. C. (2006). Vulnerability of land systems to fire: Interactions among humans, climate, the atmosphere, and ecosystems. *Mitigation and Adaptation Strategies for Global Change*, *12*(1), 33–53. https://doi.org/10.1007/s11027-006-9046-5

Leys, B., Carcaillet, C., Blarquez, O., Lami, A., Musazzi, S., & Trevisan, R. (2014). Resistance of mixed subalpine forest to fire frequency changes: the ecological function of dwarf pine (Pinus mugo ssp. mugo). *Quaternary Science Reviews*, *90*, 60–68. https://doi.org/10.1016/j.quascirev.2014.02.023

Lindner, M., Maroschek, M., Netherer, S., Kremer, A., Barbati, A., Garcia-Gonzalo, J., Seidl, R., Delzon, S., Corona, P., Kolström, M., Lexer, M. J., & Marchetti, M. (2010). Climate change impacts, adaptive capacity, and vulnerability of European forest ecosystems. *Forest Ecology and Management*, *259*(4), 698–709. https://doi.org/10.1016/j.foreco.2009.09.023

Liu, Y., Stanturf, J., & Goodrick, S. (2010). Trends in global wildfire potential in a changing climate. *Forest Ecology and Management*, *259*(4), 685–697. https://doi.org/10.1016/j.foreco.2009.09.002

Lonati, M., Gorlier, A., Ascoli, D., Marzano, R., & Lombardi, G. (2009). Response of the alien species Panicum acuminatum to disturbance in an Italian lowland heathland. *Botanica Helvetica*, *119*(2), 105–111. https://doi.org/10.1007/s00035-009-0063-3

Lyons, Nelson, Williams, Cramer, & Turner (1998). Enhanced positive cloud-to-ground lightning in thunderstorms ingesting smoke from fires. *Science (New York, N.Y.)*, *282*(5386), 77–80. https://doi.org/10.1126/science.282.5386.77

Mann, H. B. (1945). Nonparametric Tests Against Trend. *Econometrica*, *13*(3), 245. https://doi.org/10.2307/1907187

Maringer, J., Wohlgemuth, T., Neff, C., Pezzatti, G. B., & Conedera, M. (2012). Post-fire spread of alien plant species in a mixed broad-leaved forest of the Insubric region. *Flora - Morphology, Distribution, Functional Ecology of Plants*, *207*(1), 19–29. https://doi.org/10.1016/j.flora.2011.07.016

McLeod, A. I. (2011). *Kendall rank correlation and Mann-Kendall trend test [R package Kendall version 2.2]*. Comprehensive R Archive Network (CRAN). https://cran.r-project.org/package=Kendall

Migliavacca, M., Dosio, A., Camia, A., Hobourg, R., Houston-Durrant, T., Kaiser, J. W., Khabarov, N., Krasovskii, A. A., Marcolla, B., San Miguel-Ayanz, J., Ward, D. S., & Cescatti, A. (2013). Modeling biomass burning and related carbon emissions during the 21st century in Europe. *Journal of Geophysical Research: Biogeosciences*, *118*(4), 1732–1747. https://doi.org/10.1002/2013JG002444

Moretti, M., Duelli, P., & Obrist, M. K. (2006). Biodiversity and resilience of arthropod communities after fire disturbance in temperate forests. *Oecologia*, *149*(2), 312–327. https://doi.org/10.1007/s00442-006-0450-z

Moritz, M. A., Parisien, M.-A., Batllori, E., Krawchuk, M. A., van Dorn, J., Ganz, D. J., & Hayhoe, K. (2012). Climate change and disruptions to global fire activity. *Ecosphere*, *3*(6), art49. https://doi.org/10.1890/ES11-00345.1

Müller, K., Wickham, H., James, D. A., & Falcon, S. (2021). *SQLite Interface for R [R package RSQLite version 2.2.9]*. Comprehensive R Archive Network (CRAN). https://cran.r-project.org/package=RSQLite

Müller, M., Lena, V. V., Vacik, H., Mayer, C., Mayr, S., Carrega, P., Duche, Y., Lahaye, S., Böttcher, F., Maier, H., Schunk, C., Zimmermann, L., Ascoli, D., Cotterchio, A., Fiorucci, P., Gottero, F., Pirone, S., Rizzolo, R., Vacchiano, G., & Sautter, M. (2020). *Forest Fires in the Alps: State of knowledge, future challenges and options for an integrated fire management.* EUSALP Action Group 8. https://doi.org/10.13140/RG.2.2.15609.42081

Nationalparkverwaltung Berchtesgarden (2001). *Nationalparkplan.* Bayerisches Staatsministerium für Landesentwicklung und Umweltfragen. https://www.nationalpark-berchtesgaden.bayern.de/medien/publikationen/index.htm

Neuwirth, E. (2014). *ColorBrewer Palettes [R package RColorBrewer version 1.1-2]*. Comprehensive R Archive Network (CRAN). https://cran.r-project.org/package=RColorBrewer

Parisien, M.-A., & Moritz, M. A. (2009). Environmental controls on the distribution of wildfire at multiple spatial scales. *Ecological Monographs*, *79*(1), 127–154. https://doi.org/10.1890/07-1289.1

Pellizzaro, G., Cesaraccio, C., Duce, P., Ventura, A., & Zara, P. (2007). Relationships between seasonal patterns of live fuel moisture and meteorological drought indices for Mediterranean shrubland species. *International Journal of Wildland Fire*, *16*(2), 232. https://doi.org/10.1071/WF06081

Petros, G., Mantzavelas, A., & Tsakaldimi, M. (2011). Development of an adapted empirical drought index to the Mediterranean conditions for use in forestry. *Agricultural and Forest Meteorology*, *151*(2), 241–250. https://doi.org/10.1016/j.agrformet.2010.10.011

Pohlert, T. (2020). *Non-Parametric Trend Tests and Change-Point Detection [R package trend version 1.1.4]*. Comprehensive R Archive Network (CRAN). https://cran.r-project.org/package=trend

R Core Team (2020). *R: A language and environment for statistical computing [Version 4.1.2]*. R Foundation for Statistical Computing. https://www.R-project.org/

Reardon, J., Curcio, G., & Bartlette, R. (2009). Soil moisture dynamics and smoldering combustion limits of pocosin soils in North Carolina, USA. *International Journal of Wildland Fire*, *18*(3), 326. https://doi.org/10.1071/WF08085

Rego, F. C., Morgan, P., Fernandes, P., & Hoffman, C. (2021). *Fire Science*. Springer International Publishing. https://doi.org/10.1007/978-3-030-69815-7

Reineking, B., Weibel, P., Conedera, M., & Bugmann, H. (2010). Environmental determinants of lightning- v. human-induced forest fire ignitions differ in a temperate mountain region of Switzerland. *International Journal of Wildland Fire*, *19*(5), 541. https://doi.org/10.1071/WF08206

Rosenfeld, D. (1999). TRMM observed first direct evidence of smoke from forest fires inhibiting rainfall. *Geophysical Research Letters*, *26*(20), 3105–3108. https://doi.org/10.1029/1999GL006066

Royston, J. P. (1982). An Extension of Shapiro and Wilk's W Test for Normality to Large Samples. *Journal of the Royal Statistical Society. Series C (Applied Statistics)*, *31*(2), 115. https://doi.org/10.2307/2347973

Salguero, J., Li, J., Farahmand, A., & Reager, J. T. (2020). Wildfire Trend Analysis over the Contiguous United States Using Remote Sensing Observations. *Remote Sensing*, *12*(16), 2565. https://doi.org/10.3390/rs12162565

San-Miguel-Ayanz, J., Durrat, T., Boca, R., Libertà, G., Branco, A., de Rigo, D., Ferrari, D., Maianti, P., Artés-Vivancos, T., Oom, D., Pfeiffer, H., Nuijten, D., & Leray, T. (2019). *Forest Fires in Europe, Middle East and North Africa 2018*. Luxembourg. Publications Office of the European Union. https://doi.org/10.2760/1128

San-Miguel-Ayanz, J., Durrat, T., Boca, R., Maianti, P., Libertà, G., Artés-Vivancos, T., Oom, D., Branco, A., de Rigo, D., Ferrari, D., Pfeiffer, H., Grecchi, R., Nuijten, D., &

Leray, T. (2020). *Forest Fires in Europe, Middle East and North Africa 2019*. Luxembourg. Publications Office of the European Union. https://doi.org/10.2760/468688

Schelhaas, M.-J., Nabuurs, G.-J., & Schuck, A. (2003). Natural disturbances in the European forests in the 19th and 20th centuries. *Global Change Biology*, *9*(11), 1620–1633. https://doi.org/10.1046/j.1365-2486.2003.00684.x

Schunk, C., Wastl, C., Leuchner, M., & Menzel, A. (2017). Fine fuel moisture for site- and species-specific fire danger assessment in comparison to fire danger indices. *Agricultural and Forest Meteorology*, *234-235*, 31–47. https://doi.org/10.1016/j.agrformet.2016.12.007

Seidl, R., & Rammer, W. (2021). *iLand hub*. https://iland-model.org/iLand+Hub

Seidl, R., Rammer, W., Scheller, R. M., & Spies, T. A. (2012). An individual-based process model to simulate landscape-scale forest ecosystem dynamics. *Ecological Modelling*, *231*, 87–100. https://doi.org/10.1016/j.ecolmodel.2012.02.015

Seidl, R., Rammer, W., & Spies, T. A. (2014). Disturbance legacies increase the resilience of forest ecosystem structure, composition, and functioning. *Ecological Applications*, *24*(8), 2063–2077. https://doi.org/10.1890/14-0255.1

Seidl, R., Schelhaas, M.-J., & Lexer, M. J. (2011). Unraveling the drivers of intensifying forest disturbance regimes in Europe. *Global Change Biology*, *17*(9), 2842–2852. https://doi.org/10.1111/j.1365-2486.2011.02452.x

Seidl, R., Schelhaas, M.-J., Rammer, W., & Verkerk, P. J. (2014). Increasing forest disturbances in Europe and their impact on carbon storage. *Nature Climate Change*, *4*(9), 806–810. https://doi.org/10.1038/nclimate2318

Seidl, R., Thom, D., Kautz, M., Martin-Benito, D., Peltoniemi, M., Vacchiano, G., Wild, J., Ascoli, D., Petr, M., Honkaniemi, J., Lexer, M. J., Trotsiuk, V., Mairota, P., Svoboda, M., Fabrika, M., Nagel, T. A., & Reyer, C. P. O. (2017). Forest disturbances under climate change. *Nature Climate Change*, *7*(6), 395–402. https://doi.org/10.1038/nclimate3303

Sen, P. K. (1968). Estimates of the Regression Coefficient Based on Kendall's Tau. *Journal of the American Statistical Association*, *63*(324), 1379–1389. https://doi.org/10.1080/01621459.1968.10480934

Senf, C., & Seidl, R. (2021). Storm and fire disturbances in Europe: Distribution and trends. *Global Change Biology*, *27*(15), 3605–3619. https://doi.org/10.1111/gcb.15679

Snyder, R. L., Spano, D., Duce, P., Baldocchi, D., Xu, L., & Paw U, K. T. (2006). A fuel dryness index for grassland fire-danger assessment. *Agricultural and Forest Meteorology*, *139*(1-2), 1–11. https://doi.org/10.1016/j.agrformet.2006.05.006

Spano, D., Duce, P., Snyder, R. L [R. L.], Zara, P., & Ventura, A. (2005). Assessment of fuel dryness index on mediterranean vegetation. In *Proceedings of the Sixth Symposium on Fire and Forest Meteorology,* Cammore, Canada.

Sparks, J. C., Masters, R. E., Engle, D. M., & Bukenhofer, G. A. (2002). Season of Burn Influences Fire Behavior and Fuel Consumption in Restored Shortleaf Pine-Grassland Communities. *Restoration Ecology*, *10*(4), 714–722. https://doi.org/10.1046/j.1526-100X.2002.01052.x

Stähli, M., Finsinger, W., Tinner, W., & Allgower, B. (2006). Wildfire history and fire ecology of the Swiss National Park (Central Alps): new evidence from charcoal, pollen and plant macrofossils. *The Holocene*, *16*(6), 805–817. https://doi.org/10.1191/0959683606hol967rp

Taufik, M., Setiawan, B. I., & van Lanen, H. A. (2015). Modification of a fire drought index for tropical wetland ecosystems by including water table depth. *Agricultural and Forest Meteorology*, *203*, 1–10. https://doi.org/10.1016/j.agrformet.2014.12.006

Thom, D., Rammer, W., Laux, P., Smiatek, G., Kunstmann, H., & Seidl, R. (2022). Will forest dynamics continue to accelerate throughout the 21st century in the Northern Alps? *Global Change Biology*, *00*(1-15). https://doi.org/10.1111/gcb.16133

Tosca, M. G., Randerson, J. T., Zender, C. S., Flanner, M. G., & Rasch, P. J. (2010). Do biomass burning aerosols intensify drought in equatorial Asia during El Niño? *Atmospheric Chemistry and Physics*, *10*(8), 3515–3528. https://doi.org/10.5194/acp-10-3515-2010

Turner, M. G. (2010). Disturbance and landscape dynamics in a changing world. *Ecology*, *91*(10), 2833–2849. https://doi.org/10.1890/10-0097.1

Van Butsic, Kelly, M., & Moritz, M. (2015). Land Use and Wildfire: A Review of Local Interactions and Teleconnections. *Land*, *4*(1), 140–156. https://doi.org/10.3390/land4010140

Van der Werf, G. R., Randerson, J. T., Giglio, L., van Leeuwen, T. T., Chen, Y., Rogers, B. M., Mu, M., van Marle, M. J. E., Morton, D. C., Collatz, G. J., Yokelson, R. J., & Kasibhatla, P. S. (2017). Global fire emissions estimates during 1997–2016. *Earth System Science Data*, *9*(2), 697–720. https://doi.org/10.5194/essd-9-697-2017

Van Vuuren, D. P., Edmonds, J., Kainuma, M., Riahi, K., Thomson, A., Hibbard, K., Hurtt, G. C., Kram, T., Krey, V., Lamarque, J.-F., Masui, T., Meinshausen, M., Nakicenovic, N., Smith, S. J., & Rose, S. K. (2011). The representative concentration pathways: an overview. *Climatic Change*, *109*(1-2), 5–31. https://doi.org/10.1007/s10584-011-0148-z

Vergani, C., Werlen, M., Conedera, M., Cohen, D., & Schwarz, M. (2017). Investigation of root reinforcement decay after a forest fire in a Scots pine (Pinus sylvestris) protection forest. *Forest Ecology and Management*, *400*, 339–352. https://doi.org/10.1016/j.foreco.2017.06.005

WaldSchweiz (2021). *Schönbrunner Rindenabzugstabelle.* WaldSchweiz. https://www.waldschweiz.ch/fileadmin/user_upload/user_upload/Forstwirtschaft/Vermarktung/D_Schoenbrunner-Tabelle.pdf

Walker, A. P., Kauwe, M. G. de, Bastos, A., Belmecheri, S., Georgiou, K., Keeling, R. F., McMahon, S. M., Medlyn, B. E., Moore, D. J. P., Norby, R. J., Zaehle, S., Anderson-Teixeira, K. J., Battipaglia, G., Brienen, R. J. W., Cabugao, K. G., Cailleret, M., Campbell, E., Canadell, J. G., Ciais, P., Craig, M. E., Ellsworth, D. S., Farquhar, G. D.; Fatichi, S., Fisher, J. B., Frank, D. C., Graven, H., Gu, L., Haverd, V., Heilman, K., Heimann, M., Hungate, B. A., Iversen, C. M., Joos, F., Jiang, M., Keenan, T. F., Knauer, J., Körner, C., Leshyk, V. O., Leuzinger, S., Liu, Y., MacBean, N., Malhi, Y., McVicar, T. R., Penuelas, J., Pongratz, J., Powell, A. S., Riutta, T., Sabot, M. E. B., Schleucher, J., Sitch, S., Smith, W. K., Sulman, B., Taylor, B., Terrer, C., Torn, M. S., Treseder, K. K., Trugman, A. T., Trumbore, S. E., van Mantgem, P. J., Voelker, S. L., Whelan, M. E., & Zuidema, P. A. (2021). Integrating the evidence for a terrestrial carbon sink caused by increasing atmospheric CO2. *The New Phytologist*, *229*(5), 2413–2445. https://doi.org/10.1111/nph.16866

Wastl, C., Schunk, C., Leuchner, M., Pezzatti, G. B., & Menzel, A. (2012). Recent climate change: Long-term trends in meteorological forest fire danger in the Alps. *Agricultural and Forest Meteorology*, *162-163*, 1–13. https://doi.org/10.1016/j.agrformet.2012.04.001

Wastl, C., Schunk, C., Lüpke, M., Cocca, G., Conedera, M., Valese, E., & Menzel, A. (2013). Large-scale weather types, forest fire danger, and wildfire occurrence in the Alps. *Agricultural and Forest Meteorology*, *168*, 15–25. https://doi.org/10.1016/j.agrformet.2012.08.011

Weibel, P., Elkin, C., Reineking, B., Conedera, M., & Bugmann, H. (2010). Waldbrandmodellierung - Möglichkeiten und Grenzen | Forest fire modeling - limits and possibilities. *Schweizerische Zeitschrift Fur Forstwesen*, *161*(11), 433–441. https://doi.org/10.3188/szf.2010.0433

Westerling, A. L. (2016). Increasing western US forest wildfire activity: Sensitivity to changes in the timing of spring. *Philosophical Transactions of the Royal Society of London. Series B, Biological Sciences*, *371*(1696). https://doi.org/10.1098/rstb.2015.0178

Wickham, H. (2021). *Easily Install and Load the 'Tidyverse' [R package tidyverse version 1.3.1]*. Comprehensive R Archive Network (CRAN). https://cran.r-project.org/package=tidyverse

Wickham, H., Chang, W., Henry, L., Lin Pedersen, T., Takahashi, K., Wilke, C., Woo, K., Yutani, H., & Dunningtion, D. (2021). *Create Elegant Data Visualisations Using the Grammar of Graphics [R package ggplot2 version 3.3.5]*. Comprehensive R Archive Network (CRAN). https://cran.r-project.org/package=ggplot2

Wilcoxon, F. (1945). Individual Comparisons by Ranking Methods. *Biometrics Bulletin*, *1*(6), 80. https://doi.org/10.2307/3001968

Winkler, A. J., Myneni, R. B., Hannart, A., Sitch, S., Haverd, V., Lombardozzi, D., Arora, V. K., Pongratz, J., Nabel, J. E. M. S., Goll, D. S., Kato, E., Tian, H., Arneth, A., Friedlingstein, P., Jain, A. K., Zaehle, S., & Brovkin, V. (2021). Slowdown of the greening trend in natural vegetation with further rise in atmospheric CO_2. *Biogeosciences*, *18*(17), 4985–5010. https://doi.org/10.5194/bg-18-4985-2021

Wu, M., Knorr, W., Thonicke, K., Schurgers, G., Camia, A., & Arneth, A. (2015). Sensitivity of burned area in Europe to climate change, atmospheric CO_2 levels, and demography: A comparison of two fire-vegetation models. *Journal of Geophysical Research: Biogeosciences*, *120*(11), 2256–2272. https://doi.org/10.1002/2015JG003036

Yutani, H. (2021). *Highlight Lines and Points in 'ggplot2' [R package gghighlight version 0.3.2]*. Comprehensive R Archive Network (CRAN). https://rdrr.io/cran/gghighlight/

Zheng, B., Ciais, P., Chevallier, F., Chuvieco, E., Chen, Y [Yang], & Yang, H. (2021). Increasing forest fire emissions despite the decline in global burned area. *Science Advances*, *7*(39), eabh2646. https://doi.org/10.1126/sciadv.abh2646

Zumbrunnen, T., Bugmann, H., Conedera, M., & Bürgi, M. (2009). Linking Forest Fire Regimes and Climate—A Historical Analysis in a Dry Inner Alpine Valley. *Ecosystems*, *12*(1), 73–86. https://doi.org/10.1007/s10021-008-9207-3

Appendix

A. Future Fire Regime – Spatio-temporal distribution and fire characteristics

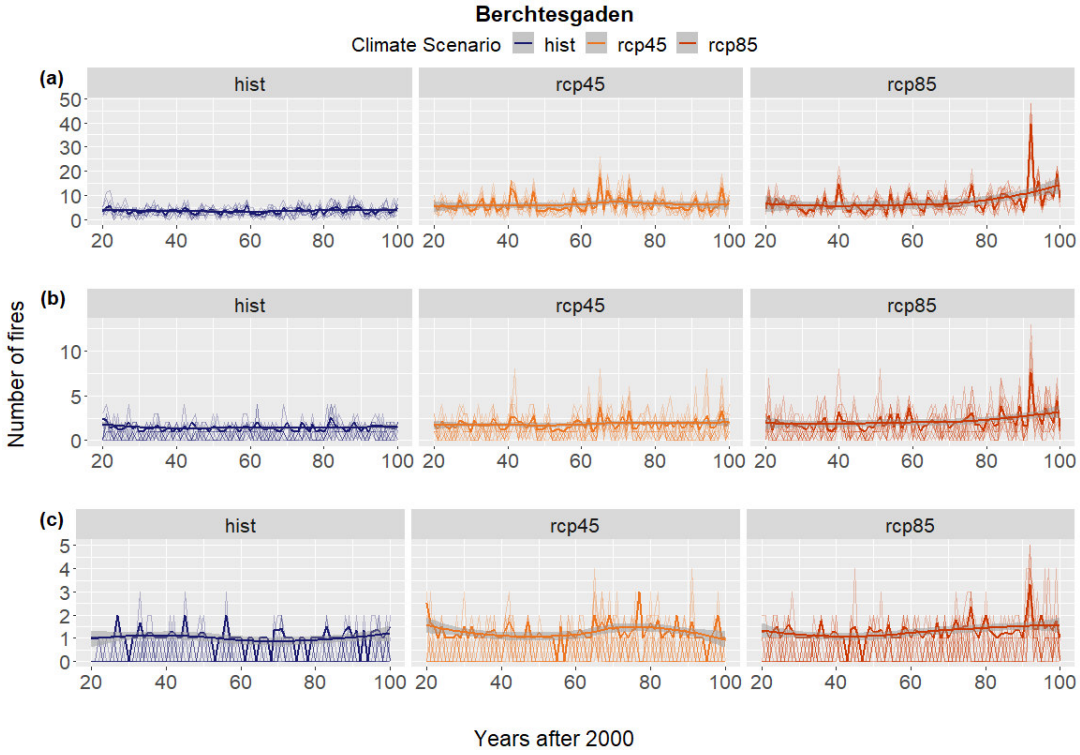

Figure A: Annual number of fires in BG throughout the simulation period under the three climate scenarios for (a) the minimum return interval of 124 years, (b) the mean return interval of 534 years, and (c) the maximum return interval of 1520 years. Thin lines show the ten individual iterations while the bold lines represent annual means as well as the overall mean, smoothed using the loess method.

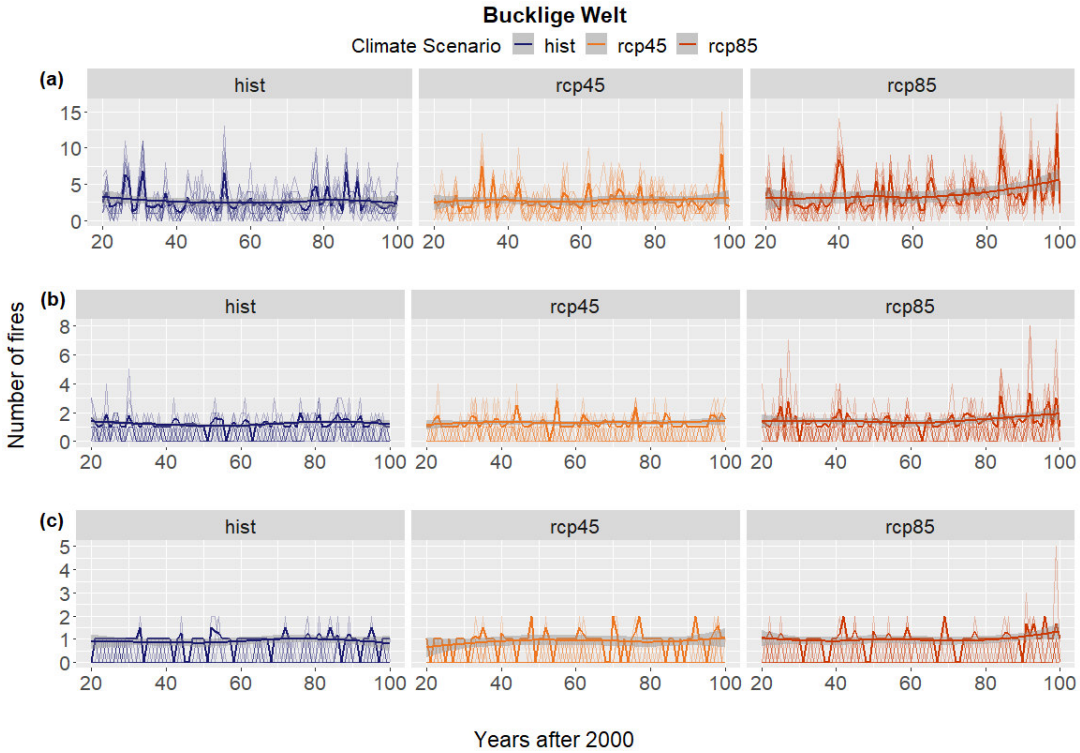

Figure B: Annual number of fires in BuWe throughout the simulation period under the three climate scenarios for (a) the minimum return interval of 124 years, (b) the mean return interval of 534 years, and (c) the maximum return interval of 1520 years. Thin lines show the ten individual iterations while the bold lines represent annual means as well as the overall mean, smoothed using the loess method.

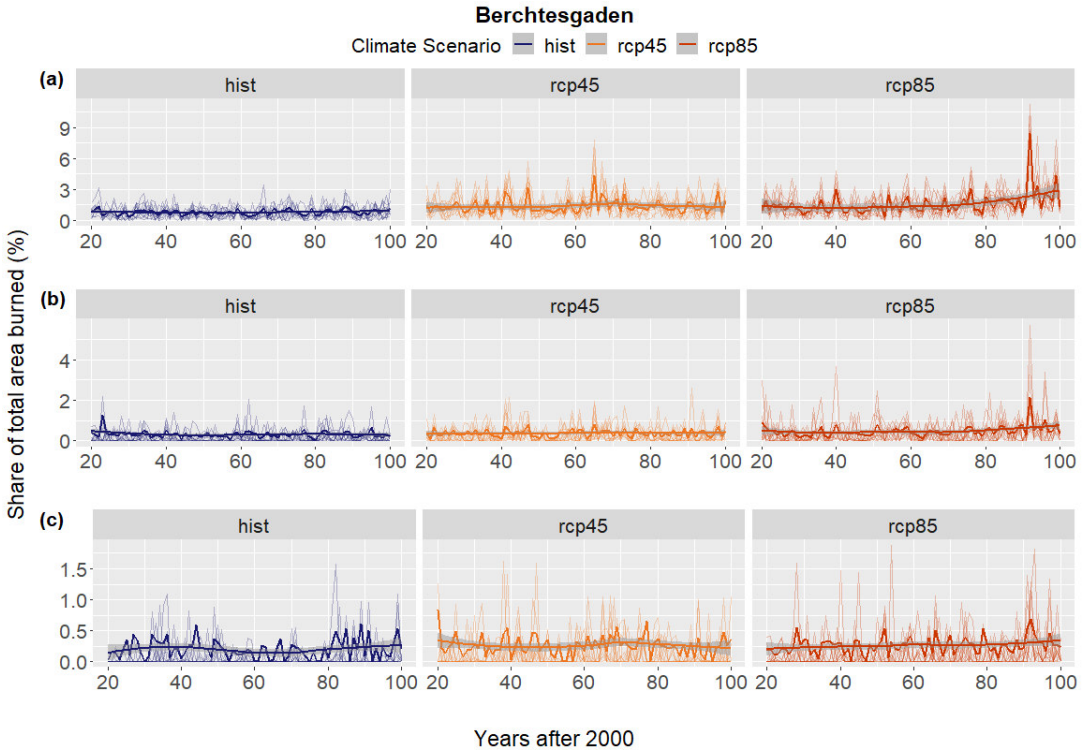

Figure C: Annual share of the total area burned in BG throughout the simulation period under the three climate scenarios for (a) the minimum return interval of 124 years, (b) the mean return interval of 534 years, and (c) the maximum return interval of 1520 years. Thin lines show the ten individual iterations while the bold lines represent annual means as well as the overall mean, smoothed using the loess method.

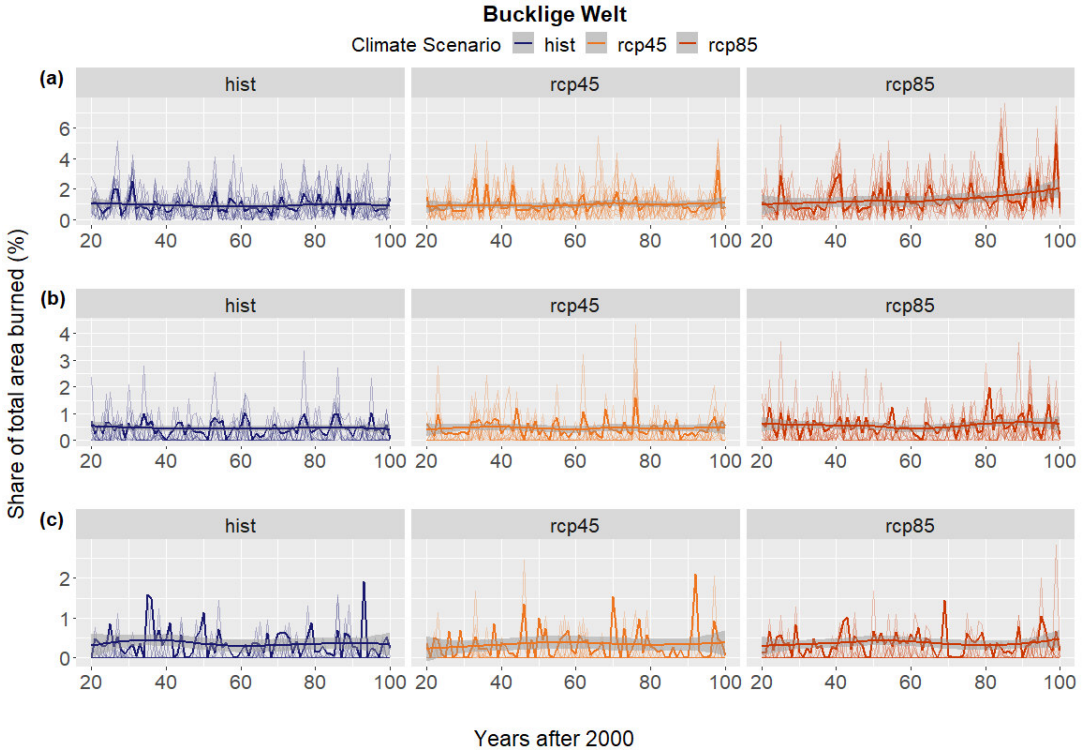

Figure D: Annual share of the total area burned in BuWe throughout the simulation period under the three climate scenarios for (a) the minimum return interval of 124 years, (b) the mean return interval of 534 years, and (c) the maximum return interval of 1520 years. Thin lines show the ten individual iterations while the bold lines represent annual means as well as the overall mean, smoothed using the loess method.

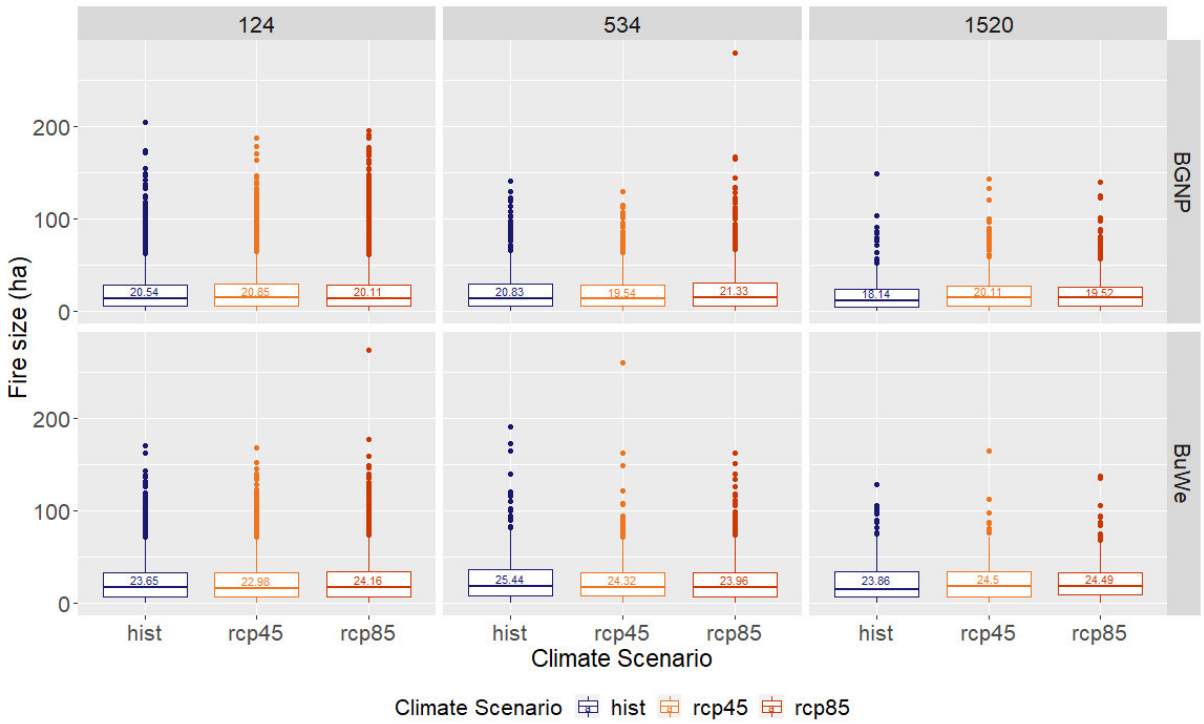

Figure E: Boxplots showing summary statistics of the individual fire sizes (in ha) throughout the entire simulation period in BGNP (first row) and BuWe (second row) for the three return intervals in all ten iterations. The bold line and numbers show the mean, the lower and upper hinges indicate the first and third quartiles, and the whiskers expand from the upper and lower hinges to the largest and smallest value, respectively, which are no further than 1.5 * IQR from them. Dots show individual outliers beyond the range of the whiskers.

Table A: Mean annual number of fires and share of the total area burned averaged over all ten iterations per scenario in both study areas in the future period (simulation years 20 – 100) and the EOC period (simulation years 80 – 100).

Study Area	Climate Scenario	Return Interval	Mean annual number of fires		Mean annual share of the total area burned (%)	
			Future	EOC	Future	EOC
BGNP	Baseline	124	3.32	3.70	0.725	0.794
		534	0.80	0.98	0.179	0.207
		1520	0.27	0.33	0.056	0.080
	RCP4.5	124	5.99	5.86	1.330	1.270
		534	1.30	1.23	0.267	0.245
		1520	0.50	0.49	0.106	0.094
	RCP8.5	124	7.27	10.80	1.540	2.300
		534	1.67	2.45	0.375	0.562
		1520	0.58	0.80	0.118	0.163
BuWe	Baseline	124	2.34	2.60	0.825	0.914
		534	0.56	0.61	0.212	0.224
		1520	0.20	0.24	0.073	0.078
	RCP4.5	124	2.41	2.47	0.842	0.860
		534	0.54	0.55	0.197	0.191
		1520	0.18	0.16	0.065	0.051
	RCP8.5	124	3.38	4.57	1.230	1.660
		534	0.81	1.06	0.305	0.409
		1520	0.25	0.35	0.089	0.107

Table B: Summary of future and end-of-century intervals of all simulated scenarios, rounded up to full years.

Study Area	Climate Scenario	Historic Interval	Future Interval (2020 – 2100)	EOC Interval (2080 – 2100)
BuWe	Historical	124	122	110
BGNP	Historical	124	139	126
BuWe	RCP4.5	124	119	117
BGNP	RCP4.5	124	76	79
BuWe	RCP8.5	124	82	61
BGNP	RCP8.5	124	65	44
BuWe	Historical	534	472	447
BGNP	Historical	534	558	484
BuWe	RCP4.5	534	509	524
BGNP	RCP4.5	534	375	409
BuWe	RCP8.5	534	329	245
BGNP	RCP8.5	534	267	178
BuWe	Historical	1520	1378	1277
BGNP	Historical	1520	1803	1246
BuWe	RCP4.5	1520	1530	1964
BGNP	RCP4.5	1520	944	1063
BuWe	RCP8.5	1520	1128	932
BGNP	RCP8.5	1520	846	615

B. Future Fire Regime – Conditions of fire occurrence

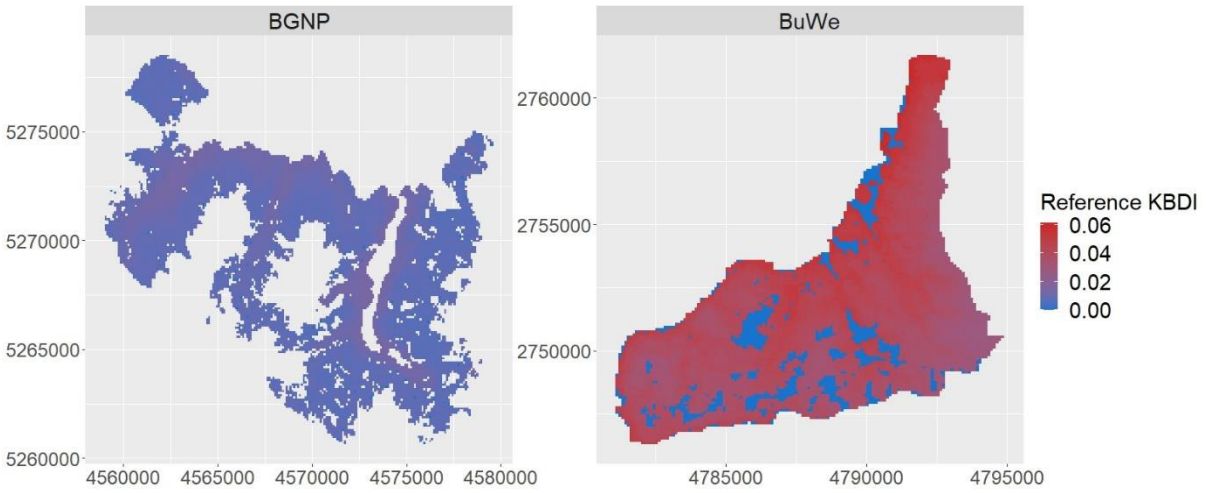

Figure F: KBDI reference values at RU-level across both landscapes.

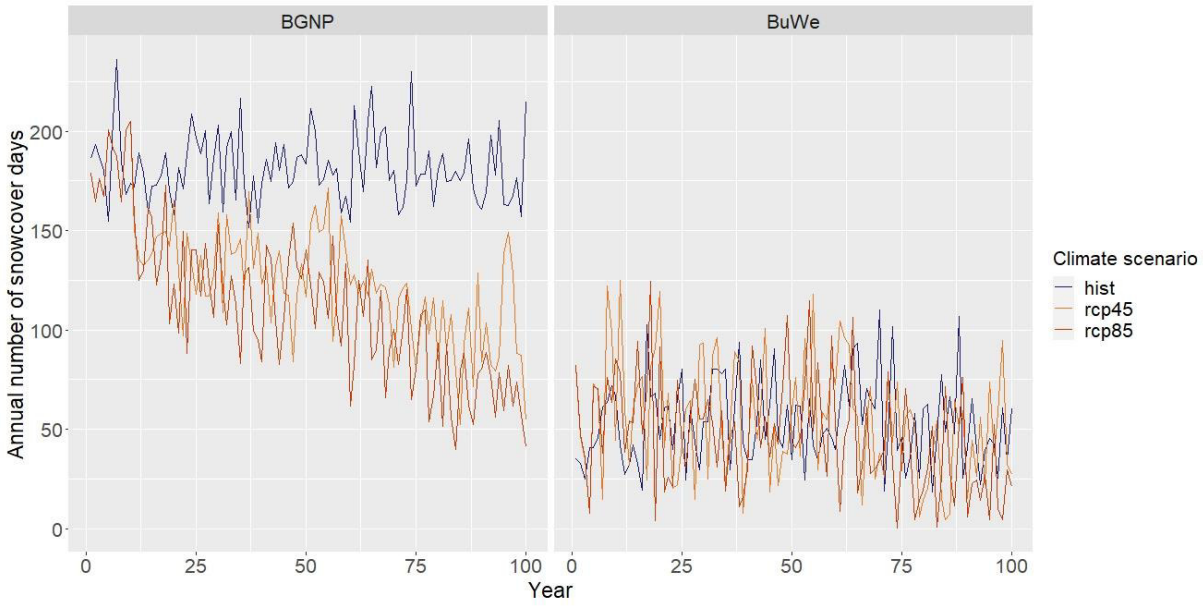

Figure G: Annual number of days with snow cover above 0 mm under the three climate scenarios across the entire BNGP (left column) and BuWe (right column) landscapes.

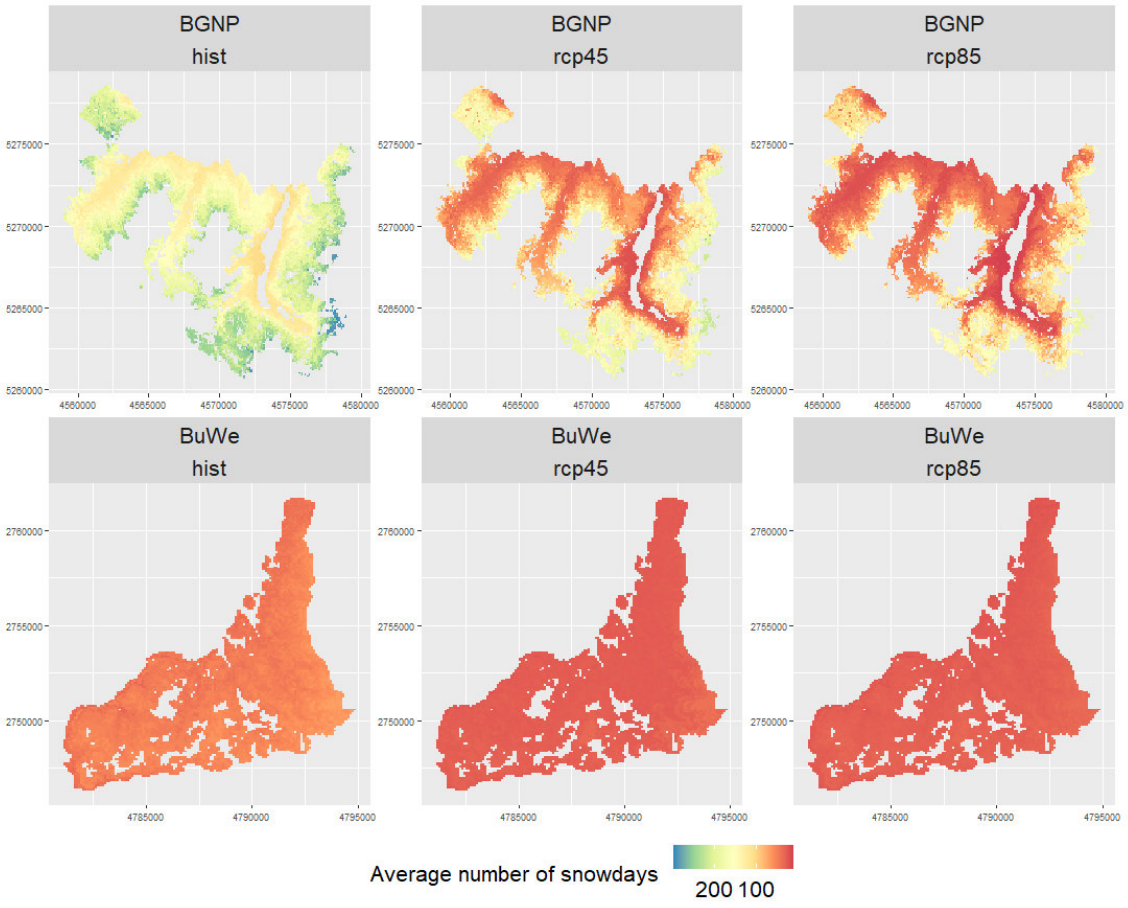

Figure H: Annual number of days with snow cover above 0 mm under the three climate scenarios in each RU of the BNGP (first row) and BuWe (second row) landscapes during the EOC period.

C. Future Fire Regime – Immediate effects

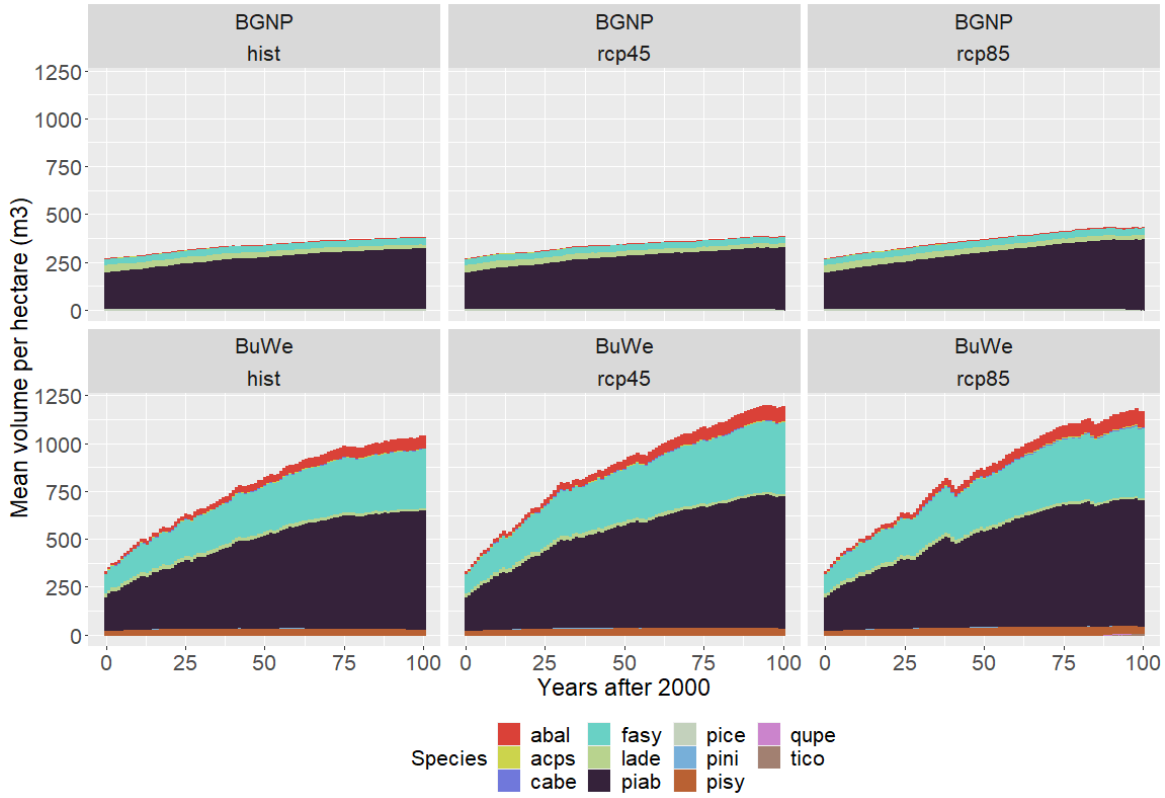

Figure I: Mean annual volume per hectare (m^3) in the BGNP (first row) and the BuWe (second row), averaged over the ten iterations. Limited to the main tree species with a volume of more than 1 m^3.

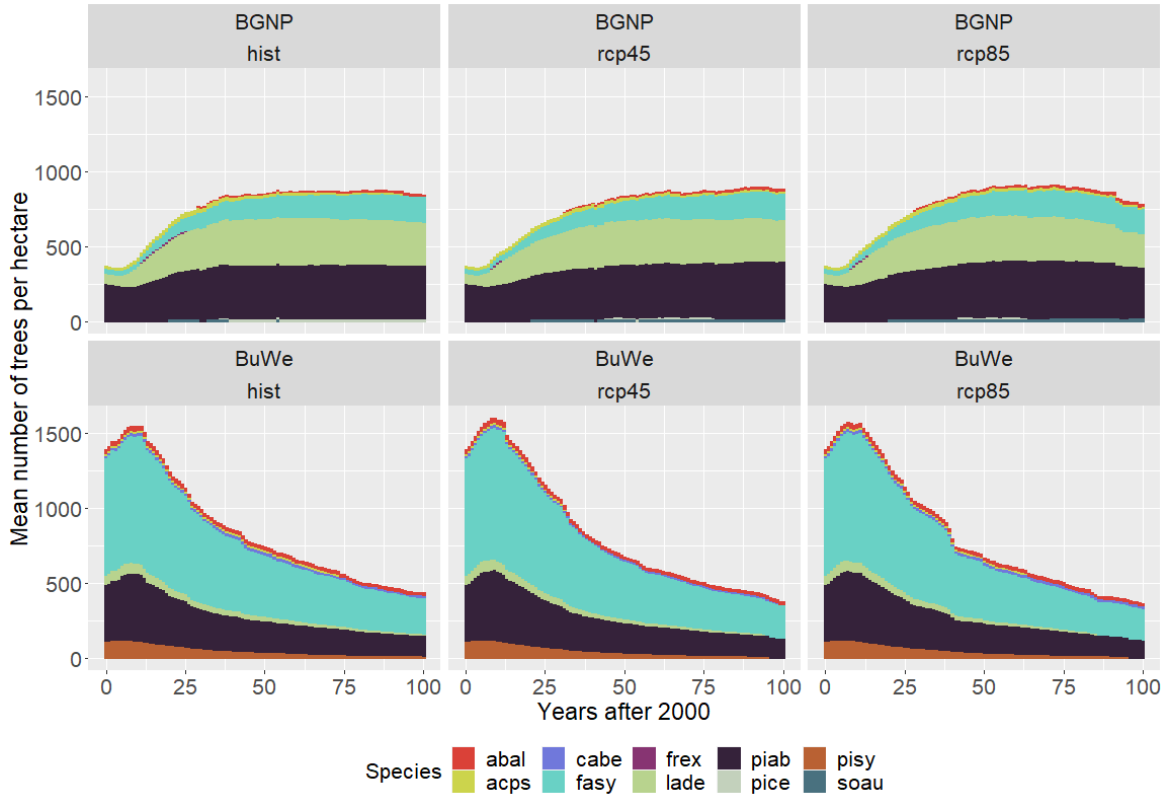

Figure J: Mean annual number of trees per hectare in the BGNP (first row) and the BuWe (second row), averaged over the ten iterations. Limited to the main species with more than 10 trees per hectare.

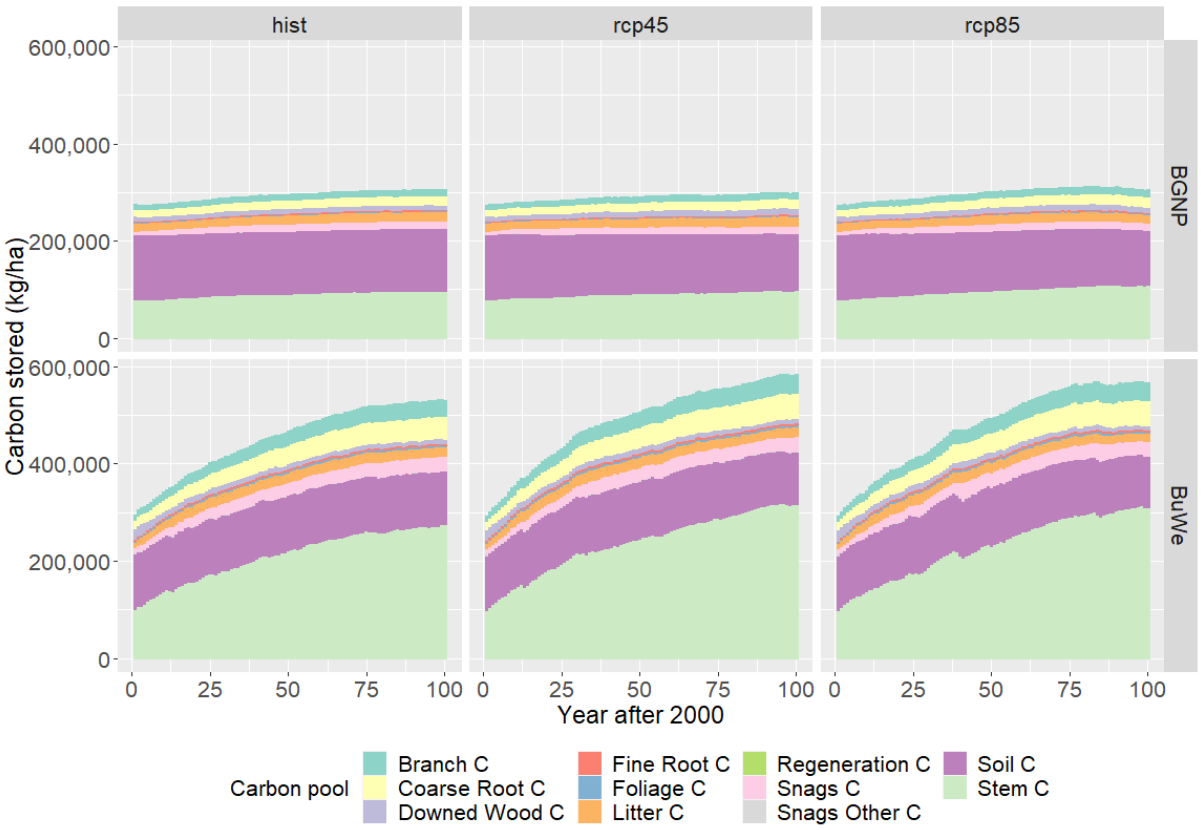

Figure K: Annual amount of carbon stored in different carbon pools (in kg/ha) in the study landscapes in the three climate scenarios.